The development of a model for the absorber component of an Aqua-Ammonia absorption heat pump

E van Niekerk

21840458

Dissertation submitted in fulfilment of the requirements for the degree *Magister* in Mechanical Engineering at the Potchefstroom Campus of the North-West University

Supervisor: Prof CP Storm

May 2016

It all starts here ™

NORTH-WEST UNIVERSITY
YUNIBESITI YA BOKONE-BOPHIRIMA
NOORDWES-UNIVERSITEIT ®

ABSTRACT

In recent years, South Africa as a country has increasingly faced challenges in regards to electricity provision. Modern society is highly dependent on refrigeration technology in order to refrigerate food, not only industrially, but also domestically. Humans are also dependent on air-conditioning, since they now inhabit parts of the world, which were previously less habitable.

The electricity woes of South Africa are obviously a threat to refrigeration capability, as most refrigeration systems use the vapour-compression cycle, which in turn uses electricity from the national grid. An alternative method of refrigeration is thus needed in order to make provision for future problems as well as becoming less dependent on the national electricity provider.

One alternative system, which can potentially satisfy this need, is the aqua-ammonia heat pump, which incorporates different principles than the conventional vapour-compression heat pump cycle. This desorption/absorption system utilizes heat input rather than electricity input, and is thus an ideal candidate. In recent years, work has indeed been done on this system, as it consists of several working components. The absorber component is a critical component of this system, and needs to be investigated and designed carefully. All the absorber designs considered in this study, have some component present or some undesirable aspect which make these designs unsuitable for a system which needs to work with thermal syphoning only. Thus, it was necessary to investigate an absorber component variation which avoid these pitfalls.

Several theoretical heat transfer models were developed for an absorber and compared with each other. Surrounding issues such as heat generated *in situ* were addressed and incorporated into the standard ε-NTU method for solving heat exchangers. The developed EES-programs can now solve with only minimal (but realistic) input parameters given. Theoretical issues with ammonia's solubility in water were also addressed, in order to enhance insight into the system. A few physical experiments were done in order to obtain values for parameters, which come into play in the practical design.

The absorber component was characterised using the different models developed. The different cooling tube configurations were compared and the best one chosen. The influence on the absorber performance of input parameters such as cooling water inlet temperature

and system pressure were investigated. Absorber performance for winter and summer conditions and inputs was also investigated.

This study resulted in a much better overall understanding of the absorber component in the aqua-ammonia heat pump, which is planned to be built. Problem areas and physical sensitivities were identified and solubility misunderstandings cleared up. Working computer models were developed which will enable future designers of the overall cycle, as well as the absorber component to make predictions. The study also enabled a first iteration for a design.

OPSOMMING

In die afgelope jare het Suid-Afrika as ’n land toenemend uitdagings in die gesig gestaar wat elektrisiteitsvoorsiening betref. Die moderne samelewing is hoogs afhanklik van verkoelingstegnologie, sodat voedsel verkoel kan word op beide huishoudelike sowel as industriële vlak. Die mens is ook afhanklik van lugversorging, aangesien dele van die wêreld nou bewoon word wat voorheen minder bewoonbaar was.

Die kopsere met elektrisiteit in Suid-Afrika is uit die aard van die saak ’n bedreiging vir verkoelings-vermoeë, aangesien die meeste stelsels van die damp-samedrukking-siklus gebruik maak, wat op sy beurt weer elektrisiteit van die nasionale netwerk verbruik. `n Alternatiewe metode van verkoeling word dus benodig sodat voorsiening vir die toekoms se probleme gemaak kan word, asook om minder afhanklik te word van die nasionale elektrisiteitsvoorsiener.

Een alternatiewe stelsel wat potensieel die bogenoemde behoefte kan bevredig, is die aqua-ammoniak hittepomp wat van ander beginsels gebruik maak as die konvensionele damp-samedrukking-hittepomp-siklus. Hierdie desorpsie/absorpsie stelsel maak gebruik van hitte inset eerder as ’n elektrisiteit inset, en is dus ’n ideale kandidaat. In die afgelope jare is werk gedoen op hierdie stelsel, aangesien dit uit verskillende werkende komponente bestaan. Die absorbeerder komponent is ’n krities belangrike deel van die stelsel en dit noodsaak deeglike ondersoek en ontwerp. Al die absorbeerder ontwerpe wat in aanmerking geneem is in hierdie studie, het een of ander komponent teenwoordig of een of ander onwenslike aspek wat hulle onvanpas maak vir ’n stelsel wat slegs met termiese syfering werk. Dus was dit nodig om ’n absorbeerder komponent variasie te ondersoek wat hierdie slaggate vermy.

Verskeie teoretiese hitte oordrag modelle is ontwikkel vir ’n absorbeerder en met mekaar vergelyk. Omliggende kwessies soos hitte wat *in situ* gegenereer word, is aangespreek en bygewerk by die standaard ε-NTU metode wat hitteruiler probleme oplos. Die ontwikkelde EES-programme kan nou oplos met slegs minimale (maar realistiese) inset parameters wat gegee word. Teoretiese kwessies met ammoniak se oplosbaarheid in water is ook aangespreek, sodat insig in die stelsel verkry kon word. ’n Paar fisiese eksperimente is gedoen sodat waardes vir fisiese parameters gevind kan word wat met die fisiese komponent verband hou.

Die absorbeerder komponent is gekarakteriseer deur gebruik te maak van verskillende modelle wat ontwikkel is. Die verkoelingsbuise se verskillende konfigurasies is vergelyk, en

die beste een gekies. Die invloed op die absorbeerder prestasie van inset parameters soos verkoelingswater inlaat temperatuur en stelsel druk is ondersoek. Absorbeerder prestasie vir winter en somer toestande en insette is ook ondersoek.

Hierdie studie het tot die gevolg dat ‘n beter algehele begrip ontwikkel is van die absorbeerder komponent in die aqua-ammoniak hittepomp, wat beplan word om gebou te word. Probleem areas en fisiese sensitiwiteite is uitgelig en ammoniak oplosbaarheids misverstande uit die weg geruim. Werkende rekenaarmodelle is ontwikkel wat toekomstige ontwerpers van die oorhoofse siklus, sowel as die absorbeerder komponent in staat sal stel om voorspellings te maak. Hierdie studie het ook ‘n eerste iterasie van ‘n ontwerp moontlik gemaak.

DECLARATION

I, Eleana van Niekerk, hereby declare that:

- I understand what plagiarism is and am aware of the University's policy in this regard.
- I know that "plagiarism" means using another person's work and ideas without acknowledgement, and pretending that it is one's own. I know that plagiarism not only includes verbatim copying, but also the extensive (albeit paraphrased) use of another person's ideas without acknowledgement. I know that plagiarism covers this sort of use of material found in textbooks, journal articles, theses AND on the internet.
- "The Design and Optimization of an Absorber for an Aqua-Ammonia Absorption Heat Pump" submitted in the fulfilment in the requirement for the Master's degree in Mechanical Engineering (M.Eng) is my own original work.
- Where other people's work has been used (either from a printed source, Internet or any other source), this has been properly acknowledged and referenced in accordance with departmental requirements.
- I have not used work previously produced by another student or any other person to hand in as my own.
- I have not allowed, and will not allow, anyone to copy my work with the intention of passing it off as his or her own work.

Eleana van Niekerk

13/11/2015

Date

DEDICATION

This work is dedicated to my mother Marlene, and my grandfather (E.P. van der Merwe) who encouraged me from an early age to study and obtain a university degree, who supported me emotionally and who prayed for me through all the difficult years of studying engineering. Though neither had a degree at the time of writing, they wanted to make sure that their child/grandchild had the best education possible. Their encouragement was a strong motivation.

KEYWORDS

Absorber
Alternative energy
Ammonia/water
Aqua-ammonia
Effectiveness-NTU method
Heat generation
Heat pump
Heat transfer model
Refrigeration

ACKNOWLEDGEMENTS

I would like to thank my supervisor Prof. C.P. Storm for his time, guidance and trouble to help me complete this study, without whose academic and technical support this work would not have been possible.

I would also like to thank Cronier van Niekerk, Ph.D. candidate for giving technical and moral support when this project was in difficult stages. Each individual on the aqua-ammonia project team who gave useful insight or assistance, is thanked. This includes my under-graduate student Ané Janse van Rensburg, for taking some of the workload off me and for her practical assistance.

A special thanks to each body who provided funding for this project. In particular, the North West University as well as THRIP.

Last, but not least, the final acknowledgement goes the Lord Jesus Christ, our Creator and Saviour, for His abundant love and providence.

TABLE OF CONTENT

COVER PAGE
TITLE PAGE
ABSTACT....ii
OPSOMMING....iv
DECLARATION....vi
DEDICATION....vii
KEYWORDS....viii
ACKNOWLEDGEMENTS....ix
TABLE OF CONTENT....x
LIST OF TABLES....xiv
LIST OF FIGURES....xv
NOMENCLATURE....xvii
LIST OF SYMBOLS....xviii

1. INTRODUCTION....1-1

1.1 BACKGROUND....1-2
1.1.1 An alternative to the vapour-compression cycle....1-5
1.2 PROBLEM STATEMENT....1-5
1.3 OBJECTIVE....1-6
1.4 SCOPE AND LIMITATIONS....1-6
1.5 RESEARCH METHODOLOGY....1-6
1.6 SUMMARY OF THE DISSERTATION....1-7
1.6.1 Chapter 1: introduction....1-7
1.6.2 Chapter 2: Literature survey and existing technology....1-7
1.6.3 Chapter 3: Theoretical principles....1-7
1.6.4 Chapter 4: Theoretical Model....1-7
1.6.5 Chapter 5: results....1-7
1.6.6 Chapter 6: Droplet Experiments....1-7
1.6.7 Chapter 7: Conclusions and Recommendations....1-8

2. LITERATURE SURVEY AND EXISTING TECHNOLOGY....2-1

2.1 INTRODUCTION....2-1
2.2 GENERAL OBSERVATIONS....2-1
2.2.1 General observations about the diffusion absorption refrigerator (DAR)....2-4
2.3 COMPATIBILITY WITH METALS....2-5
2.3.1 Ammonia gas....2-5
2.3.2 Ammonium Hydroxide....2-7
2.4 THE ROLE OF CO_2 WITH REGARDS TO SOLUBILITY OF AMMONIA IN WATER....2-8

2.5 BUBBLE PUMP COMPONENT 2-9
..... 2-10
2.6 PREVIOUS RESEARCH DONE ON THE ABSORBER COMPONENT 2-10
2.6.1 Study done on a packed bed configuration absorber 2-10
2.6.2 Study done on absorption using vertical tubular bubble-absorbers 2-11
2.6.3 An experimental study done with bubble-absorption on a pre-manufactured plate heat exchanger 2-13
2.6.4 A validated numerical model for absorption in a bubble absorber using micro-channels 2-16
2.7 CONCLUDING REMARKS 2-18

3. THEORETICAL PRINCIPLES 3-1

3.1 INTRODUCTION 3-1
3.1.1 The ammonia fountain experiment 3-1
3.2 THE SOLUBILITY OF GASES IN WATER 3-3
3.2.1 Key influencing parameters 3-3
3.2.2 Henry' law for the solubility of gases 3-4
3.2.3 Pitfalls of Henry's law 3-4
3.2.4 Different measures of concentration and solubility 3-5
3.3 THE MAXIMUM SOLUBILITY OR CONCENTRATION OF AMMONIA GAS IN WATER 3-7
3.3.1 Different sources for solubility of ammonia gas in water 3-8
3.3.2 Conversions between different measures of solubility 3-11
3.3.3 Usefulness of the 'mass ratio' measure for concentration 3-14
3.3.4 Comparisons between the different sources for solubility 3-15
3.3.5 Expansion of solubility data to non-standard pressures 3-19
3.3.6 Developing a correlation for calculation of maximum solubility of ammonia in water 3-24
3.3.7 Constant concentration curves 3-26
3.4 OBSERVATIONS OF OTHER RESEARCHERS 3-28

4. THEORETICAL MODEL 4-1

4.1 INTRODUCTION 4-1
4.1.1 Choice of software used 4-1
4.1.2 Context of the absorber component 4-1
4.1.3 Motivations for this particular layout of the absorber component 4-3
4.2 ASSUMPTIONS MADE IN THE THEORETICAL MODEL 4-4
4.3 PRINCIPLES SURROUNDING THE THEORETICAL MODEL 4-6
4.3.1 The approach followed to simulate the absorber component 4-6
4.3.3 The single cylinder vs. the tube bank approach 4-7
4.3.4 Unknown parameters solved 4-9
4.3.5 The designed concentrations 4-10

4.4 EXPOSITION OF THE THEORETICAL MODEL 4-11
4.4.1 Convection heat transfer 4-11
4.4.2 External flow 4-12
4.4.3 Internal flow 4-13
4.4.4 Applying the ε-NTU-method before absorption 4-14
4.4.5 Concentration calculations 4-16
4.4.6 Calculation of the amount of heat generated due to the exothermic absorption process 4-18
4.4.7 Incorporating the heat generated into the ε-NTU method 4-20
4.4.8 The conservation of mass and energy in the system 4-22
4.4.9 Observations surrounding the theoretical model 4-23
4.4.10 Heat capacity versus enthalpy values for calculations 4-23
4.4.11 Possible improvement on the method for the incorporation of generated heat in the ε-NTU-method 4-24
4.4.12 Other thermodynamic properties and EES 2016 4-24
4.5 CONCLUDING REMARKS 4-26

5. RESULTS 5-1

5.1 INTRODUCTION 5-1
5.2 SEVEN SIMULATIONS DEVELOPED AND OPTIMIZED 5-1
5.2.1 Explanation of the seven simulation models 5-1
5.2.2 Results from the seven configurations 5-5
5.2.3 Observations regardingthe parallel configuration. 5-8
5.2.4 Further general observations surrounding the different configurations. 5-10
5.3 CONFIGURATION CHOSEN 5-12
5.4 FURTHER CHARACTERIZATIONS OF THE ABSORBER COMPONENT 5-13
5.4.1 The influence of the gas pressure on the absorber performance. 5-13
5.4.2 The influence of the cooling water inlet temperature 5-17
5.5 RESULTS FOR GIVEN INPUT VALUES FROM A SIMULATED CYCLE 5-18
5.6 MASS AND ENERGY BALANCES 5-20
5.7 GENERAL OBSERVATIONS ABOUT THE EES-MODELS OR PROGRAMS 5-20
5.8 VERIFICATION 5-21
5.9 VALIDATION 5-22

6. DROPLET EXPERIMENTS 6-1

6.1 INTRODUCTION 6-1
6.2 PURPOSE 6-1
6.3 EXPERIMENTAL METHODOLOGY 6-2
6.3.1 Experiment no. 1 6-3
6.3.2 Experiment no. 2 6-3

6.3.3 Experiment no. 3 6-4

6.4 RESULTS 6-7

6.4.1 Experiment no. 1 6-7

6.4.2 Experiment no. 2 6-8

6.4.3 Experiment no. 3 6-9

6.5 CONCLUSIONS DRAWN FROM THE EXPERIMENTS 6-11

6.6 SUMMARY OF THE DATA OBTAINED FROM THE EXPERIMENTS 6-12

7. CONCLUSIONS AND RECOMMENDATIONS 7-1

7.1 INTRODUCTION 7-1

7.2 CONTRIBUTIONS OF THIS STUDY 7-1

7.3 RECOMMENDATIONS FROM THIS STUDY 7-2

8. REFERENCES AND BIBLIOGRAPHY 8-1

REFERENCES 8-1

BIBLIOGRAPHY 8-5

9. APPENDICES 9-1

APPENDIX A 9-1

APPENDIX B 9-11

APPENDIX ON CD 9-20

LIST OF TABLES

TABLE 1.1: SUMMARIZING TABLE OF ELECTRICITY PROVISION PROBLEMS 1-3
TABLE 2.1: METAL COMPATIBILITY WITH AMMONIA GAS (CRAIG & ANDERSON (2002)). 2-5
TABLE 2.2: METAL COMPATIBILITY WITH AMMONIUM HYDROXIDE 2-7
TABLE 3.1: SOLUBILITY DATA FOR AMMONIA GAS IN WATER FROM ATSDR 3-9
TABLE 3.2: SOLUBILITY DATA FOR AMMONIA GAS IN WATER FROM AIRGAS SPECIALITY PRODUCTS 3-9
TABLE 3.3: SOLUBILITY DATA FOR AMMONIA GAS IN WATER FROM ENGINEERING TOOLBOX 3-10
TABLE 3.4: SOLUBILITY DATA FROM THREE SOURCES IN $[NH_3/(NH_3 + H_2O)]_{KG}$ 3-15
TABLE 3.5: SOLUBILITY DATA FROM THREE DIFFERENT SOURCES IN $[NH_3/H_2O]_{KG}$ 3-16
TABLE 3.6: SOLUBILITY DATA FROM THREE DIFFERENT SOURCES EXPRESSED IN MOLE FRACTION. 3-17
TABLE 4.1: RELATIONS FOR EPSILON FOR THE NTU-METHOD (ADAPTED FROM INCORPERA ET AL. (2007)) 4-15
TABLE 4.2: OUTLET TEMPERATURE DIFFERENCE DUE TO WATER VS BRINES PROPERTIES 4-25
TABLE 5.1: EXPLANATION OF THE CONFIGURATION NOMENCLATURE 5-4
TABLE 5.2: INPUT VALUES FOR COMPARISON BETWEEN DIFFERENT ABSORBER CONFIGURATIONS 5-5
TABLE 5.3: INPUT AND OUTPUT VALUES FOR THE ABSORBER COMPONENT FOR SIMULATED RESULTS 5-18
TABLE 5.4: INPUT VALUES USED FOR VERIFICATION WITH MICROSOFT EXCEL 5-21
TABLE 5.5: COMPARISON OF RESULTS YIELDED BY EXCEL AND EES FOR SOLVING THE ABSORBER PROBLEM 5-22
TABLE 6.1: RESULTS OBTAINED IN DROPLET EXPERIMENT 2 6-8
TABLE 6.2: RESULTS FOR A PRESSURE HEAD OF 3.5 CM 6-10
TABLE 6.3: RESULTS FOR A PRESSURE HEAD OF 3 CM 6-10
TABLE 6.4: SUMMARY OF PARAMETER VALUES OBTAINED FROM DROPLET EXPERIMENTS 6-12

LIST OF FIGURES

FIGURE 1.1: APPROXIMATE LIFE TIME OF BASIC TYPES OF FOOD, AS A FUNCTION OF TEMPERATURE (STOECKER, 1998) 1-2
FIGURE 1.2: SCHEMATIC DIAGRAM OF A BASIC VAPOUR-COMPRESSION REFRIGERATION CYCLE/HEAT PUMP. 1-4
FIGURE 2.1: SCHEMATIC DIAGRAM OF A BASIC DIFFUSION ABSORPTION HEAT PUMP (PENN STATE, 2015). 2-2
FIGURE 2.2: A BASIC ILLUSTRATION OF A BUBBLE PUMP (ZOHAR ET AL., 2008). 2-10
FIGURE 2.3: A BASIC ILLUSTRATION OF THE ABSORBER DESIGN OF FERNÁNDEZ-SEARA ET AL. (2005). 2-12
FIGURE 2.4: CONCEPTUAL ILLUSTRATION OF THE TWO-PHASE FLOW IN THE VERTICAL TUBES (FERNÁNDEZ-SEARA ET AL., 2005). . 2-13
FIGURE 2.5: BASIC ILLUSTRATION OF THE CORRUGATED PLATE HEAT EXCHANGER OF ALFA LAVAL (MATRIX PROCESS SOLUTIONS, 2015). 2-14
FIGURE 2.6: INTRODUCTION OF AMMONIA GAS INTO THE HEAT EXCHANGER COMPONENT (CEREZO ET AL., 2009). 2-14
FIGURE 2.7: CONCEPTUAL ILLUSTRATION OF THE CARDENAS ABSORBER DESIGN (CARDENAS & NARAYANAN, 2010). 2-16
FIGURE 3.1: AMMONIA FOUNTAIN EXPERIMENTAL SETUP (NC STATE UNIVERSITY, 2015). 3-1
FIGURE 3.2: AMMONIA FOUNTAIN PRODUCED (CREDIT: UNIVERSITY OF CALIFORNIA, BERKELEY, 2012). 3-2
FIGURE 3.3: GRAPH COMPARING DIFFERENT SOURCES FOR SOLUBILITY OF AMMONIA IN WATER IN $[NH_3/(H_2O+ NH_3]_{KG}$ 3-18
FIGURE 3.4: GRAPH COMPARING DIFFERENT SOURCES FOR SOLUBILITY OF AMMONIA IN WATER IN $[NH_3/H_2O]_{KG}$ 3-18
3-21
FIGURE 3.5: SOLUBILITY CHART FOR AQUA-AMMONIA USING 'WEIGHT PERCENT' 3-21
FIGURE 3.6: HENRY'S LAW CONSTANT AS A FUNCTION OF TEMPERATURE. 3-25
FIGURE 3.7: CONSTANT MAXIMUM CONCENTRATION GRAPH FOR AQUA-AMMONIA BETWEEN 20% AND 50% 3-27
FIGURE 3.8: CONSTANT MAXIMUM CONCENTRATION GRAPH FOR AQUA-AMMONIA BETWEEN 25% AND 55% 3-27
FIGURE 3.9: CONSTANT CONCENTRATION GRAPH FOR AQUA-AMMONIA FROM (AIRGAS SPECIALITY PRODUCTS, 2010). 3-28
FIGURE 4.1: SCHEMATIC ILLUSTRATION IN THE CROSS-SECTION OF THE BASIC ABSORBER LAYOUT (ILLUSTRATION BY THE AUTHOR)... 4-2
FIGURE 4.2: FLUID FLOW PATTERN IN A TUBE BANK (ILLUSTRATION BY THE AUTHOR). 4-8
FIGURE 4.3: SCHEMATIC ILLUSTRATION OF THE CYLINDERS IN THE ABSORBER 4-19
FIGURE 5.1: BASIC ILLUSTRATION OF THE SINGLE CYLINDER MODEL (FROM INCROPERA ET AL., 2007). 5-2
FIGURE 5.3: ABSORBER CONFIGURATION WITH 4 ROWS OF COOLING TUBES 5-3
FIGURE 5.2: SINGLE CYLINDER HEAT EXCHANGER PERFORMANCE WITH ABSORPTION 5-3
FIGURE 5.4: STRONG SOLUTION OUTLET TEMPERATURE VS COOLING WATER MASS FLOW FOR 3 ROWS AND 10 CYLINDERS 5-7
FIGURE 5.5: STRONG SOLUTION OUTLET TEMPERATURE VS COOLING WATER MASS FLOW FOR 4 ROWS AND 14 CYLINDERS 5-7
FIGURE 5.6: COOLING WATER OUTLET TEMPERATURE VS COOLING WATER MASS FLOW 5-9
FIGURE 5.7: STRONG SOLUTION OUTLET TEMPERATURE FOR A SERIES CIRCUIT WITH 3 AND 4 ROWS, RESPECTIVELY. 5-10
FIGURE 5.9: STRONG SOLUTION OUTLET TEMPERATURE FOR A SERIES-PARALLEL CIRCUIT WITH 3 AND 4 ROWS, RESPECTIVELY. 5-11
FIGURE 5.8: STRONG SOLUTION OUTLET TEMPERATURE FOR A PARALLEL CIRCUIT WITH 3 AND 4 ROWS, RESPECTIVELY. 5-11
FIGURE 5.10: THE EFFECT OF SYSTEM PRESSURE ON WARM STRONG SOLUTION OUTLET TEMPERATURE. 5-14
FIGURE 5.11: THE EFFECT OF AMMONIA PRESSURE ON WARM STRONG SOLUTION OUTLET TEMPERATURE. 5-14
FIGURE 5.12: T-ΔS DIAGRAM DEMONSTRATING STEAM BEING BLED OFF AT DIFFERENT PRESSURES IN A RANKINE CYCLE. 5-16
FIGURE 5.13: THE EFFECT OF COOLING WATER INLET TEMPERATURE ON THE STRONG SOLUTION OUTLET TEMPERATURE. 5-17

FIGURE 6.1: SCHEMATIC ILLUSTRATION OF THE DROPLET FALLING HEIGHT AND WIDTH ON TUBE (ILLUSTRATION BY THE AUTHOR). ... 6-2
FIGURE 6.2: PHOTOGRAPH SHOWING THE MILLIMETRE MARKS ON AN ALUMINIUM CYLINDER ... 6-3
FIGURE 6.3: PHOTOGRAPH SHOWING A DROPLET FALLING ON THE CYLINDER ... 6-4
FIGURE 6.4: PLASTIC TUBE WITH SERIES OF HOLES ... 6-5
FIGURE 6.6: HORISONTAL TUBE WITH HOLES AND THE PRESSURE HEIGHT IN EXPERIMENT 3 ... 6-6
FIGURE 6.5: ADJUSTABLE CLAMP USED FOR THE TUBE WITH HOLES IN EXPERIMENT NO. 3. ... 6-6
FIGURE 6.7: THE DIFFERENT SIZES OF HOLES IN THE PLASTIC TUBE ... 6-7

NOMENCLATURE

CFC's	Chlorofluorocarbons
COP	Coefficient of Performance
DAHP	Diffusion absorption heat pump
GWP	Global Warming Potential
HCFC's	Hydro-chlorofluorocarbons
HFC's	Hydro-fluorocarbons
R-717	The ASHRAE code for NH_3 (Ammonia) as a refrigerant
THRIP	Technology and Human Resources for Industry Programme

LIST OF SYMBOLS

A	Area in [m²]
α	Heat transfer convection coefficient
c_p	Specific heat at constant pressure [kJ/kg.K]
D	Diameter
h	Enthalpy [kJ/kg]
H_2O	Water (Aqua)
k	Conductivity
L	Length
M	Molecular weight
$\dot{m}$	Mass flow rate [kg/s]
μ	Viscosity
NH_3	Ammonia
Nu	Nusselt number
Pr	Prandl number
$\dot{Q}$	Energy or heat rate [kW]
$\dot{q}$	Specific energy or heat rate [kJ/kg]
R	Thermal resistance
ρ	The density [kg/m^3]
Re	Reynolds number (in general)
T	Temperature in [K], unless otherwise stated.
x	Concentration (in weight percent)

1. INTRODUCTION

There can be little doubt that modern existence of humanity has become highly dependent on heating technology, but especially refrigeration technology for cooling applications. Applications for refrigeration are indeed very wide, and can range from air-conditioning (domestic, vehicular, or large scale) to *industrial* refrigeration. The latter includes the preservation and processing of food, heat removal from petroleum, chemical and petrochemical plants, as well as various other applications (Stoecker & Jones, 1982:1).

Air-conditioning alone has become more than just a luxury in many cases. Stoecker & Jones (1982:5) point out that there has been a shift in some of the USA's population towards the so-called 'sun-belt' of the country in the 20th century, and that this would likely not have been possible was it not for air conditioning in the work place, businesses, and homes. Moreover, refrigeration has become an absolute necessity in regards to food storage and distribution. It is a well-known fact that the storage life of most foods, whether it be fruits, vegetables, meats or fish, is significantly extended by lower temperatures, as well as that of dairy products and beverages (Stoecker & Jones, 1982:6). Figure 1.1 illustrates this point for seven basic food types (apples are represented by both 6 and 8), of which the numbering on the chart corresponds as follows:

1) Chicken,
2) Lean fish,
3) Beef,
4) Bananas,
5) Oranges,
6) Apples,
7) Eggs,
8) Apples

This enables not only various industrial food-related activities, but also the general household to store up food supplies. More important even, is that refrigeration technology has enabled the world to transport, import, and export mass amounts of food over long distances and between different regions and countries. It should be obvious that these activities can be lifesaving, as it can save millions of people from starvation. Refrigeration can also balance the load between production and demand, and thus prevents waste in this regard too.

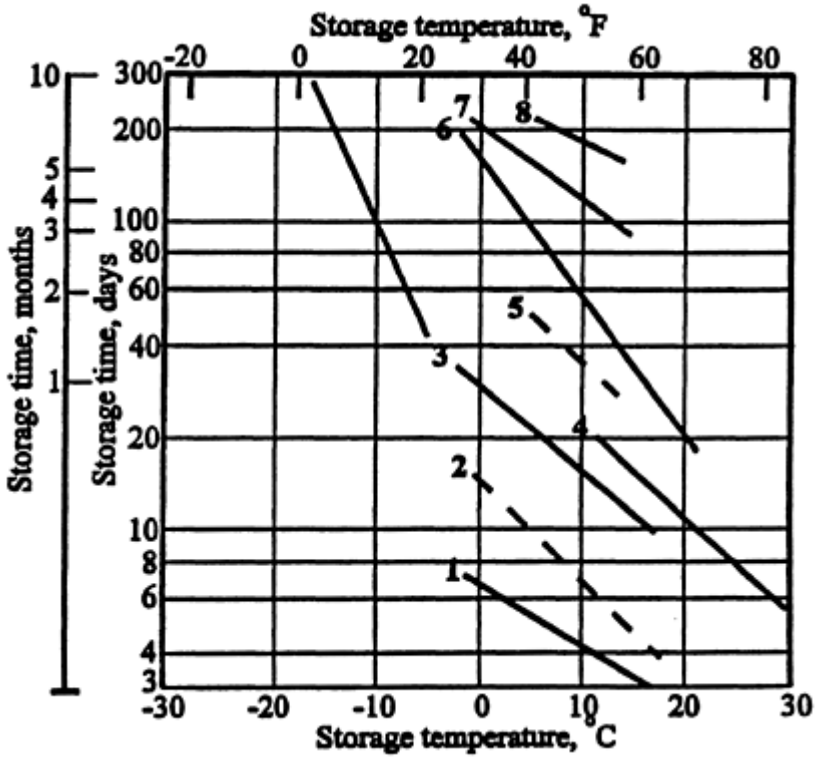

FIGURE 1.1: APPROXIMATE LIFE TIME OF BASIC TYPES OF FOOD, AS A FUNCTION OF TEMPERATURE (STOECKER, 1998)

1.1 BACKGROUND

Unfortunately, in the recent past few years, refrigeration and heating technology has been facing several challenges, in South Africa, but also internationally. In South Africa, consumers have been experiencing numerous problems with electricity supply, some coming from the national electricity provider, Eskom, and others due to factors beyond Eskom's control.

One of the largest challenges is that electricity prices have risen significantly over the last few years, and continue to do so significantly, even at the time of writing (Fin24, 2014a). Furthermore, the electricity provider has become somewhat unreliable. In 2008, for example, the country experienced a series of power outages, which forced some large mines to a temporarily halt operation, having serious economic implications (McGreal, 2008). The following table gives a summary of additional problems related to electricity provision in general, and Eskom in particular. The table is compiled from media reports.

TABLE 1.1: SUMMARIZING TABLE OF ELECTRICITY PROVISION PROBLEMS

PROBLEM DESCRIPTION	MEDIA REPORT HEADLINE	REFERENCE
The price of electricity keeps on increasing.	*Eskom welcomes decision*	Fin24 (2014c)
	More gloom amid bigger electricity hikes	Fin24 (2014b)
	Eskom gets nod to increase prices	Fin24 (2014a)
Problems with pylons.	*Power disruptions in Johannesburg after pylon theft*	News24 (2014h)
	Eskom rebuilds collapsed pylons	News24 (2014i)
Electricity provision is tight.	Switch off and save electricity - Eskom	Fin24 (2014d)
	Eskom warns of tight electricity system	Fin24 (2014e)
Strikes hinder completion at the two new coal fired power plants.	*Strike puts brakes on Medupi, Kusile*	Fin24 (2014f)
SA Municipalities owe Eskom billions of Rands	*Municipalities owe Eskom R1.4bn*	Sapa (2013)
	Municipalities owe Eskom R10bn	Pressly (2014)
Fears of total electricity blackout in SA	*Over 50% chance of total blackout, NERSA hears*	Areff (2015)
Eskom's technical infrastructure is decaying	*Eskom: Load shedding a must to avoid blackout* [Due to a coal silo that collapsed at Majuba]	Fin24 (2014g)
Eskom's technical infrastructure is decaying	*"600 MW minder krag vir dié winter"* (600 MW less power this winter). [Due to a steam boiler explosion at an Eskom power station]	De Lange (2014)

It can be seen from briefly looking at the information summarized in the above table, that the problems are serious concerning electricity provision. As in 2008, in the second half of 2014, South Africans started to experience chronic load shedding again. Bearing the above-mentioned problems in mind with regards to Eskom, it can be pointed out that the traditional

vapour-compression cycle, as efficient as it is, has one big drawback: It uses electrical power from the national grid as shaft power for its compressor. As it has been observed in the recent events unfolding in South Africa, this particular trait is becoming more and more undesirable. The diagram below (Figure 1.2) illustrates a basic vapour-compression cycle or heat pump, which is commonly used worldwide due to its high coefficient of performance (COP) and subsequent efficiency. As can be seen, the compressor component of the cycle requires shaft power from the national electricity grid, in order to do the required work.

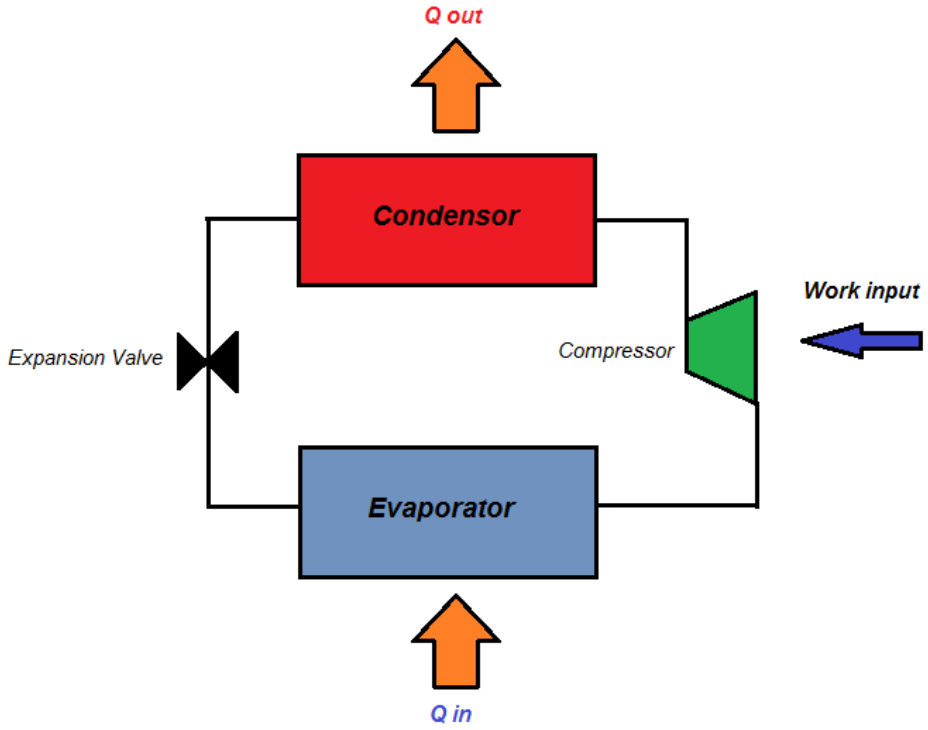

FIGURE 1.2: SCHEMATIC DIAGRAM OF A BASIC VAPOUR-COMPRESSION REFRIGERATION CYCLE/HEAT PUMP.

Furthermore, the latest concern in regards to refrigerants in general, is the impact that these substances may have on global warming or climate change. The current consensus is that the global average air and ocean temperatures are rising, and that it is due to anthropogenic factors (thus, human-made). Several “greenhouse gases” have been identified, and are typically ascribed a value for global warming potential (GWP). The Kyoto Protocol of 1997 has been issued in order to address these problems. Typically, most refrigerants today, such as HCFC’s and HFC’s are targeted for either phase-out or restriction by this protocol (Calm, 2008). A need has thus arisen to look for alternative options in regards to heating and refrigeration technology (Van Niekerk, 2013:12). It can be added, that absorption heat

pumps and processes have no ozone depletion potential (Selim & Elsayed, 1999:284), unlike the CFC's of the past, used in typical vapour-compression cycles previously.

1.1.1 AN ALTERNATIVE TO THE VAPOUR-COMPRESSION CYCLE

The question must thus inevitably be asked: Is there an alternative to the standard vapour-compression cycle, which is currently so widely in use, that can work without the electrical shaft power as source? The answer is fortunately in the affirmative. The *desorption-absorption refrigeration* (DAR) cycle/heat pump (also sometimes referred to as a diffusion absorption heat pump (DAHP)) offers an alternative, especially the variation that uses water and ammonia (H_2O & NH_3). Whereas the normal vapour-compression cycle, as describer earlier, is classified as a *work-operated cycle*, due to the compressor shaft work required, the DAR cycle is classified as a *heat-operated cycle.* This is the case because of the fact that heat input is used to mainly operate the process, by driving off ammonia vapour from water or strong solution of water and ammonia (Stoecker & Jones, 1982:328). This property of the DAR cycle also makes it a worthy substitute to investigate for future applications, because:

- This process operates/requires relatively low grade heat (80°C to 120°C).
- The critical temperature of ammonia gas (NH_3) is 132,4°C (Engineering ToolBox, 2015).
- NH_3 dissociates into N_2 and H_2 at temperatures from 170 - 200°C. Therefore, heat input temperatures approaching 200°C should be avoided (Potgieter, 2013:64).

Thus, low-grade heat can possibly be obtained from:

- The sun
- Gas: Natural gas or bio-gas
- Industrial "waste" heat.

1.2 PROBLEM STATEMENT

It has been established that the *absorber* component of the this absorption heat pump is a *critical component* of the cycle, which has the ability to inhibit the entire system and increase the cost, if not carefully designed (Fernandez-Seara *et al.*, 2005:277; Potgieter, 2013:58). This component can restrict/determine the mass flow of the entire system, thus influencing the over-all performance. Furthermore, other absorber components also considered in this study all have one or more undesirable component or characteristic present in the system,

such as a pump, a pressurized bottle of ammonia-gas, or pressure heads and pressure drops. These aspects make these absorber component variations unsuitable for the applications desired in the context of this study.

1.3 OBJECTIVE

The objective of this study is to develop a heat transfer model for the absorber component of the aqua-ammonia heat pump cycle, which will enable predictions of relevant parameters and conceptual design, as well as overcome the inadequacies mentioned above.

1.4 SCOPE AND LIMITATIONS

This study will be limited to:

- The *absorber component* of the aqua-ammonia heat pump cycle, and not be focusing on the over-all cycle in general,
- The *modelling* and *conceptual design* thereof.

However, additional information about other aspects of the cycle will be obtained when needed. The study will not be conducted in an unnecessarily reductionist manner.

1.5 RESEARCH METHODOLOGY

The method of investigation will include the following activities:

- Define the problem to be researched.
- Do a literature survey on existing knowledge in the field.
- Obtain data for solubility of ammonia in water, and expand for non-standard temperatures and pressures.
- Develop a heat transfer model to do simulations for the absorber component.
- Verify the calculations of the optimised model.
- Validate certain aspects of the design (since ammonia is toxic and not easily experimented with in the open or without placed in the complete cycle with the other components.
- Develop a design for the absorber component.

1.6 SUMMARY OF THE DISSERTATION

1.6.1 CHAPTER 1: INTRODUCTION

This chapter introduces the problem, gives background to the problem, the aim of the study, the limitations and the research methodology.

1.6.2 CHAPTER 2: LITERATURE SURVEY AND EXISTING TECHNOLOGY

This chapter gives a basic explanation working method of the aqua-ammonia heat pump, as background. The main purpose is to look at current absorbers and designs available in the open literature, and incorporate important information regarding the absorber component in general. Compatible and non-compatible metals are also considered, since ammonia and ammonium hydroxide are highly corrosive to many materials.

1.6.3 CHAPTER 3: THEORETICAL PRINCIPLES

This chapter treats important theoretical issues mainly surrounding the solubility of ammonia gas in water. Topics such as pitfalls of Henry's Law, different measures of solubility and subsequent conversion factors are treated.

1.6.4 CHAPTER 4: THEORETICAL MODEL

In this chapter, the theoretical model is presented, which enables computer simulations. The issue of heat generation is treated. The particular layout of the absorber design for this study is also set forth.

1.6.5 CHAPTER 5: RESULTS

This chapter characterizes the absorber component in general, as well as giving specific results of the simulation, by using the different computer models developed. Optimization of the absorber was also attempted.

1.6.6 CHAPTER 6: DROPLET EXPERIMENTS

In this chapter, experiments which were performed are discussed. These experiments were done to further characterize the absorber component, as well as establishing the values of certain practical parameters.

1.6.7 CHAPTER 7: CONCLUSIONS AND RECOMMENDATIONS

This chapter draws conclusions from the study done, and makes recommendations based on the conclusions and the contents.

---

2. LITERATURE SURVEY AND EXISTING TECHNOLOGY

2.1 INTRODUCTION

In Chapter 1, a brief description was given as to why there is a need to start looking at different methods of refrigeration and heating technology. The problems facing current South Africa calls for something that can be operated that would prove more reliable and available, than the current electricity grid. This chapter will look at the basic literature regarding absorption refrigeration technology, as well the absorber component specifically. Firstly, a basic discussion around the aqua-ammonia heat pump will take place, such as which variations exist, and general observations about the diffusion absorption refrigerator. A fundamental description will also be given on the operation of the diffusion absorption heat pump in general.

Secondly, consideration will be given to two surrounding aspects that have important *practical* implications. This includes the compatibility of various metals with ammonia and ammonium hydroxide, as these substances can be highly corrosive. The influence of CO_2 gas on the solubility of ammonia in water will be briefly discussed as well, since this lies at the heart of absorption. A very brief overview of a Master's degree study done on the bubble pump component will be given, as this is identified as another critical component of the cycle, besides the absorber. From there, an exposition of studies will be given which were done specifically for the absorber component in an aqua-ammonia heat pump. Different designs and models come to light as well as insights delivered from these studies. This will help establish which key ideas are currently in circulation with regards to absorber technology, as well as which parameters and factors play the most important role in absorber performance. In summary, this literature survey is designed to work from the general to the specific, in order to establish a sufficient working knowledge for the absorber component.

2.2 GENERAL OBSERVATIONS

Currently, for the aqua-ammonia heat pump, there exist two clear variations of the cycle. One variation works with a small pump, while the other variation works without a pump directly in the cycle. In the first variation, the pump transports liquid solution from the absorber back to the generator component. After the ammonia vapour has been desorbed from the solution, the weak solution returns to the absorber component and has to pass through a throttling valve, which in turn causes a pressure drop (Stoecker & Jones,

1982:329). It is thus clear that this first variation has a high and a low-pressure zone, as is the case with the vapour-compression cycle.

In the second variation, the pump is disposed of completely. In the light of the problems put forth in Chapter 1, this is obviously the desirable variation. The best example of this variation is none other than the domestic and outdoor Electrolux patented refrigerator. These refrigerators work with a heat input only, which could come from either electricity, or gas (Eastop & McConkey, 1978:617). This variation needs to be especially carefully designed, as it exploits several physical operations, such as thermal syphoning, Dalton's principle of partial pressures in the evaporator with an auxiliary gas, in order to lower the pressure of the ammonia gas, and finally, a specially designed generator which uses a bubble pump.

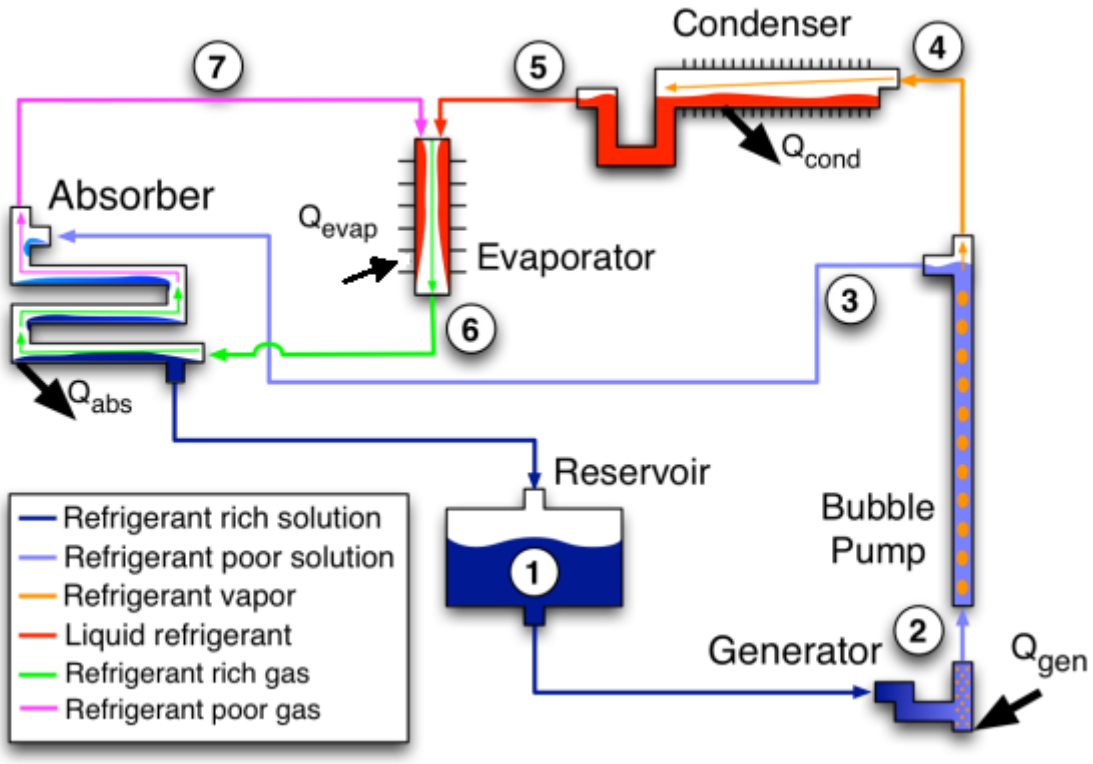

FIGURE 2.1: SCHEMATIC DIAGRAM OF A BASIC DIFFUSION ABSORPTION HEAT PUMP (PENN STATE, 2015).

In this section, a brief overview is given about the basic operation principles of the diffusion absorption heat pump. Starting at (2) in the above illustration, a strong solution of water and ammonia (collectively called aqua-ammonia) is present in a component which encompasses a 'generator' and a 'bubble pump'. Heat (alone) is added to the generator, and bubbles form as the ammonia gas starts to desorb from the solution, forming a vapour of ammonia gas.

The bubbles forming at this stage, are critically important, as they are carefully utilized in a pipe to act as a 'pump', so that volumes of liquid can be transported and lifted along with them (Van der Walt, 2012:10). Exiting the bubble pump will thus be both weak solution of aqua-ammonia as well as vapour. The now weak solution goes back to the absorber component.

The vapour is unfortunately not pure ammonia, but ammonia gas mixed with water vapour. An important component not shown in the above illustration is the rectifier. The mixture of water and ammonia vapour passes through a rectifier, which carefully strips the ammonia gas of water vapour. This is crucially important, as water vapour mixed with the ammonia gas will raise the temperature in the evaporator component, (Stoecker & Jones, 1982:348) which is undesirable for refrigeration purposes. After being stripped of water vapour, the ammonia gas travels to the condenser component where it will change phase and transform into a liquid. This process gives off heat. From the condenser the liquid travels to the evaporator. Here, the liquid is exposed to an inert gas atmosphere (typically, hydrogen or helium is used. See Potgieter (2013)). This causes the liquid to start to evaporate to form gas again, and a cooling effect is accomplished (Eastop & McConkey, 1978:617). In accordance with Dalton's Law of partial pressures, the ammonia vapour will be at a lower pressure due to the auxiliary gas, than the system pressure in the condenser. This is an essential requirement for evaporation in the DAHP (Eastop & McConkey, 1978:618) in the absence of a pump.

The ammonia gas and the auxiliary gas then travel to the absorber component, where it meets the weak aqua-ammonia solution. The weak solution absorbs the ammonia gas, in order to form a strong solution again, which returns to the generator and bubble-pump to complete the cycle. The auxiliary gas returns to the evaporator component to complete its function there (Eastop & McConkey, 1978:618). As will be seen later in this chapter, and chapters to follow, the absorption process is exothermic, and generates significant amounts of heat. Cooling this component is thus crucial, for should the absorption process happen adiabatically, the solution will heat up to a point where absorption ceases completely (Stoecker & Jones, 1982:329).

The above description is only the very basic working operation. Eastop & McConkey (1978:618) points out that many refinements need to be made in practise. One such refinement is that one or several heat exchangers can/should be added in order to enhance cycle efficiency. Stoecker & Jones, (1982:336) for example point out that it is logical to add a

regenerative heat exchanger between the (hotter) weak solution and (cooler) strong solution flows between the absorber and generator. This is because a reasonable amount of the operating cost goes into adding heat to the strong solution in the generator, and removing heat from the weak solution as it enters the absorber. As it will also be seen in subsequent chapters, the solubility of ammonia gas in water is strongly affected by temperature.

2.2.1 GENERAL OBSERVATIONS ABOUT THE DIFFUSION ABSORPTION REFRIGERATOR (DAR)

Srikhirin & Aphornratana (2002) did a general study on the DAR-system by developing a basic mathematical model for the cycle, as well as building an experimental setup – also using no moving parts. Their general observations and methodology is be beneficial to review.

It has been noticed by these researchers that most other research, which has been carried out, at that point, utilized already commercially manufactured refrigerator units. These are designed using air at ambient temperature as coolant for the system. As a correctional action, all the usual air-cooled units were replaced with components using water as the coolant. This remedial action allowed for experimental testing over a wider range of operating conditions. Furthermore, whereas hydrogen was traditionally used as auxiliary gas, helium was selected instead, for safety reasons. The following general observations stems from this study:

- Due to the lack of physical moving parts in the DAR-cycle, noise and vibration are low, and the need for maintenance is minimum.
- By keeping the cooling water temperature in a specific range, the system pressure could be controlled.
- There exists a minimum heat input value in the generator, below which no cooling effect will be produced by the cycle. This is determined by bubble-pump characteristics.
- The COP can be enhanced, according to this study, by increasing the heat input.
- Maximum performance of the system is obtained when the entire refrigerant (ammonia gas, in this case) evaporates in the evaporator.
- For the absorber component, the rate of absorption will depend on the concentration, temperature, mass flow rate and wetted surface area.

- The design of the bubble-pump component is very important, as the flow rate of the refrigerant and that of the solution must match. Non-matched conditions will result in the waste of energy.
- The study also showed that the performance of the cycle is heavily dependent on characteristics of the bubble-pump, as well as mass transfer performance of the absorber and evaporator.

In a different study, the important general observation is made, that for absorption systems, only the water and ammonia variation is capable to produce cold temperatures as low as -10˚C (Cerezo *et al*., 2009:1005).

2.3 COMPATIBILITY WITH METALS

Ammonia gas and aqua-ammonia solutions can be highly corrosive substances. Therefore, basic compatibility with metals was considered. Craig & Anderson (2002) compiled a handy text on corrosion data, which incorporated a variation of sources into one reference. Both ammonia gas as well as ammonium hydroxide was considered for compatibility. The consideration is only relatively superficial, since material science and its compatibility is a study on its own. However, this should give a basic idea, which materials can be considered, and which will not be suitable at all.

2.3.1 AMMONIA GAS

The following table summarizes basic characteristics of compatibility of ammonia gas with various groups of metals. All information is adapted from Craig & Anderson (2002:128-129):

TABLE 2.1: METAL COMPATIBILITY WITH AMMONIA GAS (CRAIG & ANDERSON (2002)).

Category of metals:	Notes on compatibility:
Carbon steels	Generally acceptable in ammonia service, except with sensitivity to stress corrosion cracking.
Alloy steels	Storage tanks made of low-alloy steel have been used for years for ammonia storage. Stress corrosion cracking

	observed as primary problem. Air contamination is problematic. The stress corrosion cracking can be inhibited by the addition of a small amount (0.1 to 0.2%) of water to storage vessels.
Stainless steels	Stainless steels show good resistance to ammonia gas.
Aluminium	Copper-free aluminium alloys have been found to generally be resistant to dry, water-free, ammonia gas. The alloys 3003 and 1100 can also withstand pure, anhydrous ammonia in the liquid phase. However, contaminants can result in pitting.
Copper	Ammonia and ammonium compounds are corrosive substances for copper alloys, and may lead to stress corrosion cracking. However, moisture and oxygen must be present for ammonia to be corrosive to copper. Substances such as CO_2 are suspected to accelerate stress corrosion cracking. Cracking will begin in surface layers under tension. Copper and the associated alloys would only be suitable for water-free ammonia gas if it remains strictly uncontaminated by water and oxygen. Aluminium bronzes are also not suitable for service using moist ammonia.
Magnesium	Ammonia normally does not attack magnesium at standard temperatures. If water vapour is present, some corrosion may take place.

Tin	Tin is generally not reactive with ammonia.
Titanium	Titanium alloys form an oxide film, which can successfully protect them against ammonia and other gases. This protection is active even above temperatures of 150˚C.
Zirconium	Zirconium is unaffected in the presence of ammonia gas, up to temperatures of 1000˚C.

It can be concluded from the above table that many metal alloys would not be capable of withstanding corrosion due to ammonia gas if there is only a slight amount of water present. Safe choices would thus seem to be the stainless steels, tin, titanium and zirconium. Choice would depend on availability and cost.

2.3.2 AMMONIUM HYDROXIDE

Ammonium hydroxide is usually found in an aqueous solution, which is aqua-ammonia. This is obviously relevant to the system and component, which is the subject of this study. The following table gives a summary of basic compatibility of ammonium hydroxide with various groups of metals. As before, all information is adapted from Craig & Anderson (2002:148):

TABLE 2.2: METAL COMPATIBILITY WITH AMMONIUM HYDROXIDE.

Category of metals:	**Notes on compatibility:**
Stainless steels	Good resistance is shown by stainless steels to all concentrations of ammonium hydroxide (up to boiling point).
Aluminium	Alloys of aluminium will initially be rapidly attacked by diluted solutions of ammonium hydroxide. However, the rate of attack seems to decrease as the pH and concentration of ammonium

	hydroxide increases.
Copper	Copper and the alloys thereof in general, suffer from instant attacks by ammonium hydroxide. However, different rates of attack on different alloys and at different conditions are observed.
Nickel	Nickel 200 can resist attack by 1% concentration solutions, but higher concentrations can cause rapid attack to the metal.
Titanium	Titanium alloys, up to and until saturation, will resist corrosion of boiling ammonium hydroxide. Hydrogen embrittlement may develop for temperatures higher than 80˚C, and a pH higher than 12.

From the above information, it can be concluded that from a general viewpoint, only the *stainless steels* remain as a viable option for building a component, which comes into contact with both ammonia gas, as well as aqua-ammonia/ammonium hydroxide.

2.4 THE ROLE OF CO_2 WITH REGARDS TO SOLUBILITY OF AMMONIA IN WATER

Due to the very nature of the binary aqua-ammonia heat pump operation, the solubility of ammonia gas in water is relevant and important. For the absorber component, it lies at the heat of its function, as ammonia gas is absorbed back into the watery solution entering the absorber (in the bubble-pump, the ammonia gas was driven off from the solution again via the addition of heat). Hales & Drewes (1979) did an important study relevant to this subject, in regards to the solubility of ammonia in water at low concentrations, which has practical implications.

In previous years, it has been noticed that a discrepancy exits between the concentration of ammonia in rainwater, and the concentration calculated using standard solubility theory. This presented a puzzle. The researchers did practical experiments to test solubility, one setup being strictly only ammonia gas and water, and the other setup having CO_2

deliberately in the system. It was found that the presence of CO_2 influenced the solubility of ammonia gas in water, and this, largely, explained the lower ammonia concentration observations, since CO_2 is present in the natural environment. This has obvious practical implications for a future experimental setup, as well as commercial production of an aqua-ammonia heat pump, which is intended to be used for an entire household. CO_2 will first need to be removed from the physical system prior to the commissioning thereof. One way to accomplish this, would be through boiling the demineralized water to be introduced in the system (as the researchers did), and flushing the pipes, tubes and components prior to the introduction of the ammonia gas. Also, should the performance of the heat pump decrease, one of the possibilities can be CO_2 contamination via in-leakage (if the system pressure allows). Additional to the above, Bogart (1981:50) points out that CO_2 contamination via atmospheric air should also be treated with great care. It is pointed out that chemical reactions taking place between water, ammonia gas and CO_2 can produce solids. One of the significant possibilities for products is ammonium carbamate. This is highly corrosive to carbon steel.

2.5 BUBBLE PUMP COMPONENT

As has been pointed out, by Srikhirin & Aphornratana (2002), that the bubble pump is also of utmost importance for the aqua-ammonia heat pump. Therefore a brief mention of a study done on this component is given. Van der Walt (2012) did an in-depth study on the bubble pump component in this cycle, in order to establish a mathematical model, and design and optimize this component. His study helped laying the groundwork for this variation of the cycle to be revived back into industry. Indeed, part of the bubble pump's function is to displace the liquid solution from the generator to the next components in the cycle. Ammonia gas is also driven off from the strong solution, forming a weak solution of aqua-ammonia, which goes back to the absorber component. The displacement of liquid is accomplished by making use of gas bubbles that form during the boiling process when heat is added. The correct two-phase flow regime(s), such as so-called slug flow, need to develop so that the slugs (of gas) can lift the liquid in fragments to the top of the pipe (which is part of the bubble pump). The basic principle is being illustrated in Figure 2.2 below.

Van der Walt (2012) developed a mathematical model for the bubble pump for this variation of the cycle, being solar-driven. Two-phase flow theory and thermo-physical properties were incorporated in the model. This enabled the general characterization of the component, as well as testing different heat transfer correlations and important optimum points of parameters at different conditions (Van der Walt, 2012:71).

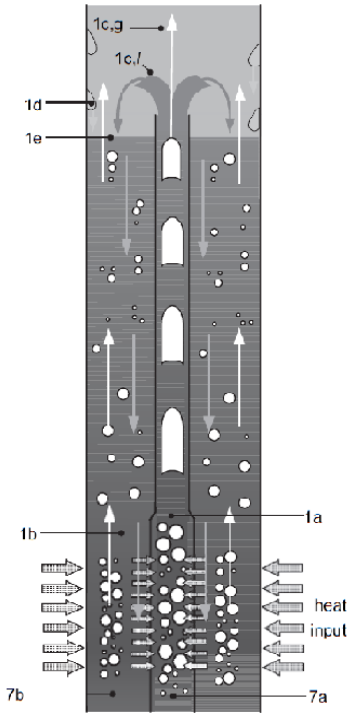

FIGURE 2.2: A BASIC ILLUSTRATION OF A BUBBLE PUMP (ZOHAR ET AL., 2008).

2.6 PREVIOUS RESEARCH DONE ON THE ABSORBER COMPONENT

Peer-reviewed and published literature about the absorber component of the aqua-ammonia heat pump is summarized below. The studies are presented in chronological sequence. Different designs for the absorber were studied by the various researchers, and different approaches taken to do the modelling thereof.

2.6.1 STUDY DONE ON A PACKED BED CONFIGURATION ABSORBER

Selim & Elsayed (1999) developed a mathematical model for an absorber component which has the design of a *packed bed*. It is pointed out by them that previous available absorber designs that were available at that time were:

- Solution cooled absorbers
- Plate-heat exchangers
- Mixed absorbers
- An absorber-evaporator unishell with a pump for recirculation
- An absorber-evaporator unishell (presumably without a pump)

However, it is further pointed out that in any absorber component, the following properties are desirable: minimal input cost, a size kept as small as possible, large enough surface area

for the heat and mass transfer to take place, and allowing enough time in the physical component for the solution and vapour to interact sufficiently.

One of the key motivations for these researchers to use a packed bed configuration was to increase the surface area on which heat and mass transfer could take place. The material of their bed enabled the breaking up of the weak solution liquid into small streams, which was believed to have achieved the mentioned goal (of enhancing the active surface area). Their study concluded that the following parameters influence the absorption process: the inlet conditions, vapour and solution flow rates, the type of material used to pack the bed with, the height of the packed bed and the volumetric heat rejection model.

However, one remark has to be made: The modellers assumed that both the ammonia gas and water vapour behave as *perfect gases*. This assumption was never explicitly justified or confirmed to be correct. It is clear from elemental thermodynamics that water vapour only behaves as an ideal gas (let alone *perfect* gas) under very special circumstances. These circumstances involve the compressibility factor, and high temperatures or very low pressures – relative to the critical temperature or critical pressure of the substance (Çengel & Boles, 2002:89-92). The system pressure was varied between 300 kPa and 600 kPa (with temperatures from the evaporator ranging from -10 to 10˚C) in one of the parametric studies. A careful analysis will have to be done to establish that this assumption is valid (even for ideal gas behaviour). This is outside the scope of this dissertation, but *perfect* gas behaviour will not be assumed correct for the purpose of this literature survey.

2.6.2 STUDY DONE ON ABSORPTION USING VERTICAL TUBULAR BUBBLE-ABSORBERS

An informative study was carried out by Fernández-Seara *et al.* (2005) on an absorber type which utilizes vertical tubes for the absorption to take place. This absorber is also of the shell-and-tube configuration, and is further classified as a bubble-type absorber. Furthermore, their model used water (and not air) as a coolant for the component. A basic demonstration was given by the authors, and is represented below: Cooling water is introduced at the top of the component outside the tubes, while both the weak liquid solution as well as the ammonia gas enters at the bottom, inside the tubes. The ammonia gas and liquid aqua-ammonia thus flow in a parallel, co-current configuration. Absorption takes place along the vertical length of the tubes, while being externally cooled by water. It is not clear

whether the experimental setup utilized a pump to overcome the pressure head, which would inevitably be present in the vertical tubes.

An important consequence of this configuration, is that a specific set of two-phase flow regimes develop in these vertical tubes, to some extent analogous to that which happens when ordinary pure substances undergo a phase change via condensation in pipes. A basic illustration of this phenomenon is given below:

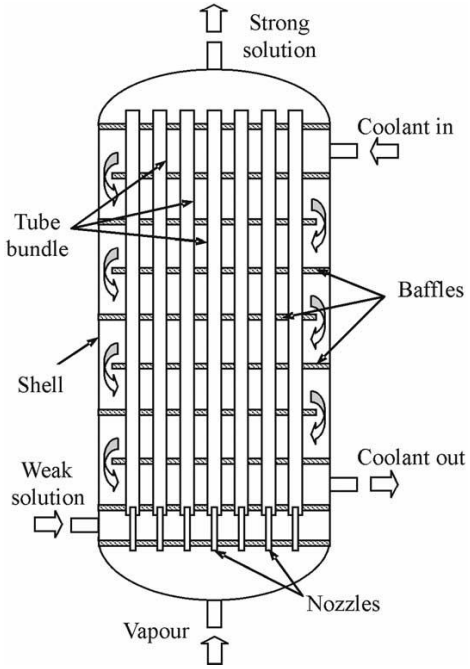

FIGURE 2.3: A BASIC ILLUSTRATION OF THE ABSORBER DESIGN OF FERNÁNDEZ-SEARA ET AL. (2005).

For obvious reasons, the introduction of this two-phase flow adds more layers of complexity to the modelling of the component and flow. The model specifically utilized for this study, treated the flow regimes of churn, slug and bubbly flow, separately.

The researchers employed an iterative methodology to solve the equations for heat and mass transfer simultaneously, and developed a specific algorithm for the iterative process. Their developed program also required specific geometry for the component as well as material thermal properties and operating conditions for the absorber component, prior to calculation.

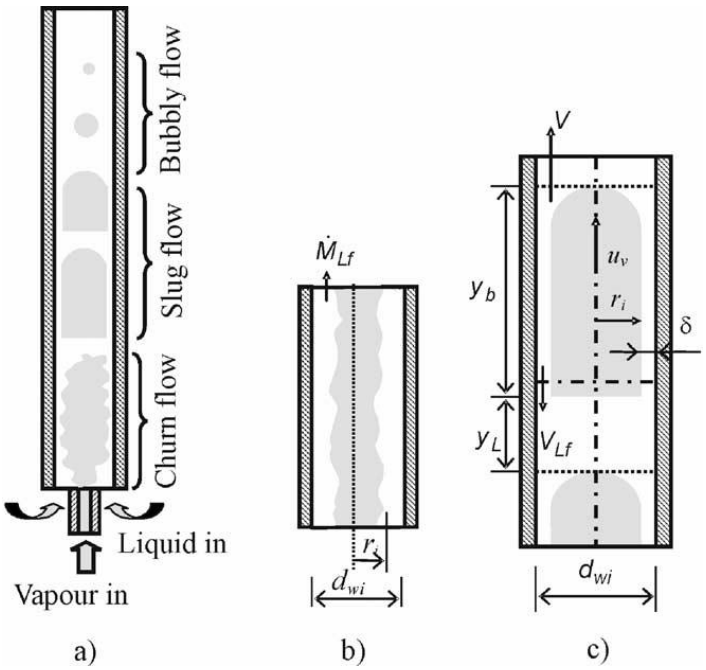

FIGURE 2.4: CONCEPTUAL ILLUSTRATION OF THE TWO-PHASE FLOW IN THE VERTICAL TUBES (FERNÁNDEZ-SEARA ET AL., 2005).

The results from the simulation showed that for this design of absorber, key design parameters include the *diameter* and the *length* of the absorption tubes. These two parameters are also closely inter-related, as an optimum tube (inner) diameter exists, which has the capability to minimize the required tube length. It was also found that the *amount* of tubes in the absorber component has a direct influence on the tube *length* required, for proper functioning.

2.6.3 AN EXPERIMENTAL STUDY DONE WITH BUBBLE-ABSORPTION ON A PRE-MANUFACTURED PLATE HEAT EXCHANGER

Cerezo *et al*. (2009) did an experimental study, which attempted to characterize the absorption process in general, but also using specifically a pre-manufactured, commercially available component for the physical absorber. The study has practical implications for both the design layout of the absorber and options available for the absorber component. It also offers insight into physical behaviour of the system and the influence of certain parameters.

Alfa Laval provided the researchers with their NB51 model, which is a corrugated plate heat exchanger. This heat exchanger is conceptually illustrated below:

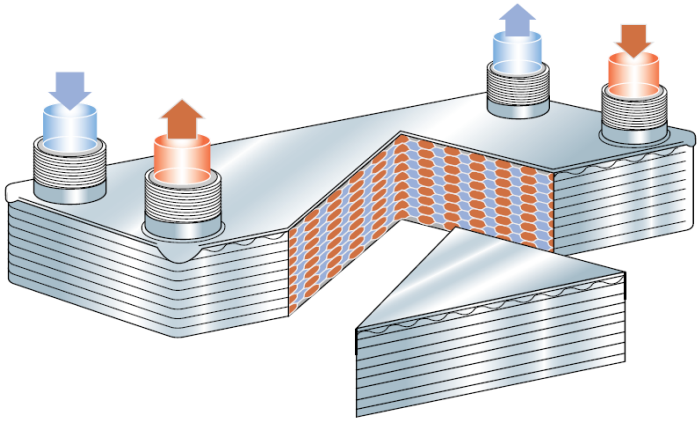

Flow principle of a nickel brazed plate heat exchanger

FIGURE 2.5: BASIC ILLUSTRATION OF THE CORRUGATED PLATE HEAT EXCHANGER OF ALFA LAVAL (MATRIX PROCESS SOLUTIONS, 2015).

As can be seen from the illustration, this is a compact type of heat exchanger, making use of wavy plates in order to maximize the heat transfer surface. The specifications further reveal that the cover plates, connections and internal plates are made of stainless steel AISI 316,

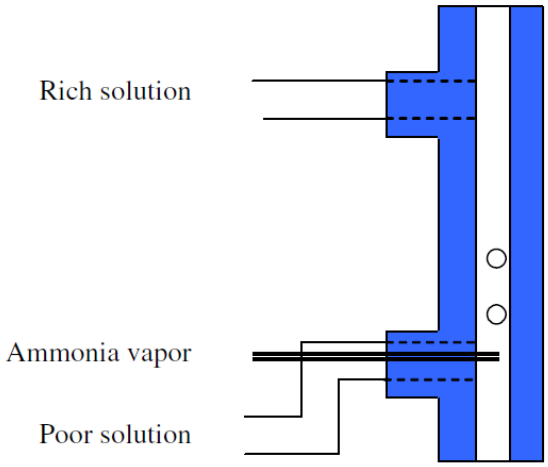

FIGURE 2.6: INTRODUCTION OF AMMONIA GAS INTO THE HEAT EXCHANGER COMPONENT (CEREZO ET AL., 2009).

and the brazing is done with nickel (more information on the nickel is not given). The absorber can withstand a maximum pressure of 18 to 21 bar, and a maximum temperature of

about 225˚C (Matrix Process Solutions, 2015). The properties make this absorber type mostly ideal for the use in an aqua-ammonia cycle. However, caution may need to be exercised nonetheless, since the brazing is done with nickel. As can be concluded from the part of this literature survey dealing with compatible materials, nickel can suffer attack from ammonium hydroxide (Craig & Anderson, 2002:148). The ammonia gas was introduced, from a pressurized bottle, to flow co-currently with the weak solution, as is illustrated below. It can further be noticed that a magnetic coupling gear pump was used in the experimental setup, as well as at least two electric heaters. Physical observations were made using Coriolis flow meters (for flow rate and density), cooling flow meters (for water flow rate), pressure gauges, and RTD temperature sensors.

The authors judged the performance of the absorption process/component in regards to the following factors:

- Mass flux in regards to absorption
- The thermal load
- The overall heat transfer coefficient
- The amount of sub-cooling that happened to the solution exiting the absorber.

One important observation made by the authors is that it was not possible to use/calculate the standard log mean temperature (which is prevalent in many heat exchanger calculations) in some of their experimental variations. This was due to the phenomenon that the outlet temperature of the cooling water (cold stream) was higher than the inlet temperature of the weak solution (hot stream). This is because of the heat generated within the aqua-ammonia solution, due to absorption. The authors developed an alternative way of calculating the log mean temperature.

The following observations were made or conclusions drawn due to this study:

- The absorber thermal load varied from 0.5 to 1.3 kW. (This will be significant for comparison later).
- Increasing the flow rate of the cooling water increased the flux of mass (NH_3) absorption.
- Increasing the pressure resulted in a *higher* mass absorption flux, and improved heat transfer for the solution. On the other hand, increasing the (inlet) solution concentration and raising temperatures of both the cooling water and aqua-ammonia solution, the effect on the first mentioned entities (mass absorption flux and heat transfer) is the opposite (thus less absorption and poorer heat transfer).

- The amount of sub-cooling of the aqua-ammonia mixture exiting the component was very low.

The authors conclude that because of this, the area of the heat exchanger was very well utilized for performing its function in the absorption process.

2.6.4 A VALIDATED NUMERICAL MODEL FOR ABSORPTION IN A BUBBLE ABSORBER USING MICRO-CHANNELS

Cardenas & Narayanan (2010) developed a one-dimensional numerical model for an absorber being also of the bubble type (contrary to falling film types). This absorber consists of micro-channels which lets the aqua-ammonia solution run counter-current to a coolant at its bottom, while having ammonia vapour/gas introduced via bubbles at the top though a porous medium. It is important to note that this particular model has been tested and validated to a reasonable extent against an experimental setup. This makes it useful for further comparison and possible validation in some areas. The model was also developed at constant pressure, which makes it even more ideal, since it will be attempted in this study to develop the variation for the aqua-ammonia heat pump which do not use a pump (thus

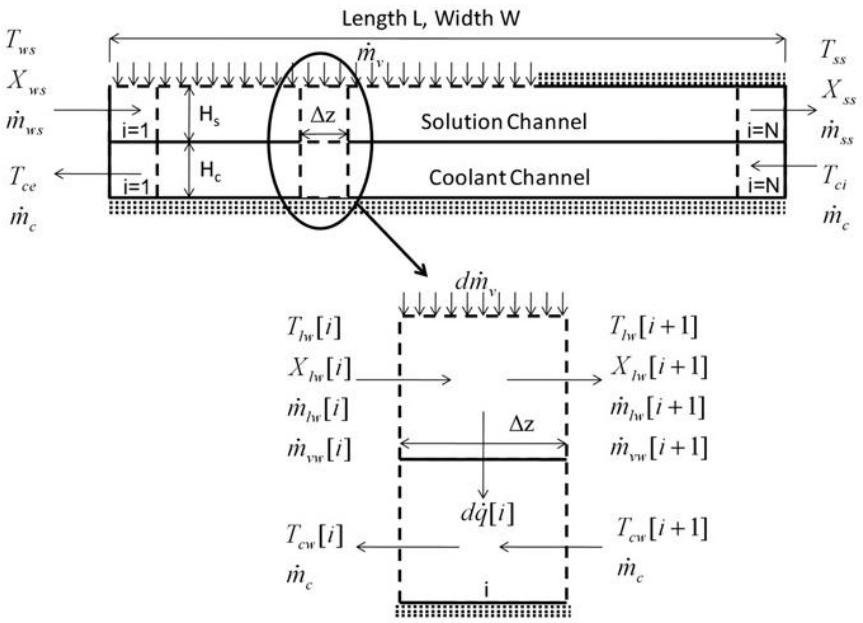

FIGURE 2.7: CONCEPTUAL ILLUSTRATION OF THE CARDENAS ABSORBER DESIGN (CARDENAS & NARAYANAN, 2010).

working at constant pressure). Following is a basic illustration of the concept for this particular absorber model:

- It is pointed out that the modelling of these components is essential, in order to facilitate optimization and good design. Also noteworthy, according to the authors, is that it can be challenging to model the absorber component, due to the fact that both heat and mass transfer need to be accounted for simultaneously.

Some important simplifying assumptions made for the theoretical model are that:

- Counter diffusion of water into the ammonia vapour is negligible.
- Steady state conditions are reached.
- Gradients perpendicular to the flow of the solution were neglected.
- The pressure drop is not significant along the channel (this was experimentally determined).
- The authors point out that the above assumptions are made by most modellers, which they have considered, and give a handy table with references as motivation for the statement.
- Moreover, Cardenas & Narayanan have utilized Engineering Equation Solver (EES) for programming their model, using the handy built-in properties especially for aqua-ammonia solutions. EES will be the preferred program used further in this study as well.
- The basic modelling technique used was to divide the channels into N amount of control volumes parallel to the flow directions of the coolant and the aqua-ammonia solution. Important known variables were introduced as boundary conditions at the entrance of the first and last control volumes of the channels. These variables include the flow rate, concentration, and temperatures of the streams.

For the experimental setup of this type of absorber, detailed engineering drawings can be found in Cardenas (2009:200). The coolant and aqua-ammonia solution channels have dimensions of 15cm by 3cm, respectively, for their length and width, while the heights differed between these two channels. The solution channel was set to 0.6 mm and that of the coolant to 1 mm. For the comparison between the numerical model and the experimental setup, the key parameters varied were the cooling water inlet temperature and the mass flow rate of the weak solution. The outcome of both the model as well as the experimental setup was measured in regards to the heat transfer rate in Watts. In some cases, it was found that the model underestimated the amount on heat transfer, for example at relatively low ammonia vapour flow rates, while for higher flow rates, the model and the experimental data

were in good agreement. The maximum difference was found to be 35% between the experimental and numerical values for the heat transferred, while the average difference between all the test data and the numerical model values was only 9%. Considering the complicated nature of fluid flow, as well as the need for empirical correlations in each heat transfer model, these results are satisfactory. More details on the validation and outcomes can be found in Cardenas (2009) and Cardenas & Narayanan (2010:1792).

After the validation has been complete, the authors performed a parametric study on several fluid flow and geometrical/physical properties of the absorber. These properties include the coolant inlet temperature, ammonia vapour injection rate, the weak aqua-ammonia solution flow rate, the physical channel height of the absorber and the number of injection sections for the ammonia vapour. Important conclusions drawn from the results are:

- Should a fix mass flow rate for ammonia vapour be chosen, there exists an optimal flow rate for the weak solution of aqua ammonia, so that complete absorption takes place.
- Absorption rate is significantly enhanced by introducing a lower inlet temperature for the coolant.
- An optimal value for the channel height of the aqua-ammonia solution exits, whereby maximum absorption will take place. Beyond this point, incomplete absorption starts to take place.

The study of Cardenas & Narayanan is thus very valuable for general characterization of the absorber component of this particular kind or type, and should preferably be consulted when designing an absorber component for an aqua-ammonia heat pump, as all aspects could not be mentioned here.

2.7 CONCLUDING REMARKS

It is clear from the above survey of literature that the absorber is a component which can bring quite a variety of different engineering principles together. This is already despite the fact that the DAHP tends to be more complex in nature than the general vapour-compression cycle. It is also clear from both Chapters 1 and 2, that the absorber component is crucial in the DAHP-cycle.

It is noticed that most researchers have moved from an air-cooled component to a water-cooled absorber, contrary to designs of earlier years. This will be done in this study as well.

Two categories of absorbers exist in the literature: a falling thin film type and a bubble type. The falling thin film is of aqua-ammonia solution, while the bubble type is of the ammonia gas bubbles forming in the weak solution. The bubbles have two-phase flow regimes consequently. Three of the four studies for absorber design considered bubble-type designs, thus relatively little literature appear to be in circulation in regards to thin film absorbers.

It is also clear that material selection may be a challenge, as relatively few metals will be compatible with both ammonia gas as well as ammonium hydroxide. Standard copper components such as tubes found in typical heat exchangers can thus not be used in this case.

---

3. THEORETICAL PRINCIPLES

3.1 INTRODUCTION

This chapter will look at some of the basic fundamental principles surrounding the absorption and solubility of ammonia gas into water. It should be obvious that the absorption process lays at the heart of the absorber component, hence its importance and discussion in this chapter.

3.1.1 THE AMMONIA FOUNTAIN EXPERIMENT

A fascinating and relevant experiment to perform with ammonia gas and water, is one named the 'ammonia fountain'. A basic setup for this experiment is given in Fig. 3.1 below:

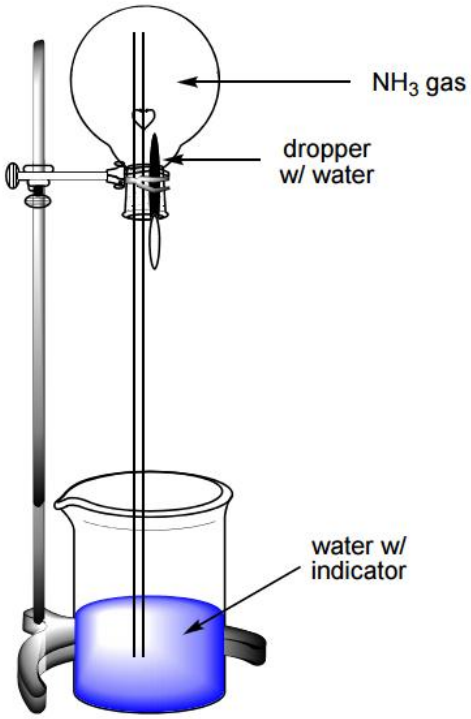

FIGURE 3.1: AMMONIA FOUNTAIN EXPERIMENTAL SETUP (NC STATE UNIVERSITY, 2015).

Dry ammonia gas is introduced into an inverted flask which is sealed off (NC State University, 2015). The process for generating the ammonia gas will not be discussed here. A 2-hole stopper, medicine dropper, 2-L beaker is set up as shown in the above illustration. The beaker is filled with about 1.5 litres of water, and a base indicator is added to the water.

The medicine dropper is filled with water, and put back into the hole-stopper. A small amount of water is squirted into the flask, and the experiment starts.

FIGURE 3.2: AMMONIA FOUNTAIN PRODUCED (CREDIT: UNIVERSITY OF CALIFORNIA, BERKELEY, 2012).

What is observed is, that the moment the ammonia gas comes into contact with water, a physical fountain is formed from water rigorously flowing into the top flask (shown by the arrow). This is despite the fact that the upper flask is situated above the water, and that a pressure height needs to be overcome.

This basic experiment demonstrates that ammonia gas is extremely soluble in water (NC State University, 2015). The fountain is caused by the ammonia gas is absorbed into the water, which leaves a significantly lower pressure in the upper flask of the setup. The atmospheric pressure pushes the water into the upper flask, due to the vacuum that forms (University of California, Berkeley, 2012).

This experiment showing the ability of ammonia gas to be absorbed into water, demonstrates the principle on which the absorber component basically works. It also shows that if designed correctly, with the right operating conditions, this affinity of ammonia gas for water, can actually do work in the physical sense. Work is defined as the force x distance (in the direction of the force) and in the illustration above, it can be seen that a force was exerted on the water over a distance to the top flask. Thus, work was done on the water.

3.2 THE SOLUBILITY OF GASES IN WATER

From the above information, it becomes clear that the solubility of gases in general, and ammonia gas in water, in particular, needs to be further investigated. It is evident in the literature that there are two main parameters that affect the solubility of any gas in a liquid solution: pressure and temperature (Kotz et al., 2009:626). Other secondary parameters which also play a role, are the presence or absence of other solutes (Schmidt-Nielsen, 2010:9). This is the reason why the role of CO_2 concerning ammonia-solubility in water has been investigated in Chapter 2.

3.2.1 KEY INFLUENCING PARAMETERS

The effects of pressure and temperature can be readily illustrated by common household operations:

Canned cold beverages are most often carbonated with CO_2 gas to give certain effects. These cans are physically pressurised. When the can is open, the solubility of the CO_2 in the drink decreases as the pressure is relieved, and the CO_2 appears as bubbles in the fluid.

Thus, in general the solubility of a gas increases when pressure increases (Kotz *et al*., 2009:626).

On the other hand, increasing the temperature has the opposite effect. This can be easily observed when a pot of water is heated on a stove. Long before the boiling point of water is reached, bubbles start to form visibly in the water. These are from gases which were dissolved in the water, but of which the solubility has now decreased due to the temperature increase (Schmidt-Nielsen, 2010:10). Furthermore, the chemical principle of Le Chatelier also dictates that the solubility of gases in water will change (decrease) with an increase in temperature (Kotz *et al*., 2009:627). These details will not be discussed here.

3.2.2 HENRY' LAW FOR THE SOLUBILITY OF GASES

A general law which normally describes gas-solubility behaviour, is called Henry's law. This law basically states that the solubility of a gas in a solvent or liquid is directly proportional to the (partial) pressure of that gas outside of the solvent (Kotz *et al*., 2009:626). It can be quantified as follows:

$$c = \frac{P}{k_H} \qquad [3\text{-}1]$$

Where *c* is the concentration, *P* is the partial pressure and k_H is the Henry's law constant. This law can be potentially helpful in determining the approximate maximum concentration or solubility of ammonia gas in water under a given set of pressures and temperatures. Where then, is the influence of temperature in the above equation? The answer lies in the constant. As it will be shown later, the Henry's law constant is not a constant in the true sense of the word, but is highly temperature dependent (see 'pitfalls of Henry's law' below). Le Chatelier's principle has also been mentioned earlier in this regards, as it comes into play with temperature change.

3.2.3 PITFALLS OF HENRY'S LAW

Smith & Harvey (2007) point out that there are important common pitfalls to avoid when using Henry's law, and the subsequent constant identified above. Important points from their article are:

- The Henry's law constant is most certainly not a constant with regards to temperature. Using a Henry's law constant at a temperature of a mere 10K too high

or too low, can lead to serious errors. Henry's law constant has a dependence on temperature which is non-linear, and is thus not truly constant in the literal sense of the word.

- Because of the fact that Henry's law is used in a wide variety of fields, the constant appears in different units. It can additionally be added that this would also be a consequence of the wide variety of measures of concentration (discussed in detail in a following section). Using a reported value for the Henry's law constant may be incorrect, if the units do not match the measure of concentration in Eq. 3-1. This can lead to serious errors. Thus, when looking up Henry's law constants, special care needs to be taken in order to make sure the value is applicable where it is about to be used.
- Henry's law is sometimes defined as:

$$C = k_H^*.P \qquad [3\text{-}2]$$

- This leads to the Henry's law constant k_H^* in Eq. 3-2 basically being the reciprocal of the definition stemming from Eq. 3-1. Smith & Harvey (2007:37) refers to these two forms as the "volatility form" and the "solubility form", respectively.
- Kotz et al. (2009:627) points out that because ammonia gas produces some NH4+ and OH- ions in water, the predictions of Henry's law may not be completely accurate. However, as will be seen, only approximations will be needed for the work done later in this study to begin with, and Henry' law will be used to characterize general behaviour and solubility. However, in the above light, the work done in regards to solubility at non-standard pressures will only be approximations. It is noted, however, that technical literature still give values for the Henry's law constant for ammonia gas in water at different temperatures, despite above mentioned restraints (see for example: ATSDR (2004:116), Incropera et al. (2007:953)). Thus, it is concluded that the approach that will be taken cannot be completely unacceptable or incorrect either.

3.2.4 DIFFERENT MEASURES OF CONCENTRATION AND SOLUBILITY

As with any physical quantity, it is of utmost importance that the units be understood correctly. Upon any small investigation of solutions, it will become abundantly clear that there are very different measures of solubility or concentration. These can often become quite confusing. When applying Henry's law, it is crucial to know which measure of solubility

or concentration is being dealt with. Kotz *et al*. (2009:618) gives the following handy introductory information and common measures of solubility:

- Concentration expressed as molality (mol/kg):

$$\frac{amount\ of\ solute\ (in\ mol)}{total\ mass\ of\ solvent\ (in\ kg)}$$

- Concentration expressed as a mole fraction (-):

$$\frac{n_A}{n_A + n_B + n_C + \cdots}$$

[3-3]

The above measure of concentration is thus the amount of solute in moles, as a fraction of the total amount in moles of the mixture.

- Concentration expressed as a 'weight percent':

$$\frac{mass\ of\ A\ (in\ kg)}{mass\ of\ A + mass\ of\ B + mass\ of\ C + \cdots (in\ kg)} \times 100\%$$

This measure of solubility is quite common in products used by the general public (Kotz *et al*., 2009:619). It is the measure used by the NH_3-H_2O external procedure utilized by the Engineering Equation Solver (EES) software mentioned in Chapter 2. Epithets such as 'mass fraction' have also been encountered for this particular measure of solubility, such as in Herold *et al*. (1996). The above measures of concentration are not the complete picture either. For example, added to the above could be the parts per million (ppm) measure, which is for very small quantities (Kotz *et al*. 2009:619).

It can already clearly be seen why confusion can arise regarding concentration and solubility. The above measurements already show that there are volumetric measurements (mole fraction), gravimetric measurements (weight percent), and a measurement which mixes volumetric and gravimetric bases (molality). However, even this is not the end of the concentration measurement road. Molarity (not the same as *molality*, as defined previously) is another measurement encountered, which is defined as *the amount of moles of solute per litre of solution* (Kotz *et al*. 2009:618).

Furthermore, Schmidt-Nielsen (2010) points out several ambiguities, even with the above information already given. For example, simply giving a concentration in percentage (%) (for gases or solids dissolved in a solution) can mean more than one thing, as there is not a

standard convention for how percentage is ascribed (Schmidt-Nielsen, 2010:591). This possible ambiguity is not difficult to perceive. For example, does a "2%-solution" mean:

- 2 g substance and 98g water (in a given mixture)?
- 2 g substance for every 100 g water?

Likewise, Schmidt-Nielsen (2010:592) points out that even the term 'weight percent' can be equally problematic. Indeed, when data was searched for the maximum solubility of ammonia gas in water, it was found that different measurements for percentage based on weight (thus gravimetric measurements) exist. The different sources will be given later. However, to demonstrate the difference, one source gave the standard 'weight percent' which was defined earlier in this section (that is, a percentage of the mass of a substance A (ammonia), divided by the total weight of the mixture (the ammonia + water combined)). Another source gave the solubility as 'mass of ammonia per mass of water'. These two are not the same, but can both be expressed as a percentage of weight, since percentage simply means the amount of parts per hundred parts. The above exposition of different measures of solubility was given in order to eliminate any possible misunderstanding or unit errors, when it comes to aqua-ammonia solutions. When the term 'weight percent' is applied further in this document, it will be the measure that has been described above specifically.

3.3 THE MAXIMUM SOLUBILITY OR CONCENTRATION OF AMMONIA GAS IN WATER

It has already been noted by Srikhirin & Aphornratana (2002) in Chapter 2, that the absorber performance (in regards to rate of absorption) depends on a number of parameters or characteristics. One of these parameters is the concentration of the solution in the absorber component. The maximum amount of ammonia gas that can be absorbed into water (at a given temperature and pressure) is discussed further in this chapter. Cardenas & Narayanan (2010) who did complex mass transfer calculations, continually noticed that a 'saturation concentration' exists (Cardenas & Narayanan, 2010:1794). Out of the context of their study, there seems to be a maximum concentration of (or maximum solubility for) ammonia gas in water. However, they never elaborated on this parameter. Complex mass transfer calculations will not be done in this study. Rather, a macroscopic approach will be followed which can hopefully give a good overall estimation of concentration behaviour, since the main focus of the mathematical model developed will be heat transfer, not mass transfer. However, the concentration cannot be ignored either, as was shown in the literature survey

of Chapter 2. From these considerations, a macroscopic approach seems to give the best trade-off. The methodology for developing this macroscopic approach will be as follows:

- Obtain values for the solubility of ammonia gas in water from different sources, at a range of different temperatures.
- Develop ways to reconcile some of the different measures of solubility.
- Compare the different sources with each other for verification.
- Expand the work to non-standard pressures (using Henry's law).
- Develop a way to calculate the maximum concentration at any given temperature or pressure.

3.3.1 DIFFERENT SOURCES FOR SOLUBILITY OF AMMONIA GAS IN WATER

Three different sources were consulted for solubility of ammonia gas in water. The need for this step was recognised when it became clear that the Engineering Equation Solver (EES) does not have a restriction with regards to solubility limits. It has been mentioned earlier, that doing heat transfer calculations with EES is preferable, since it contains libraries of thermos-physical properties in general. Additionally even more so, since it contains specifically a handy procedure for aqua-ammonia mixtures, which can return various needed properties. However, it has been noticed that the EES routine cannot give the user the maximum concentration aqua-ammonia which is possible at a given temperature and pressure. This leaves the designer of an aqua-ammonia cycle or component at risk of defining conditions which are physically unrealistic. For this reason, external sources were consulted and incorporated into the heat transfer model developed in EES (see Chapter 4).
An important point to make is, that values given for solubility in the sources will be taken as the maximum concentration possible for a particular temperature and pressure set (in equilibrium conditions). This is not explicitly stated, but seems to be implicitly implied. (Trends of pressure and temperature conform to the principles outlined earlier, such as a decrease in solubility with temperature increase, etc.) Furthermore, the values obtained for the solubility (of ammonia in water) will be assumed to be experimentally determined.

The three different sources that were used for obtaining data are:

- Agency for Toxic Substances and Disease Registry (ATSDR, 2004). This source is from the U.S. Department of Health and Human Services, and provides a number of handy data sheets on several substances, including ammonia gas.
- Airgas Speciality Products (2010). Airgas Speciality Products is a company that supplies a number of chemicals, which includes industrial ammonia and aqua-

ammonia. They provide a range of sources on ammonia and aqua-ammonia, including safety guidelines. Solubility data is also available from their website.

- Engineering Toolbox (2014). The Engineering Toolbox website is a handy website for engineers and any person wishing to obtain a quick but reliable reference to technical data.

The data from the above mentioned three sources will be used to complement EES calculations with regards to solubility limits.

The solubility data is presented below as it is obtained from the above sources. It is noticed that all three sources' data sets do not span over the same temperature range. The available data was utilized 'as is'. All three sources gave the data at the standard pressure of 101 kPa. The following data was obtained from the Agency for Toxic Substances and Disease Registry (ATSDR, 2004):

TABLE 3.1: SOLUBILITY DATA FOR AMMONIA GAS IN WATER FROM ATSDR

ATSDR (USA)		
TEMPERATURE		**Solubility** @ 101 [kPa]
[^{o}C]	**[K]**	**[NH_3 /(NH_3 + H_2O)]$_{kg}$**
0,0	273,150	**44,9%**
5,0	278,150	**-**
10,0	283,150	**-**
15,0	288,150	**38,0%**
20,0	293,150	**33,6%**
25,0	298,150	**34,0%**
30,0	303,150	**28,0%**
35,0	308,150	**-**
40,0	313,150	**-**
45,0	318,150	**-**
50,0	323,150	**18,0%**

It can be seen that data points were not available in neat, continuous intervals. Nonetheless, the information can be used for comparison where it is available. The following data was obtained from Airgas Speciality Products (2010):

TABLE 3.2: SOLUBILITY DATA FOR AMMONIA GAS IN WATER FROM AIRGAS SPECIALITY PRODUCTS

Airgas Speciality Products			
TEMPERATURE			**Solubility** @ 101 [kPa]
[^{o}F]	**[^{o}C]**	**[K]**	**$[NH_3/(NH_3 + H_2O)]_{kg}$**
32	**0,0**	273,150	**46,0%**
50	**10,0**	283,150	**41,0%**
68	**20,0**	293,150	**35,0%**
86	**30,0**	303,150	**29,5%**
104	**40,0**	313,150	**24,5%**
122	**50,0**	323,150	**19,5%**
140	**60,0**	333,150	**15,0%**
158	**70,0**	343,150	**11,0%**
176	**80,0**	353,150	**6,5%**
194	**90,0**	363,150	**3,0%**
212	**100,0**	373,150	**0,0%**

The above data set was given in degrees Fahrenheit. When subsequent conversion was done to degrees Celsius, it was noticed that the intervals for this measure of temperature was neatly spaced. It is also noticed that this data set gives the widest temperature range of all three data sets. The following data was obtained from the Engineering Toolbox (2014):

TABLE 3.3: SOLUBILITY DATA FOR AMMONIA GAS IN WATER FROM ENGINEERING TOOLBOX

Engineering Toolbox		
TEMPERATURE		**Solubility** @ 101 [kPa]
[^{o}C]	**[K]**	**$[NH_3 / H_2O]_{kg}$**
0,0	273,150	**90,0%**
10,0	283,150	**70,0%**
20,0	293,150	**52,5%**
30,0	303,150	**41,0%**
40,0	313,150	**32,0%**
50,0	323,150	**24,5%**
60,0	333,150	**17,0%**

3.3.2 CONVERSIONS BETWEEN DIFFERENT MEASURES OF SOLUBILITY

Naturally, the reason for seeking different sources of solubility data, is so that comparisons can be drawn, and that the data of one source can be verified by another. However, on closer investigation, it can be seen that not all three sources give the solubility in the same measure. The two measures found are both gravimetric percentages, but still quite different. They are the following:

- Two of the sources give the solubility or concentration in the standard weight percent:

$$\frac{kg\ NH_3 gas}{kg\ (H_2O + NH_3)\ mixture}$$

which can also be written as:

$$\left[\frac{NH_3}{NH_3 + H_2O}\right]_{kg}$$

[3-4]

- The third source gave the solubility in mass of solute per mass of solvent. This means, for each kilogram of water (solvent), there will be a certain x-grams or kilograms of ammonia gas (solute) dissolved. This can also be written as:

$$\left[\frac{NH_3}{H_2O}\right]_{kg}$$

[3-5]

The difference between these two measures is not trivial, and will introduce a significant error should they be confused. Nowhere in the literature studied were conversion factors found to switch over between these two measures. This is possibly due to the fact that the second measure is not often encountered. Due to this deficiency, two sets of conversion factors will be derived below.

- Let the notation $\mathrm{NH_3}$ and $\mathrm{H_2O}$ each denote one unit of substance species in either kilograms (gravimetric) or moles (volumetric).
- Let:

$$x = \left[\frac{NH_3}{NH_3 + H_2O}\right] \text{ and } c = \left[\frac{NH_3}{H_2O}\right]$$

1. From $\left[\frac{NH_3}{NH_3+H_2O}\right]$ to $\left[\frac{NH_3}{H_2O}\right]$:

$$1 = \frac{NH_3 + H_2O}{NH_3 + H_2O} = \frac{NH_3}{NH_3 + H_2O} + \frac{H_2O}{NH_3 + H_2O}$$

[3-6]

$$\therefore \frac{H_2O}{NH_3 + H_2O} = 1 - \frac{NH_3}{NH_3 + H_2O}$$

[3-7]

Thus, it logically follows from the above equations that:

$$\frac{NH_3 + H_2O}{H_2O} = \left(1 - \frac{NH_3}{NH_3 + H_2O}\right)^{-1}$$

[3-8]

and:

$$\frac{NH_3}{(NH_3 + H_2O)} \times \frac{(NH_3 + H_2O)}{H_2O} = \frac{NH_3}{H_2O}$$

[3-9]

and that is the desired measure.

By substituting Eq. 3-8 in Eq. 3-9, it can clearly be seen that the conversion factor is:

$$factor\ A = \left(1 - \frac{NH_3}{NH_3 + H_2O}\right)^{-1}$$

[3-10]

Thus, to convert from $\left[\frac{\mathrm{NH_3}}{\mathrm{NH_3+H_2O}}\right]$ to $\left[\frac{\mathrm{NH_3}}{\mathrm{H_2O}}\right]$:

$$c = x \times (1 - x)^{-1}$$

[3-11]

Or put differently:

$$\left[\frac{NH_3}{H_2O}\right] = \left[\frac{NH_3}{NH_3 + H_2O}\right] \times factor\ A$$

[3-12]

From $\left[\frac{\mathrm{NH_3}}{\mathrm{H_2O}}\right]$ to $\left[\frac{\mathrm{NH_3}}{\mathrm{NH_3+H_2O}}\right]$:

In order to make the above conversion, it is logical that the following is necessary:

$$\frac{NH_3}{H_2O} \times \frac{H_2O}{NH_3 + H_2O} = \frac{NH_3}{NH_3 + H_2O}$$

[3-13]

It is obvious that Eq. 3-7 cannot be used in Eq. 3-13, since that would require that the outcome desired is needed to obtain the outcome desired, which is not possible. Note further, that in the original measure which is being converted from, which is $\left[\frac{NH_3}{H_2O}\right]$, H_2O is used as reference. Thus, divide the desired expression for conversion by the reference substance, both in the numerator as well as the denominator, or:

$$\frac{H_2O}{NH_3+H_2O}\times\frac{\frac{1}{H_2O}}{\frac{1}{H_2O}}=\frac{\frac{H_2O}{H_2O}}{\frac{NH_3}{H_2O}+\frac{H_2O}{H_2O}}$$

[3-14]

$$\therefore\frac{\frac{H_2O}{H_2O}}{\frac{NH_3}{H_2O}+\frac{H_2O}{H_2O}}=\frac{1}{\frac{NH_3}{H_2O}+1}$$

[3-15]

Thus, from the above, it follows that:

$$\frac{H_2O}{NH_3+H_2O}=\frac{1}{\frac{NH_3}{H_2O}+1}$$

[3-16]

Thus, the conversion factor in this case is:

$$factor\ B=\left(\frac{NH_3}{H_2O}+1\right)^{-1}$$

[3-17]

Thus, to convert from $\left[\frac{\mathrm{NH_3}}{\mathrm{H_2O}}\right]$ to $\left[\frac{\mathrm{NH_3}}{\mathrm{NH_3+H_2O}}\right]$:

$$x=c\times(c+1)^{-1}$$

[3-18]

Or put differently:

$$\left[\frac{NH_3}{NH_3+H_2O}\right]=\left[\frac{NH_3}{H_2O}\right]\times factor\ B$$

[3-19]

These two conversion methods will be used to reconcile the sources for solubility, as well as additional calculations, as will be seen later. It is pointed out that these two conversion factors developed can be used to convert either gravimetric measures or volumetric measures where the unit of substance is moles. For this study, only gravimetric measures needed conversion.

In addition to the above, solubility values may be found in the literature being expressed as the volumetric *mole fraction*, which need to be converted to a *weight percent*, or vice versa. For these conversions, Bogard (1981:442) gives handy conversion equations. These are given here for the sake of completeness, since the subject of different measures and conversion is treated. It is noted that Fernandez-Seara *et al.* (2005:280) used the volumetric mole fraction for their absorber calculations.

According to this source, these are given below.

- Let the following be:

  x = gravimetric 'weight percent' $\left[\frac{\mathrm{NH_3}}{\mathrm{NH_3+H_2O}}\right]_{\mathrm{kg}}$

  m = the mole fraction $\left[\frac{\mathrm{NH_3}}{\mathrm{NH_3+H_2O}}\right]_{\mathrm{mole}}$

  φ = molecular weight relation between ammonia and water: $\frac{\mathrm{M_{NH_3}}}{\mathrm{M_{H_2O}}}$ which = 0.94533

Then:

$$x = 100m/\left[m + \frac{100 - m}{\emptyset}\right] \qquad [3\text{-}20]$$

And:

$$m = 100x/[x + (100 - x) \times \emptyset] \qquad [3\text{-}21]$$

The above then completes this section on conversion factors between different solubility or concentration measures. This will enable further work done on this subject.

3.3.3 USEFULNESS OF THE 'MASS RATIO' MEASURE FOR CONCENTRATION

The question can be asked: if the measure for concentration which is $\left[\frac{NH_3}{H_2O}\right]_{kg}$ was not so frequently encountered in the literature studied in this study, why was a conversion factor developed to convert to it? Besides the fact that one source was found to be in this measure, the answer is that this measure can potentially be quite useful, practical and is essential in at least one set of calculations. To be more specific:

- As it will be seen in the following sections, it was discovered that certain solubility calculations could only be done with this gravimetric measure, and not the 'weight percent' measure.
- A practical consideration is the following: suppose an aqua-ammonia cycle or heat pump is to be commissioned. A certain concentration for strong solution is desired, but that concentration is not available on the market as ammonium hydroxide. The operators commissioning the system can then easily calculate, using this measure (which is basically a mass ratio), of how much of ammonia and water is needed. This is because this measure literally gives the mass of ammonia needed for each kilogram of water.
- Obviously, the conversion factors would be valid for more than just ammonia and water. It can basically be used for any binary-substance system, so the conversion

factors can possibly enable calculations in other fields as well. To elaborate, it is noted that this 'mass ratio' is in essence very much like an air-fuel ratio. In other words, just as an air-fuel ratio of 7:1 would mean 7 units of air for every unit of fuel, the 'mass ratio' under discussion would mean x units of ammonia for every 1 unit of water.

3.3.4 COMPARISONS BETWEEN THE DIFFERENT SOURCES FOR SOLUBILITY

Now that all three sources could be converted to the same measure of solubility, or measure of concentration, comparisons were made. Data was read into Excel spread sheets, for each source, and converted to the different measures of solubility or concentration. Following below are tables with the three different sources. Three tables represent three of the different measures found. Two of these three measures (the gravimetric ones) will be used in further calculations, while the mole fraction measure is given for the sake of completeness – to have at least one volumetric measure.

Furthermore, the two gravimetric measures each contain a column named 'reconciled data'. This column was formed by taking the average between the three sources at specific temperature intervals (e.g. 10, 20, 30 [˚C] etc.]. Between these temperature intervals (e.g. at 15, 25, 35 [˚C] etc.), average values were calculated for intermediate temperature values. This is a form of linear interpolation. Outlier values were rejected so that the profile was not disrupted. Moreover, in the case where only one source gave a value at a specific temperature, that value was used 'as is', so that the average formula don't record a zero and compromise the values. Thus, the 'reconciled data' will be used as the final solubility values and solubility profile for aqua-ammonia. Below are the tables containing the data:

TABLE 3.4: SOLUBILITY DATA FROM THREE SOURCES IN $[NH_3/(NH_3 + H_2O)]kg$

Gravimetric Solubility Comparison @ 101,325 kPa				
$[NH_3/(NH_3 + H_2O)]_{kg}$				
TEMPERATURE	**Airgas**	**ATSDR**	**ENG. Toolbox**	**Reconciled data**
[^oC]	[-]	[-]	[-]	[-]
0,0	**46,00%**	**44,90%**	**47,37%**	**46,09%**
5,0				**43,59%**
10,0	**41,00%**		**41,18%**	**41,09%**
15,0		**38,00%**		**37,71%**
20,0	**35,00%**	**33,55%**	**34,43%**	**34,33%**
25,0		**34,00%**		**31,59%**

30,0	**29,50%**	**28,00%**	**29,08%**	**28,86%**
35,0				**26,62%**
40,0	**24,50%**		**24,24%**	**24,37%**
45,0				**21,72%**
50,0	**19,50%**	**18,00%**	**19,68%**	**19,06%**
55,0				**16,91%**
60,0	**15,00%**		**14,53%**	**14,76%**
65,0				**12,88%**
70,0	**11,00%**			**11,00%**
75,0				**8,75%**
80,0	**6,50%**			**6,50%**
85,0				**4,75%**
90,0	**3,00%**			**3,00%**
95,0				**1,50%**
100,0	**0,00%**			**0,00%**

TABLE 3.5: SOLUBILITY DATA FROM THREE DIFFERENT SOURCES IN [NH_3/H_2O]kg

Gravimetric Solubility Comparison @ 101,325 kPa				
$[NH_3 / H_2O]_{kg}$				
TEMPERATURE	**Airgas**	**ATSDR**	**ENG. Toolbox**	**Reconciled data**
[^oC]	[-]	[-]	[-]	[-]
0,0	**85,19%**	**81,49%**	**90,00%**	**85,56%**
5,0				**77,65%**
10,0	**69,49%**		**70,00%**	**69,75%**
15,0		**61,29%**		**61,01%**
20,0	**53,85%**	**50,49%**	**52,50%**	**52,28%**
25,0		**51,52%**		**46,43%**
30,0	**41,84%**	**38,89%**	**41,00%**	**40,58%**
35,0				**36,40%**
40,0	**32,45%**		**32,00%**	**32,23%**
45,0				**27,89%**
50,0	**24,22%**	**21,95%**	**24,50%**	**23,56%**
55,0				**20,44%**
60,0	**17,65%**		**17,00%**	**17,32%**
65,0				**14,84%**
70,0	**12,36%**			**12,36%**

75,0				**9,66%**
80,0	**6,95%**			**6,95%**
85,0				**5,02%**
90,0	**3,09%**			**3,09%**
95,0				**1,55%**
100,0	**0,00%**			**0,00%**

Reconciliation of data was not done for the volumetric concentration data, as this will not be further used in calculations.

TABLE 3.6: SOLUBILITY DATA FROM THREE DIFFERENT SOURCES EXPRESSED IN MOLE FRACTION.

Volumetric Solubility Comparison @ 101,325 kPa			
$[NH_3/(NH_3 + H_2O)]_{mole}$			
TEMPERATURE	**Airgas**	**ATSDR**	**ENG. Toolbox**
[^oC]	[-]	[-]	[-]
0,0	**48,65%**	**47,48%**	**50,09%**
5,0			
10,0	**43,36%**		**43,55%**
15,0		**40,19%**	
20,0	**37,02%**	**35,48%**	**36,41%**
25,0		**35,96%**	
30,0	**31,20%**	**29,61%**	**30,75%**
35,0			
40,0	**25,91%**		**25,64%**
45,0			
50,0	**20,63%**	**19,04%**	**20,81%**
55,0			
60,0	**15,87%**		**15,37%**
65,0			
70,0	**11,64%**		
75,0			
80,0	**6,88%**		
85,0			
90,0	**3,17%**		
95,0			
100,0	**0,00%**		

The data for both the gravimetric measures were plotted on a graph, demonstrating all three sources. Interpolation curves were fitted to the data points.

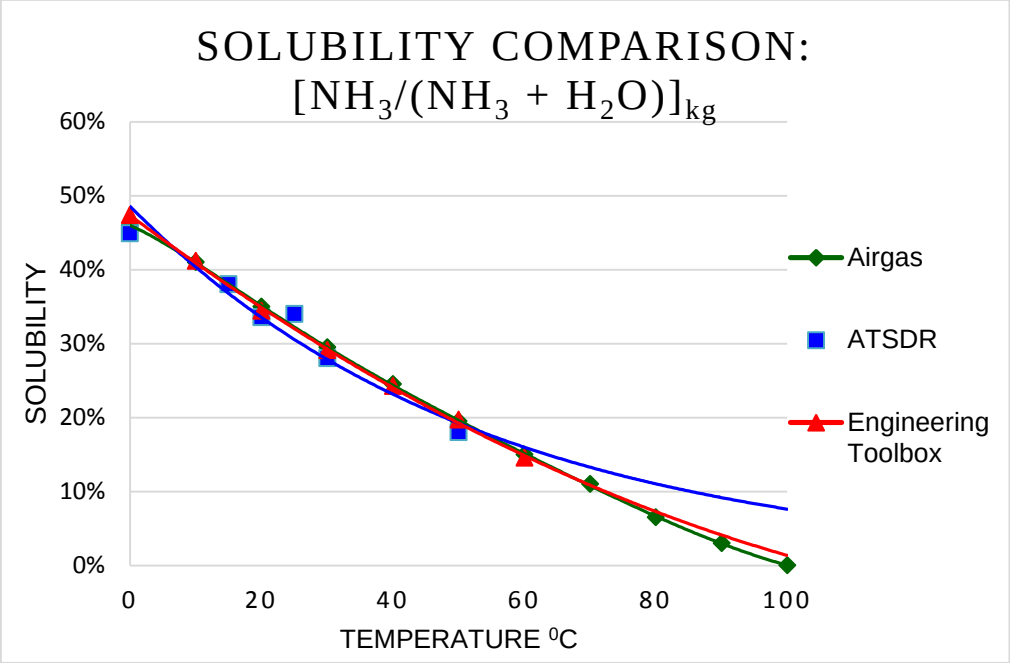

FIGURE 3.3: GRAPH COMPARING DIFFERENT SOURCES FOR SOLUBILITY OF AMMONIA IN WATER IN [NH_3/(H_2O+ NH_3]kg

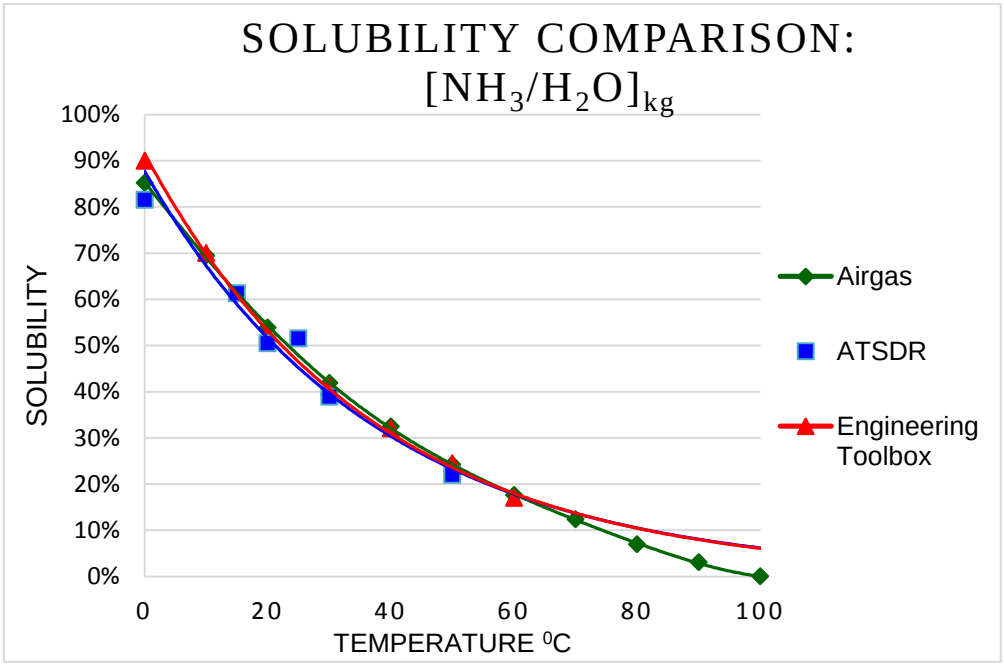

FIGURE 3.4: GRAPH COMPARING DIFFERENT SOURCES FOR SOLUBILITY OF AMMONIA IN WATER IN [NH_3/H_2O]kg

The graphs show that the solubility of ammonia in water follows a trend which approaches exponential decay. The reason why one source gives a 0% solubility for ammonia in water, is likely because of the fact that water boils at 100˚C at standard atmospheric pressure. However, when the pressure is increased, ammonia will be soluble again in water as a fluid.

It can also be seen that the sources correspond reasonably closely with one another, as no major scattering of the data points is observed. This is a preferable outcome. The fact that the sources do not give exactly the same values either, gives support to the assumption that the values found in these sources are experimentally observed values, rather than theoretically calculated values (the sources never explicitly makes it clear which it is). It was already seen in Chapter 2 (under the discussion of influence of CO_2 on the solubility), that researchers observed that practical values for the solubility of ammonia gas in water do not always correspond to the theoretically calculated values, hence the preference for experimental results.

3.3.5 EXPANSION OF SOLUBILITY DATA TO NON-STANDARD PRESSURES

The next step in regards to the expansion of the solubility question is to expand the data to non-standard pressures. All the data presented thus far, is valid only at standard atmospheric pressure. It can be seen from Henry's law as well as earlier discussions, that pressure is one of the key parameters in determining the maximum concentration possible, for a gas in water. Furthermore, this is practically also needed because it cannot be assumed that the absorber component will be operating at standard pressure conditions for either the system pressure or the partial pressure of the ammonia gas. Indeed, in the study of Cardenas & Narayanan (2010) a pressure of 6 bar is reported for operating conditions.
Furthermore, insight about the behaviour of solubility between these two substances is desired. For example, consider the following:

- Increasing the temperature of a mixture will decrease the solubility (as seen from the data).
- Increasing the pressure of a mixture will increase the solubility (as observed per Henry's law and earlier discussions).

Thus, suppose that a situation occurs for the aqua-ammonia heat pump (and absorber component) where *both* the temperature and the pressure are *increased*. What will happen to the solubility? What will the net effect be? Which parameter will "win"? To answer these

questions, solubility charts were developed in Excel, which visually display the physical behaviour of the aqua-ammonia mixture. The following is a solubility chart for weight percent.

Maximum Solubility Chart:
Kilogram ammonia gas soluble per kilogram mixture [%]
$[NH_3 / NH_3 + H_2O]_{kg}$

Ammonia is liquid in this area and reacts violently with water.

Pressure [kPa]	0,0	5,0	10,0	15,0	20,0	25,0	30,0	35,0	40,0	45,0	50,0	55,0	60,0	65,0	70,0	75,0	80,0	85,0	90,0	95,0
1200								81,2%	79,2%	76,8%	73,6%	70,8%	67,2%	63,7%	59,4%	53,3%	45,2%	37,3%	26,8%	15,5%
1150								80,5%	78,5%	76,0%	72,8%	69,9%	66,3%	62,7%	58,4%	52,3%	44,1%	36,3%	26,0%	14,9%
1100							81,5%	79,8%	77,8%	75,2%	71,9%	68,9%	65,3%	61,7%	57,3%	51,2%	43,0%	35,3%	25,1%	14,4%
1050							80,8%	79,0%	77,0%	74,3%	70,9%	67,9%	64,2%	60,6%	56,2%	50,0%	41,9%	34,2%	24,3%	13,8%
1000							80,0%	78,2%	76,1%	73,4%	69,9%	66,9%	63,1%	59,4%	55,0%	48,8%	40,7%	33,1%	23,4%	13,2%
950						81,3%	79,2%	77,3%	75,1%	72,3%	68,8%	65,7%	61,9%	58,2%	53,7%	47,5%	39,5%	32,0%	22,5%	12,7%
900						80,5%	78,3%	76,4%	74,1%	71,2%	67,7%	64,5%	60,6%	56,9%	52,3%	46,2%	38,2%	30,8%	21,6%	12,1%
850						79,6%	77,3%	75,3%	73,0%	70,1%	66,4%	63,2%	59,2%	55,5%	50,9%	44,8%	36,8%	29,6%	20,6%	11,5%
800					80,5%	78,6%	76,2%	74,2%	71,8%	68,8%	65,0%	61,7%	57,8%	54,0%	49,4%	43,3%	35,4%	28,4%	19,6%	10,9%
750					79,5%	77,5%	75,0%	72,9%	70,5%	67,4%	63,6%	60,2%	56,2%	52,3%	47,8%	41,7%	34,0%	27,1%	18,6%	10,3%
700				80,8%	78,3%	76,2%	73,7%	71,5%	69,0%	65,8%	61,9%	58,5%	54,5%	50,6%	46,1%	40,0%	32,4%	25,8%	17,6%	9,7%
650				79,6%	77,0%	74,9%	72,2%	70,0%	67,4%	64,1%	60,2%	56,7%	52,6%	48,8%	44,2%	38,2%	30,8%	24,4%	16,6%	9,0%
600				78,3%	75,6%	73,3%	70,6%	68,3%	65,6%	62,3%	58,2%	54,8%	50,6%	46,8%	42,3%	36,4%	29,2%	22,9%	15,5%	8,4%
550			79,1%	76,8%	73,9%	71,6%	68,8%	66,4%	63,6%	60,2%	56,1%	52,6%	48,5%	44,6%	40,2%	34,4%	27,4%	21,4%	14,4%	7,7%
500			77,5%	75,1%	72,1%	69,6%	66,7%	64,2%	61,4%	57,9%	53,8%	50,2%	46,1%	42,3%	37,9%	32,3%	25,5%	19,9%	13,2%	7,1%
450		77,5%	75,6%	73,0%	69,9%	67,3%	64,3%	61,8%	58,9%	55,3%	51,1%	47,6%	43,5%	39,7%	35,4%	30,0%	23,6%	18,2%	12,1%	6,4%
400	77,2%	75,4%	73,4%	70,7%	67,4%	64,7%	61,6%	59,0%	56,0%	52,4%	48,2%	44,7%	40,6%	36,9%	32,8%	27,6%	21,5%	16,5%	10,9%	5,8%
350	74,7%	72,8%	70,7%	67,8%	64,4%	61,6%	58,4%	55,7%	52,7%	49,1%	44,9%	41,4%	37,4%	33,9%	29,9%	25,0%	19,4%	14,8%	9,7%	5,1%
300	71,7%	69,7%	67,4%	64,4%	60,8%	57,9%	54,6%	51,9%	48,8%	45,2%	41,1%	37,7%	33,9%	30,5%	26,8%	22,2%	17,1%	12,9%	8,4%	4,4%
250	67,9%	65,7%	63,2%	60,1%	56,3%	53,4%	50,0%	47,3%	44,3%	40,8%	36,8%	33,5%	29,9%	26,8%	23,4%	19,2%	14,6%	11,0%	7,1%	3,7%
200	62,8%	60,5%	57,9%	54,6%	50,8%	47,8%	44,5%	41,8%	38,9%	35,5%	31,7%	28,7%	25,5%	22,7%	19,6%	16,0%	12,1%	9,0%	5,8%	3,0%
150	55,9%	53,5%	50,8%	47,5%	43,6%	40,7%	37,5%	35,0%	32,3%	29,2%	25,9%	23,2%	20,4%	18,0%	15,5%	12,5%	9,3%	6,9%	4,4%	2,2%
101,3	46,1%	43,7%	41,1%	37,9%	34,3%	31,7%	28,9%	26,7%	24,4%	21,8%	19,1%	17,0%	14,8%	12,9%	11,0%	8,8%	6,5%	4,8%	3,0%	1,5%

Temperature in [°C]

FIGURE 3.5: SOLUBILITY CHART FOR AQUA-AMMONIA USING 'WEIGHT PERCENT'.

The above chart shows the solubility trends under various temperatures and pressures via both a numerical percentage as well as a colouring scheme. The temperature ranges from 0 to 95˚C and the pressure ranges from 101 to 1200 kPa total pressure, respectively. The colour scale is as follows: strong blue indicates most soluble, while strong pink indicates least soluble conditions, with white being in between the two extremes. Because of practical considerations, it was realised that at some point in the pressure range, ammonia was going to condense to liquid. These values were taken into account, and where ammonia gas transforms into liquid, it is indicated as purple. Solubility calculations are no longer meaningful in this pressure range. The values for these pressures at various temperatures, were obtained from EES, and worked in by hand into the chart.

It should also be realised that like the points where ammonia transforms into a liquid, certain points on the chart may not be correct, due to practical chemistry. Other non-realistic points may be present which are not so obvious. The rest of the chart was developed as follows:

- Each data point or value for solubility was carried over to the *x*-axis of the chart, from the 'reconciled data' column in the relevant tables above and entered at 101 kPa for the entire temperature range.
- Under each temperature value, having both the pressure and value for the solubility, a Henry's law constant was calculated using Eq. 3-1 just with the subject changed. Thus,

$$k_H = \frac{P}{c} \qquad [3\text{-}22]$$

This effort to calculate a new Henry's law constant, avoids two important pitfalls of Henry's law. Firstly, it takes into account that the 'constant' changes over temperature. Secondly, the units for k_H will be correct for further calculations for this particular measure of solubility (since it was calculated from it to begin with).

- Having done the above, the new maximum concentration could now be calculated at any desired pressure, using the original form of Henry's law in Eq. 3-1, since the constant is now known at each temperature set. This was done for all the desired pressures of the chart.
- Microsoft Excel's very useful conditional formatting function was then used to create the colour scale.

Finally, after all the above, the solubility chart was complete, and gives a very handy overall picture of the solubility behaviour as a function of pressure and temperature. The following observations are made concerning the chart:

- There is clearly a non-linear relationship between these two parameters.
- If both the temperature and pressure keep on being marginally increased, it seems that the net effect will be that the solubility still decrease. Thus, the temperature parameter has the strongest influence.
- In the process of drawing up the charts, it was observed that for the concentration, the measure of the standard weight percent $\left[\frac{NH_3}{NH_3+H_2O}\right]_{kg}$ cannot be used for calculation with Henry's law, in the algorithm just described above (with other words, it cannot be used in Eq. 3-1 to calculate a new concentration). When this measure is used, it is observed that at some point with pressure increase, values of 100% or greater are given. This is mathematically/logically impossible, since the amount of NH_3 cannot be greater than the sum of NH_3 + H_2O in the mixture. To demonstrate this problem, an example is given:

For a temperature T, let:

- The observed maximum concentration be *x* = 46% as weight percent (deliberately chosen).
- The pressure be 101.3 kPa.

  From Henry's law, it follows that the constant is:

$$k_H = \frac{P}{c} \therefore k_H = \frac{101.3}{0.46} = 220.2\ kPa$$

  Now, it is desired with this value that the new maximum concentration at the same temperature be calculated at 300 kPa. Thus,

$$c = \frac{P}{k_H} \therefore c = \frac{300}{220.2} = 1.362 = 136.2\ \%$$

  which is impossible. This illustrates the problem.

- This means that another pitfall of Henry's law has been identified.
- What makes this problem more subtle, is that at 200 kPa pressure, for example, the error introduced would not be apparent, since the value obtained would still be under 100% concentration. Nonetheless, the value is significantly incorrect. At a pressure of 200 kPa and a temperature of 5˚C, the incorrect method gives a maximum

solubility of 86%, while the correct method gives a value of 60.5%, which is a 42% error. Moreover, a Henry's law constant given in a pressure unit (such as kPa) must be checked that it avoided this pitfall, since having calculated a value with both the weight percent as well as $\left[\frac{NH_3}{H_2O}\right]_{kg}$ will yield a value for Henry's law constant with the unit of kPa. The correct way to calculate a new concentration with Henry's law, would be to use the measurement of $\left[\frac{NH_3}{H_2O}\right]_{kg}$ using the method and equations outlined above. Then, after a new concentration in the above measure is obtained for new, non-standard pressures, the values can be converted to the weight percent measure via the conversion factors developed. Indeed, this was the methodology followed which yielded the handy solubility chart given in this chapter. And it can be clearly seen in the chart, that nowhere does the weight percent yield a value of 100% or higher. All the values are realistic.

- Lastly, it is emphasised that the above method for calculating solubilities at non-standard pressures, are just approximations, and not exact analytical answers due to the formation of ions (as has previously been stated). However, approximations are all that is needed, as shall be seen. In addition, as previously stated, despite the ion-formation problem, values for the Henry's law constant are found in chemical technical literature for ammonia gas in water (or even mentioned by university distant learning tuition videos, such as University of California, Berkeley (2012)).

3.3.6 DEVELOPING A CORRELATION FOR CALCULATION OF MAXIMUM SOLUBILITY OF AMMONIA IN WATER

The solubility chart developed thus far is quite handy in giving an overall picture (literally and figuratively) of the solubility behaviour for aqua-ammonia, especially by inspection. This can aid in pre-concept design ideas. But it will not be easy to use such a chart in the EES program, unless unnecessarily complex programming is introduced. Yet, when the heat transfer model is programmed, the solubility will need to be taken into account. To achieve this, the Henry's law constant was plotted against temperature from the data previously obtained, as can be seen in Fig 3.6 below:

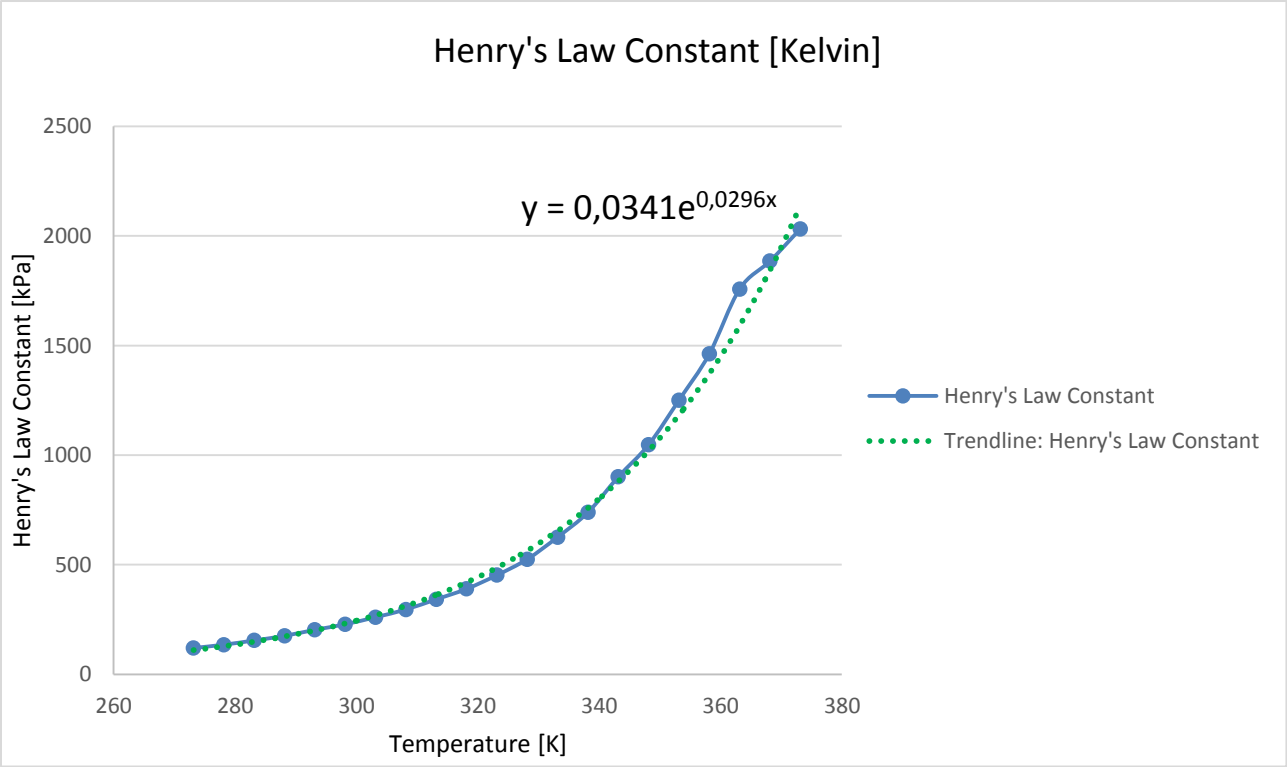

FIGURE 3.6: HENRY'S LAW CONSTANT AS A FUNCTION OF TEMPERATURE.

An exponential interpolation curve was fitted to the data points of the constant, and an equation was obtained. The equation is:

$$k_{HK} = 0{,}0341e^{0{,}0296T}$$

[Eq. 2-23]

where k_{HK} is the Henry's law constant for ammonia gas in water, and T the temperature in Kelvin. The essence of Eq. 2-23 is that the constant can now be calculated for any given temperature, even between the data points. When the constant is obtained, the solubility can simply be calculated at any pressure using Henry's law itself (Eq. 3-1). It should be remembered that this is the "volatility form" of the constant as pointed out earlier in this chapter, and should be used as such.

As can be seen from the graph of Henry's law constant above, there is a slight deviation by the exponential function from the experimental values. The differences between the correlation and the values were calculated at all the temperature data points, and the results are as follows:

- Minimum difference = 1.5%
- Maximum difference = 9.5%
- Average difference = 4.7%

The above results fall into an acceptable range of deviation for an empirical correlation, and is deemed satisfactory.

Furthermore, it should be kept in mind that the restrictions, which are on the solubility chart, are also applicable on the calculations using the correlation of Eq. 2-23. Thus, where the pressure gets close to the saturated liquid pressure for ammonia, or where the temperature gets to the boiling point of water, the calculations will obviously no longer be valid. The freezing point of pure water, however, does not seem to be a problem. This is because the presence of ammonia in water lowers the freezing point significantly, forming a phase diagram (Airgas Speciality Products, 2010). Lastly, it should always be kept in mind, when carrying out the methodology above, that the pressure P in Henry's law is the partial pressure of the ammonia gas above/outside the solution. Thus, if an auxiliary gas is present, care needs to be taken so that the total pressure is not accidentally used.

3.3.7 CONSTANT CONCENTRATION CURVES

Having developed the above correlation and method, it is now possible to draw up constant concentration curves. These wil be handy for overall cycle design. For example, if the designer wants to maintain a constant concentration for the solution in the bubble pump, but has the problem of varying pressure or input temperatures, he/she can consult the constant concentration curves in order to see which pressure should accompany which temperature, for example.

The curves were developed using the correlation given above by Eq. 2-23, and the subsequent algorithm explained. This was programmed into EES, and parametric tables were drawn up for various concentrations. The curves were drawn up for the standard 'weight percent' and are presented below. The graphs were drawn up by using intervals of 10% for the concentration.

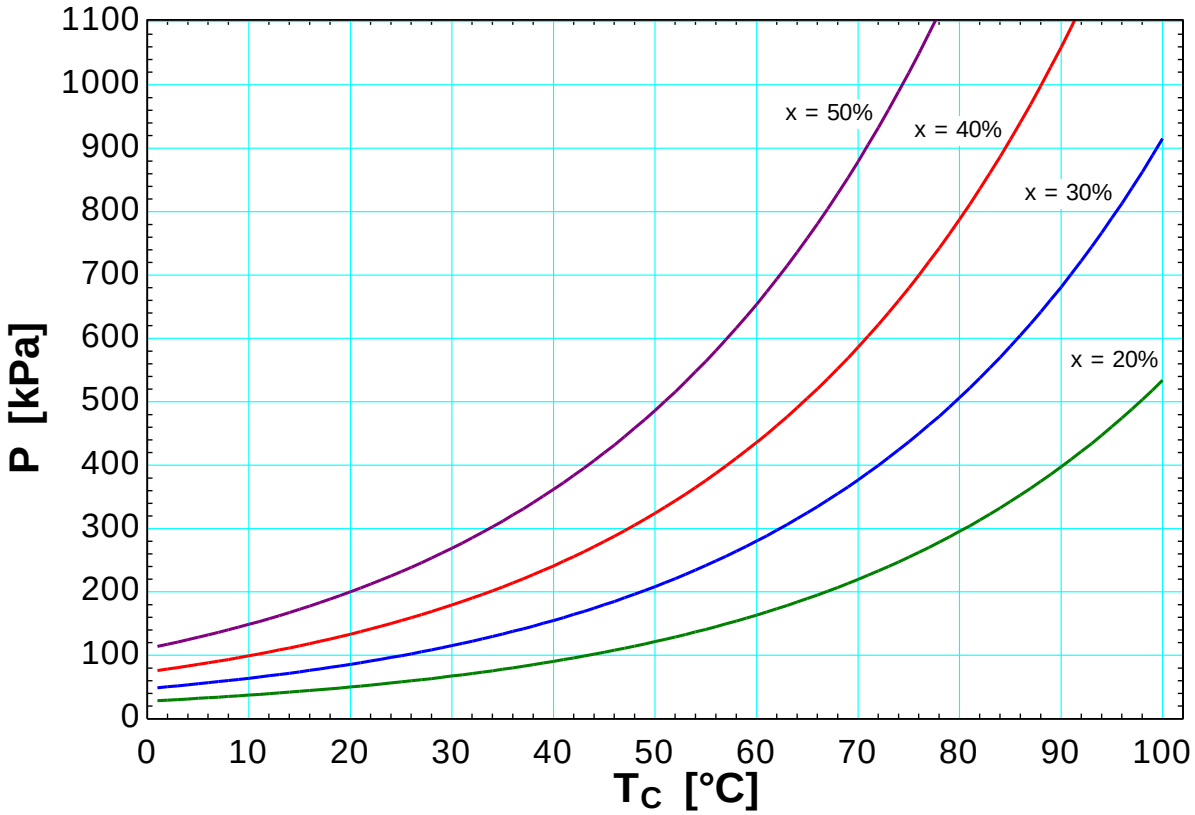

FIGURE 3.7: CONSTANT MAXIMUM CONCENTRATION GRAPH FOR AQUA-AMMONIA BETWEEN 20% AND 50%

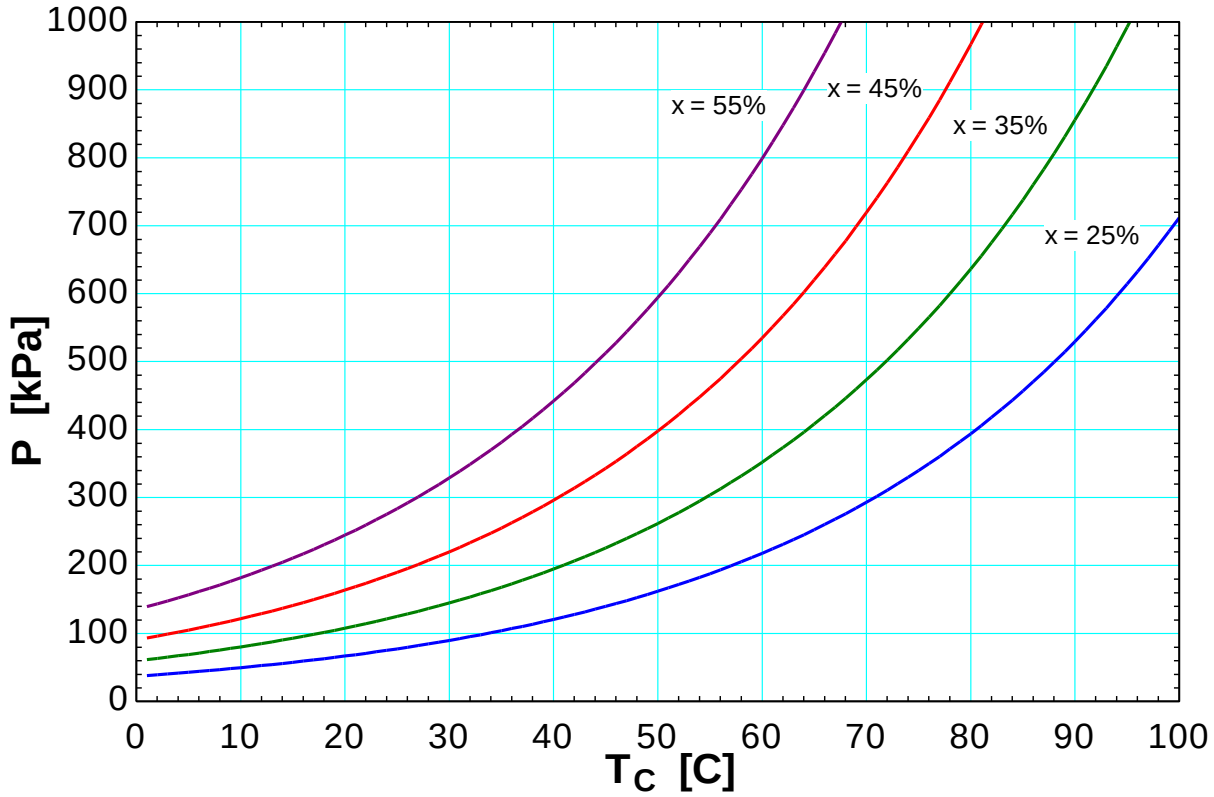

FIGURE 3.8: CONSTANT MAXIMUM CONCENTRATION GRAPH FOR AQUA-AMMONIA BETWEEN 25% AND 55%

Airgas Speciality Products (2010) also published one constant concentration graph in their technical procedure. It is less expanded than the graphs developed and given above, and not in standard SI units. However, it is assuring to note that exactly the same trends are observed for constant concentration in their graph, as the ones seen in the developed graphs. Thus, for visual verification, the graph from Airgas Speciality Products is given below:

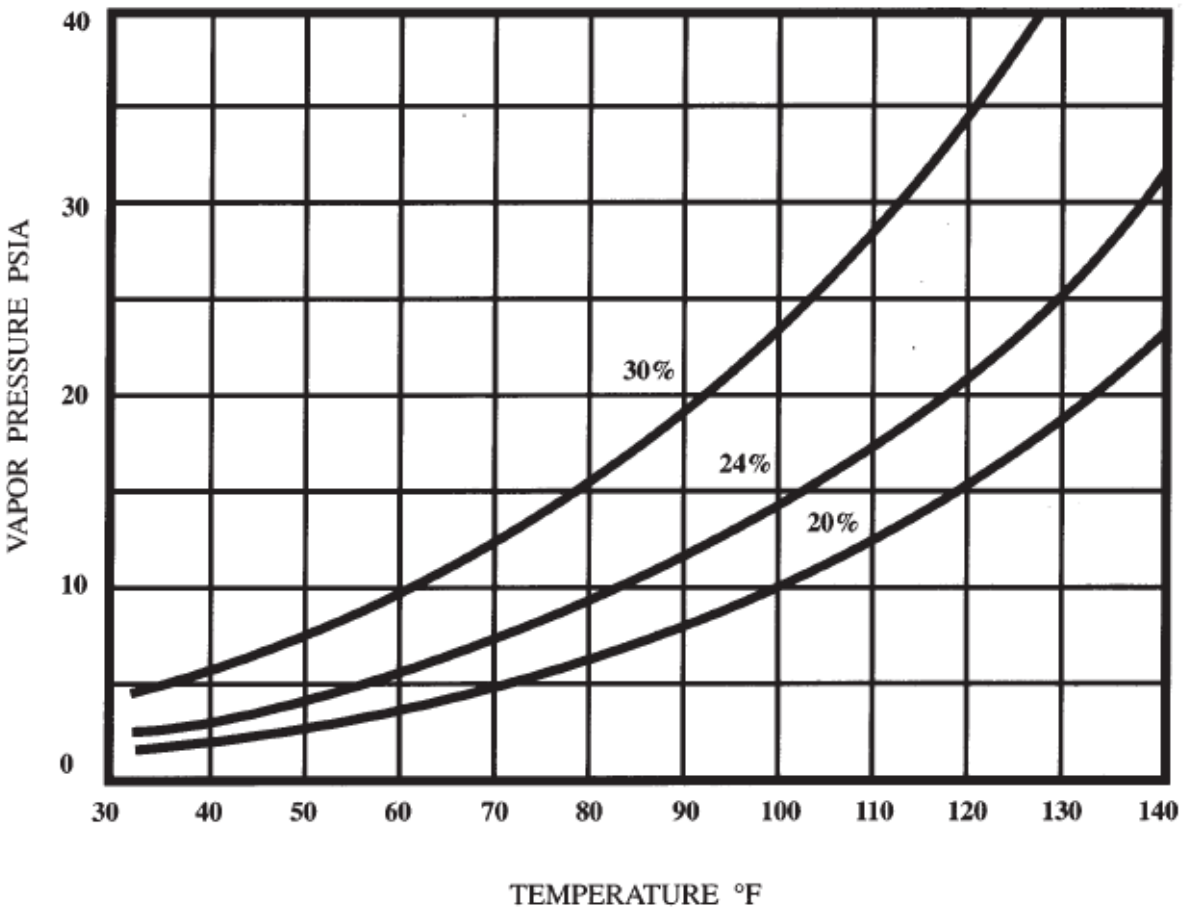

FIGURE 3.9: CONSTANT CONCENTRATION GRAPH FOR AQUA-AMMONIA FROM (AIRGAS SPECIALITY PRODUCTS, 2010).

Once again, as before, the possible restrictions which are valid for the solubility chart and solubility algorithm, are valid here as well. Thus, a designer would need to check properties before final use.

3.4 OBSERVATIONS OF OTHER RESEARCHERS

In this section, a few observations of other researchers on this topic, are noted.

- Cerezo *et al*. (2009:1009) note that when their absorber pressure was increased from 1.6 bar to 2.0 bar, the mass transfer flux increased with about 85%. The mass transfer flux is basically the rate at which the ammonia absorbed into the weak solution.

- Cardenas & Narayanan (2010:1797) noticed that lowering the coolant inlet temperature to the absorber, significantly enhanced the absorption rate.
- Cardenas & Narayanan (2010:1794) also noticed that a saturation concentration exists for the ammonia in water.

All three the above observations are consistent with possible predictions from the developed solubility chart and model. An increase in pressure would indeed lead to a higher amount of ammonia gas in water, as per the solubility chart, if the operating temperature was not increased. Lowering the coolant inlet temperature would lower the temperature of the aqua-ammonia solution, which is in the process of absorbing ammonia gas, and the result found by Cardenas & Narayanan would also fit in very neatly with the predictions of the solubility chart. Lastly, the observation of a 'saturation concentration' seems to be basically the same as the 'maximum solubility' identified earlier in the chapter. The constant concentration curves developed from the work done in this chapter also show the same general trend to those provided by Airgas Speciality Products (2010), which is a pleasing result.

The above observations mean that the work done in this chapter generally agree with the work of others, and is very likely to be generally valid, especially if the identified pitfalls are avoided and cautions taken seriously. This can hopefully provide a good macroscopic approach to the subject of solubility and absorption of ammonia gas in water.

---

4. THEORETICAL MODEL

4.1 INTRODUCTION

In this chapter, the basic theoretical model which was developed to simulate the absorber component, will be set forth. The basic architecture of the absorber for this study is explained, assumptions stated, motivations for choices given, and the mathematical equations given.

4.1.1 CHOICE OF SOFTWARE USED

It has already been stated briefly that the software which is used for simulation, is *f-Chart Software's* Engineering Equation Solver (EES). The reason for this choice, is because of EES's very handy built-in thermodynamic properties in general, as well as the useful NH_3H_2O-procedure which is capable of calculating properties, specifically for aqua-ammonia mixtures. Furthermore, EES's major developer, S.A. Klein, is also a co-author of a widely circulated text on absorption systems (Herold *et al*., 1996). The easy call of thermodynamic functions saves a lot of time in programming, but more important, enables easy parametric studies and system optimization.

4.1.2 CONTEXT OF THE ABSORBER COMPONENT

As was explained in Chapter 2, the absorber component does not function in isolation, but rather in a system which forms a heat pump. Moreover, the absorber has already been identified as a critical component by several observers reviewed in Chapter 2. The wider context of the aqua-ammonia project at the North West University, Potchefstroom, as has been previously stated in Chapter 1, is to grow independent of Eskom, South Africa's national electricity provider. The project specifically aims to use solar energy for a supply of heat input. This heat pump would instead fulfil all the basic heating and cooling needs of a typical middle class South African household, in the ideal situation.

Should the solar energy alone not be sufficient, the option exists to add natural gas as an energy source to the system. Theunissen (2011) did a study on a heat sink for the system. At the North West University, several Master's studies have already been done on this particular project. The illustration in Figure 4.1 gives a schematic presentation (in cross-section) of the basic layout of the absorber.

Potgieter (2013) has done an overall evaluation of the DAHP in the context of solar options for South Africa.

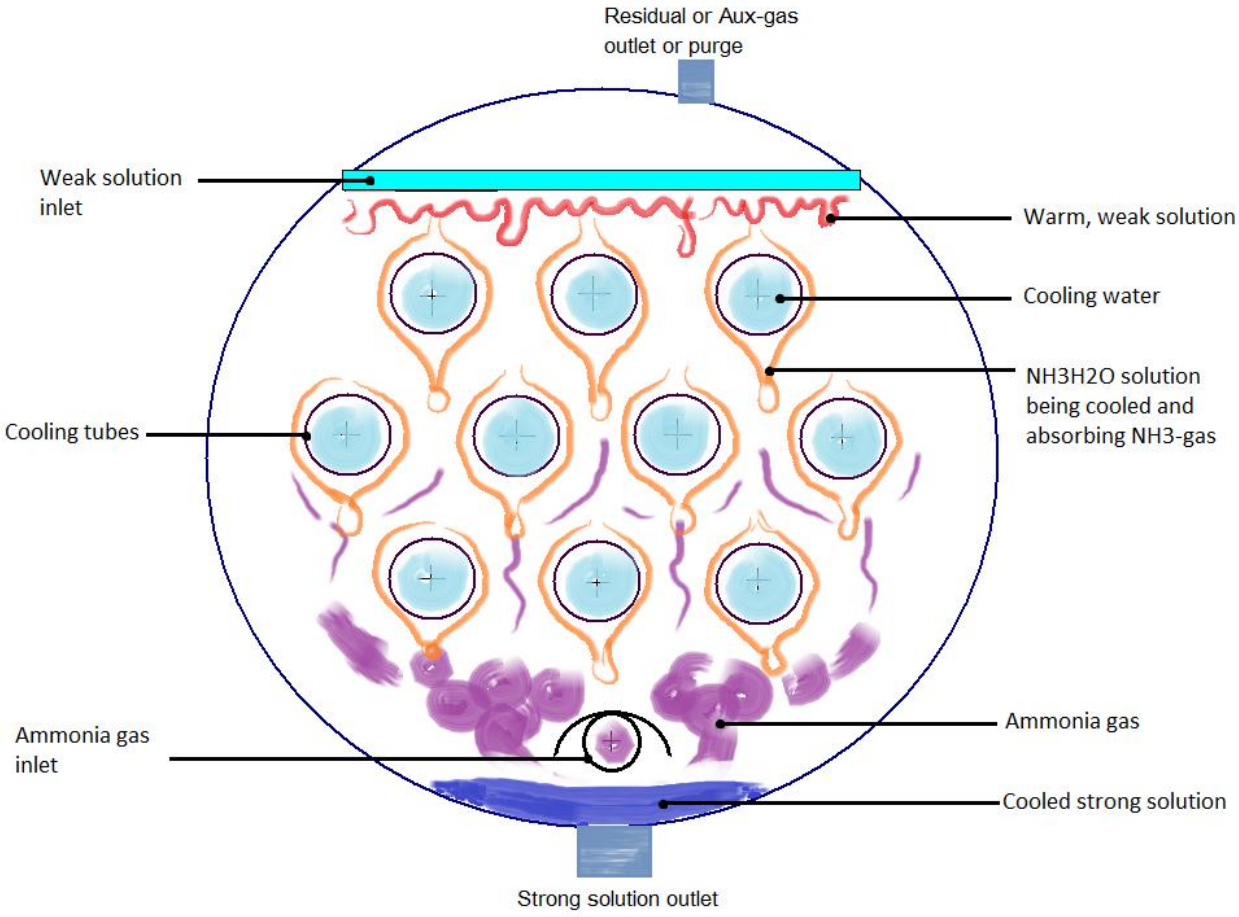

FIGURE 4.1: SCHEMATIC ILLUSTRATION IN THE CROSS-SECTION OF THE BASIC ABSORBER LAYOUT (ILLUSTRATION BY THE AUTHOR).

Van der Walt (2012) did an in-depth study of the bubble pump. This study is to help complete the project by doing the absorber component, with other Master's studies running parallel to it. A Ph.D. candidate is doing intensive simulations of the overall cycle of the

entire heat pump, in order to help facilitate and aid overall design. This is important, as input data is acquired from him. The Ph.D. candidate will thus be referred to later, due to interdependence, but it is noted that no official thesis can be referenced, since his study is not yet completed. The final task of building the physical absorber component was assigned to a final year B.Eng engineering student. Engineers working in teams are an integral process of engineering, so this should not be seen as a problem.

The physical layout of the absorber component is given in this section. It is important to visualise the layout, as the mathematical absorber models for this study, were specifically developed for this layout. As can be seen from the illustration above, this absorber will fall under the falling film absorber type, as the weak solution drips on the cooling tubes and forms a thin film. Warm, weak aqueous-ammonia solution enters the absorber from the top. From there, it systematically drips on the various tubes containing cooling water, thus flowing in a cross-flow configuration. Ammonia gas is introduced at the bottom of the absorber so that it can run in a counter-flow configuration to the weak solution film on the tubes, and get absorbed. At the bottom, the now strong solution gathers and exits the absorber. At the very top of the shell, any residual ammonia gas (which did not get absorbed) or auxiliary gas (which ended up in the absorber), are purged and taken back into the relevant components of the system. Helium or hydrogen gas (which will be used as auxiliary gas) is lighter than ammonia gas, so will end up at the top, and is thus not anticipated to build up. It must further be noted that the cooling tubes lie in a horizontal configuration, and not vertical (contrary to at least one study described in Chapter 2). Also, the inlet of the weak solution is not a continuous bar as is presented in the schematic illustration, but will actually consist of seven separate feed tubes which are carefully situated exactly above each column of cooling water tubes. Small holes will be drilled in these feed tubes that carefully lets the weak solution drip on the cooling tubes.

4.1.3 MOTIVATIONS FOR THIS PARTICULAR LAYOUT OF THE ABSORBER COMPONENT

There exists a number of reasons or motivations for the choice of this particular layout of the absorber. Some of these motivations come from having studied the work of others, while other considerations were practical of nature.

- A falling film type of absorber is chosen, because the falling film maximises the contact area between the ammonia gas and weak solution liquid. This was a major reason why Selim & Elsayed (1999) chose the falling film configuration for their study.
- No pump or compressor is allowable in the main circuit of the water and ammonia. This means that the cycle is dependent on the bubble “pump” component mentioned in Chapter 2 (which is not an electrical pump of any sort) and thermal syphoning for circulation of the refrigerant (ammonia gas) and the absorbent (aqua-ammonia solution). This means that bubble-type absorbers such as that of Fernández-Seara et al. (2005) are avoided. This is due to the fact that a pressure head will inevitably

have to be overcome in their design, since the ammonia gas is introduced at the bottom (Figure 4.1). With the current concept and layout, this pressure head would not be present, since ammonia gas would not be at the bottom of a continuous water column. Only drops of liquid will surround the feed tube of the ammonia gas, with enough open space for the gas to fill up. In the case of the study of Cerezo et al. (2009) (which is also a bubble-type of absorber), ammonia gas was fed from a pressurized bottle, and pumps were indeed present in their circuit as well. Here too, ammonia gas was introduced at the bottom of a channel of water.

- It was not clear from the paper of Cardenas & Narayanan (2010) whether they used a pump or not. This was an important question, since the ammonia gas needed to be squeezed through a porous medium, which would inevitably need some form of pressurization. A deeper look into the Master's Dissertation of Cardenas (2009:52) revealed that the test facility not only contained a pump, but that ammonia gas was in this case also fed from a pressurized bottle. This too, would be too problematic, since the desired outcome of this study, is a heat pump, which not only does not contain a pump in this circuit, but also recycles the ammonia gas. Thus, feeding ammonia gas from a bottle would miss the bigger aim of the development of this heat pump system.
- It has been seen from the study of Fernández-Seara et al. (2005) that bubble-type of absorbers result in complex two-phase flow regimes developing. The choice of a falling film absorber avoids this phenomenon which introduces an unnecessary layer of complexity to the calculations. Two-phase flow is a speciality field of its own.

It is believed that the proposed layout of the absorber component will avoid all of the above problems, and will satisfy the need of the total system. Both gravity, as well as a pressure head in the bubble pump will drive the weak solution. Experimentation will be presented later in this study, which determined the ideal liquid level height (from which the pressure head comes) for proper functioning.

4.2 ASSUMPTIONS MADE IN THE THEORETICAL MODEL

A number of assumptions need to be made for the theoretical mathematical model, which is developed in this chapter. Some of these assumptions are common in absorber models, some are needed to simplify the model, and some are introduced out of practical considerations of the physical layout.

The following assumptions are made in this study, but have also been made by the study of Fernandez-Seara *et al*. (2005:280):

- The absorber component and its subsequent processes are operating at steady-state conditions.
- Heat transfer to the surrounding environment is negligible.
- No significant amount of direct heat transfer takes place between the vapour (or gas) in the absorber component, and the cooling water in the tubes. (Refer to Figure 4.1 to see why this assumption is also reasonable for this design. The cooling tubes are covered with liquid all the time in the ideal situation).
- The coolant and liquid properties are constant in the directions perpendicular to their respective flow directions (this assumption is reasonable, but also necessary in order to simplify the model and calculations).

The following assumptions are made and well-motivated by the study of Cardenas & Narayanan (2010), and will also be made for this study:

- The absorber component operates at constant pressure.
- No significant counter-diffusion takes place of water into the ammonia gas. Cardenas & Narayanan (2010:1790) points out that counter-diffusion of water into ammonia are 4% or less of the flux of ammonia absorption in water.

The following assumptions are made which are particular to this study. These assumptions are made from looking at the geometry of the component, as well as an attempt to avoid unnecessary complexity in the theoretical model. These assumptions are:

- Referring to Figure 4.1, absorption mainly takes place only in the two bottom rows of the cooling tubes. This is in large part due to the fact that the ammonia gas is introduced at the bottom of the absorber component, well below the rows of cooling tubes. Another reason is because of the strong affinity for ammonia gas and water (as can be seen from the ammonia fountain experiment), and subsequently the fact that the cycle operating conditions are designed well below the maximum solubility of ammonia in water.
- There is sufficient “residence time” for all the ammonia gas to absorb into the weak solution.

- The distribution of ammonia gas in water is more-or-less uniform between the seven tubes (of the bottom two rows) between which the ammonia gas gets absorbed.

4.3 PRINCIPLES SURROUNDING THE THEORETICAL MODEL

The purpose of the theoretical model and simulation is to be capable of predicting outcome parameters for a given set of input conditions. Having developed the basic model and simulation program which can predict desired output parameters, the absorber component can then further be characterized by doing parametric studies and possible optimization. Predictability (within reasonable error margins for convection heat transfer) is of utmost importance, since this is a crucial step in the design of the absorber component, as well as the design of the overall heat pump cycle. The mathematical model basically solves a complex heat transfer problem. This means solving a heat exchanger, which is the primary subset of the absorber component. What makes the solving of this heat exchanger different as well as a challenge is the fact that additional heat is generated *in situ* within the hot fluid stream itself. This heat needs to be firstly calculated and secondly accounted for. Nowhere in the engineering under-graduate course of heat transfer, is such a phenomenon treated (see: Van Eldik (2012)).

4.3.1 THE APPROACH FOLLOWED TO SIMULATE THE ABSORBER COMPONENT

A specific methodology has been followed in order to model the heat transfer problem in the absorber component. It is assumed that the reader already has fundamental knowledge of heat transfer theory, so each and every principle will not be explained anew. The approach for exposition of the theory is to brake up the theoretical principles in several categories.

4.3.2 THE EFFECTIVENESS NTU-METHOD AND THE ADAPTATION THEREOF.

The effectiveness NTU-method (hereafter the ε-NTU-method) is used to solve the heat transfer problem. This is in contrast to the Log Mean Temperature Difference (LMTD) method, also commonly encountered in heat transfer courses. It is noted by Cerezo *et al*. (2009:1007) that in many situations or experiments, the conventional *log mean temperature* cannot be calculated and used (in the standard LMTD-method), since the temperature at the outlet of the cooling water stream ends up to be higher than that of the inlet temperature of the hot stream (which is the weak solution). This is due to the heat generated during the absorption process. Furthermore, the LMTD-method is not preferred, due to the fact that cumbersome iterations are needed to solve the heat exchanger if the outlet temperatures of

the two streams are unknown (Van Eldik, 2012:11.6). This will be the case in this study as well, hence another reason to use the ε-NTU-method.

The following methodology or strategy has been developed in order to deal with the problem of heat generation using the ε-NTU method to simulate the heat transfer in the absorber:

- Do calculations with the ε-NTU method for the hot and cold streams of the fluid – without absorption (or considering any gases such as the ammonia gas which enters the absorber). Obtain *preliminary* outlet temperatures for both the hot fluid stream and cold fluid stream.
- Calculate the heat generated (Q̇-gen) by the absorption process using EES thermo-properties in a mass-energy balance.
- Calculate the new temperature of the hot stream only, using Q̇-gen and the preliminary temperature obtained earlier, and obtain a transitional enthalpy and temperature.
- Do a "halfway ε-NTU method" between the transitional properties of the hot fluid, and the preliminary outlet properties of the cold fluid.
- Calculate new and final outlet properties for both hot and cold fluids.

Having followed the above steps, it was possible to solve the problem of heat transfer and to simulate the absorber component. The equations will be given later in this chapter.

4.3.3 THE SINGLE CYLINDER VS. THE TUBE BANK APPROACH

The cooling tubes are simulated and solved as a collection of single cylinders, rather than a conventional tube bank. There are three main reasons for this choice:

- Optimization will be attempted later with the model. This means that different configurations will be created for how the cooling tubes (cylinders) are connected to one another. Approaching and solving the problem as a tube bank cannot and does not make provision for this.
- Secondly, it is assumed that the absorption process of ammonia gas in water only takes place around the bottom two rows of the array of cooling tubes. Thus, these two rows are treated separately from the first row. The tube bank approach cannot consider this, whereas treating the cooling tubes as a set of individual cylinders can.

- The third and most important reason for considering the set of cooling tubes as a collection of individual cylinders rather than a tube bank, is due to the very nature of the fluid flow pattern itself, found in this particular design and layout of the absorber.

To explain, the following illustration is given:

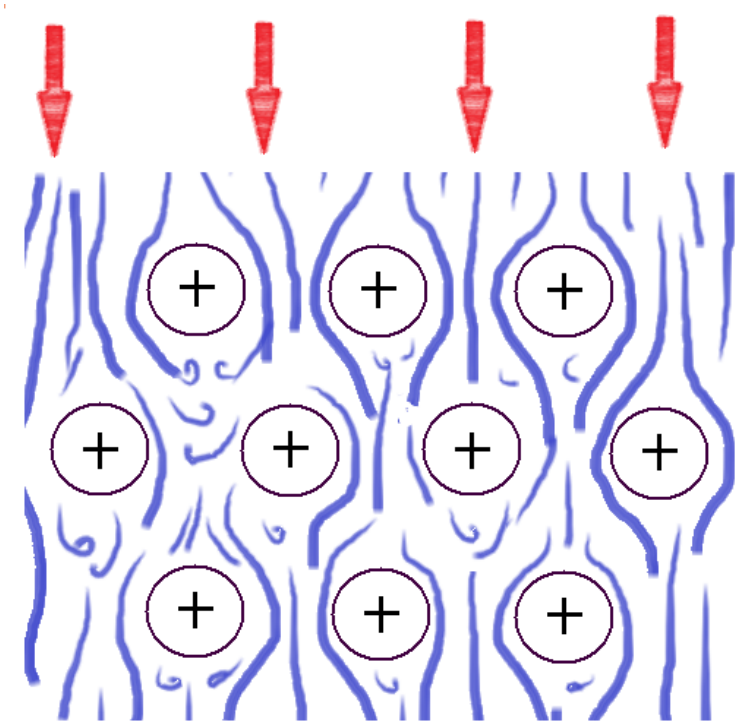

FIGURE 4.2: FLUID FLOW PATTERN IN A TUBE BANK (ILLUSTRATION BY THE AUTHOR).

The flow pattern of the fluid in a tube bank is given in Figure 4.2. The arrows represent the main direction of flow of the incoming fluid, whilst the blue lines represent the streamlines of the fluid flow. It is of utmost importance to notice that there exists a continuous amount of the hot or the cold incoming fluid between each and every tube in the tube bank. It can clearly be seen from studying Section 7.6 in the text of Incropera *et al*. (2007:436) that the distance between each column of tubes (denoted S_L in their text) influences the heat transfer outcome.

The flow pattern found in the proposed absorber layout and design will not be like that of a tube bank described above, even though it may superficially appear to be the case. Refer to Figure 4.1 once more. There will not be a continuous flow of hot aqueous-ammonia fluid between each of the *vertical columns* of tubes. Instead, each of the seven vertical columns will have a tube above it, which supplies hot aqua-ammonia fluid. The fluid will carefully drip (from small holes) on each individual cylinder which lies exactly vertically below the feed tube. The incoming weak solution of the one cylinder will not touch the weak solution on the

cylinder situated *horizontally* next to it. The liquid will simply move as a thin film on the active cylinder, which received the liquid from the feed tube. From there, it will drip as droplets on the cylinder directly vertically below it. In between each cylinder will be open space, which will be filled with either ammonia gas getting absorbed, or inert auxiliary gas (such as hydrogen or helium). One of the major reasons for this approach has already been explained: so that the ammonia gas does not have to be "pumped" in against a pressure head of a fluid column. Physical experiments were done with droplets, cylinders, feed tubes and holes in order to characterize this dripping process, which will be explained in a subsequent chapter.

In summary, the theoretical model will approach the *external flow* (in regards to convection heat transfer) using the theory of the single cylinder. Each cylinder's properties will be calculated *separately*, and in the case of the top two rows, the outputs of the one cylinder will be the inputs for the cylinder right below it. At the bottom, the properties of the final stream of liquid will be calculated from all the streams of liquid coming from the tubes.

4.3.4 UNKNOWN PARAMETERS SOLVED

Generally, heat exchanger calculations fall into two main categories:

- Solving for the *outlet temperatures* of the streams, while having the physical dimensions of the heat exchanger already known. This problem is usually seen as an *analysis* problem.
- Selecting a heat exchanger type, specifying the outlet temperatures beforehand and then solving for the contact surface area needed of the tubes or plates which keep the different fluids apart. This problem is usually seen as a design problem (Van Eldik, 2012:11.8).

The absorber component in this study will once again be an exception to these rules. Although the problem at hand is a design problem (since the heat exchanger type and architecture needs to be selected), the most important unknown parameters that will be solved for in this case are the outlet temperatures of the cold and hot streams of fluid. (Though, naturally, other useful parameters such as outlet concentration and heat generated will be calculated as well). The reason for solving for the outlet temperatures and not the contact surface area is twofold:

- Each and every cylinder will have a different outlet temperature for the hot stream which cannot be known beforehand. It is thus not possible to solve for the contact area of the tubes.
- Fixed mass flow rates were received from the Ph.D. candidate (via personal communication). It was realized, that for a given fixed mass flow of the warm weak solution, the wetted area of the tubes will also be fixed. This is because the warm liquid forms a thin film on the cooling tubes. Thus, the tube lengths are basically fixed for a given mass flow of warm liquid solution due to limited wetted area of the thin film. This was confirmed experimentally via droplet experiments, which will be treated in a following chapter.

In order to study characteristics, parametric tables are drawn up using EES, which has the ability to vary influential parameters.

4.3.5 THE DESIGNED CONCENTRATIONS

As has been mentioned earlier, the overall cycle of the aqua-ammonia desorption absorption heat pump is being modelled and designed by a Ph.D. candidate. The Ph.D. candidate designed the cycle to be reasonably below the maximum concentration possible at various points in the cycle, but specifically also in the absorber. There exists good motivation for having done this, in external literature:

- It was noticed by Fernández-Seara et al. (2005:287) that by keeping the weak solution concentration relatively low, mass transfer (thus absorption of the ammonia gas in water) was enhanced. This reduced the absorption tube lengths in their particular design.
- Cerezo et al. (2009:1008) decreased their inlet solution concentration from 33% (weight percent) to 29%, respectively, and noticed a significant increase in absorption flux.
- Cardenas & Narayanan (2010:1794) observed that when their weak solution inlet mass flow was at the lowest flow rate, complete absorption did not take place, as a higher concentration of aqua-ammonia was reached. They report a ‘driving force’ for mass transfer (absorption in this context) with lower concentrations, which become weaker when inlet concentrations were increased.

Indeed, a 'driving force' can physically be observed in the ammonia fountain experiment described in Chapter 3, where water is sucked up against a pressure height from a beaker at the bottom of the experiment to a flask at the top. This 'suction effect' is also desirable for the absorber component.

4.4 EXPOSITION OF THE THEORETICAL MODEL

The mathematical model which eventually calculates the heat transfer, consists of several different aspects which need consideration. These aspects include *convection for external flow*, *convection for internal flow*, the *general application of the ε-NTU-method*, the *calculation of the amount of heat generated* during the absorption process, *incorporating the heat generated heat into the ε-NTU-method*, dealing with the *solution concentration* and finally the *conservation laws*. Not all the background for the heat transfer calculations will be given from fundamental principles.

Furthermore, the equations given in this chapter for the standard heat transfer calculations were obtained from the detailed text of Incropera *et al*. (2007), with the study course notes of Van Eldik (2012) as supplement. The exceptions to using these two sources are: the concentration calculations, the calculation of the amount of heat transferred, incorporating the amount of heat generated in the ε-NTU-method and the conservation of mass and energy calculations.

The handy thermo-physical properties of EES were also used throughout, including the NH_3H_2O-procedure already mentioned. Whereas the basic principles are described in the coming sections, seven working models in EES were developed using these principles. One of them being a simplified model for easy reference, the other being for optimization purposes, which will be elaborated on in a subsequent section. Each aspect of the heat transfer model is now treated.

4.4.1 CONVECTION HEAT TRANSFER

Convection heat transfer takes place when heat is transferred between the surface of a solid, and a fluid moving over the surface (Incropera *et al*., 2007:348). The rate equation for convection heat transfer is generally characterized by the following equation, better known as Newton's Law of cooling:

$$q = \alpha A_s(T_s - T_\infty)$$

[4 - 1]

where q is the heat transfer rate, α the convection heat transfer coefficient, A_s the surface area over which heat transfer takes place, T_s the surface temperature and T_∞ the free stream temperature. Solving the heat transfer coefficient is at the heart of solving the problem of convection.

Further important parameters for convection heat transfer, are the following dimensionless parameters:

- The Reynolds number: $$Re = \frac{\rho V D}{\mu}$$

[4 - 2]

- The Prandtl number: $$P_r = \frac{c_p \mu}{k} = \frac{\nu}{\alpha}$$

[4 - 3]

- The Nusselt number: $$Nu = \frac{\alpha D}{k}$$

[4 - 4]

For the solving heat exchangers, the problem of convection is usually further divided into external flow and internal flow. These two cases are further treated below.

4.4.2 EXTERNAL FLOW

The external flow in this study takes place around the cylinder tubes inside the absorber component, with the warm, weak solution. The Reynolds number is for this purpose defined as a function of mass flow, and not velocity, since the velocity of the fluid over the tubes is not so easy to calculate:

$$Re_{hf} = \frac{4 \cdot \dot{m}_{hf}}{\pi \cdot D_o \cdot \mu_{hf}}$$

[4 - 5]

where $\dot{m}_{hf}$is the mass flow of the hot fluid, D_o is the outer diameter of the cylinder and μ_{hf} the viscosity of the fluid. The Nusselt number is calculated using the following empirical correlation, which is generally valid for both laminar and turbulent flow:

$$Nu_{hf} = 0.3 + \frac{0.62 \cdot Re_{hf}^{0.5} \cdot Pr_{hf}^{1/3}}{\left[1 + \left(\frac{0,4}{Pr_{hf}}\right)^{\frac{2}{3}}\right]^{0.25}} \cdot \left[1 + \left(\frac{Re_{hf}}{282000}\right)^{\frac{5}{8}}\right]^{\frac{4}{5}}$$

[4 - 6]

The Prandtl number (Pr) is easily calculated using a function in EES. Having calculated the Nusselt number above, the convection heat transfer coefficient is now calculated using the Nusselt number:

$$\alpha_{hf} = \frac{Nu_{hf} \cdot k_{hf}}{D_o}$$

[4 - 7]

Where α_{hf} is the convection heat transfer coefficient for the hot fluid and k_{hf} the conductivity of the hot fluid. Having used the above equations, the problem of external convection can now be solved.

4.4.3 INTERNAL FLOW

The internal cross sectional area of the cylinder is calculated:

$$A_i = \pi \cdot \left[\frac{D_i}{2}\right]^2$$

[4 - 8]

The velocity of the cold fluid flowing inside the cooling cylinder is calculated, so that it can be used in the Reynolds number calculation given by Eq. 4-2:

$$V_{cf} = \frac{\dot{m_{cf}}}{\rho_{cf} \cdot A_i}$$

[4 - 9]

The Nusselt number for the internal flow is calculated using the famous Dittus-Boelter correlation, which is applied differently for different conditions:

For $Re_{cf} < 2300$:

$$Nu_{cf} = 4.36$$

[4 - 10]

For $\mathrm{Re_{cf}} \geq 2300$:

$$Nu_{cf} = 0.23 \cdot Re_{cf}^{\frac{4}{5}} \cdot Pr^n$$

[4 - 11]

with $n = 0.4$ for the fluid heating and $n = 0.3$ for the fluid cooling.

With the above calculations done, the convection heat transfer coefficient can be calculated using Eq. 4-4, which solves the problem of internal convection.

4.4.4 APPLYING THE Ɛ-NTU-METHOD BEFORE ABSORPTION

Outlet temperatures without absorption were first calculated. The outlet conditions resulting from these calculations were named 'preliminary' conditions in the program. Since the average heat transfer coefficients for both external as well as internal fluid flow have been determined using the above equations, the thermal resistance can be calculated. The thermal conductivity *k* for the solid (in this case stainless steel) was easily called from EES's libraries and using the average temperature between the hot fluid inlet and cold fluid inlet.

The total thermal resistance (R_{tot}) is calculated as follows, starting with the convection of the hot fluid outside, going to the conduction of the stainless steel cylinder walls, and ending with the cold fluid inside the tubes:

$$R_{tot} = \frac{1}{\alpha_{hf} \cdot \pi \cdot D_o \cdot L_{pipe}} + \frac{ln\left(\frac{D_o}{D_i}\right)}{2 \cdot \pi \cdot k_{SSteel} \cdot L_{pipe}} + \frac{1}{\alpha_{cf} \cdot \pi \cdot D_i \cdot L_{pipe}} \quad [4 - 12]$$

with k_{SSteel} being the conductivity of stainless steel and L_{pipe} the length of the cylinders.

The following equations are standard to the ε-NTU-method. Let the subscripts 'hf' and 'cf' notate 'hot fluid' and 'cold fluid' respectively.

$$UA = \frac{1}{R_{tot}} \quad [4 - 13]$$

$$C_{cf} = \dot{m_{cf}} \cdot cp_{cf} \quad [4 - 14]$$

$$C_{hf} = \dot{m_{hf}} \cdot cp_{hf} \quad [4 - 15]$$

$$C_r = \frac{C_{min}}{C_{max}} \quad [4 - 16]$$

$$C_{min} = \min(C_{cf}; C_{hf}) \quad [4 - 17]$$

$$C_{max} = \max(C_{cf}; C_{hf}) \quad [4 - 18]$$

with *cp* being the specific heat capacity, C the overall heat capacity and C_r the heat capacity ratio.

$$\dot{Q}_{max} = (\dot{m}c_p)_{min}(T_{hf,i} - T_{cf,i})$$

[4 - 19]

$$NTU = \frac{UA}{C_{min}}$$

[4 - 20]

TABLE 4.1: RELATIONS FOR EPSILON FOR THE NTU-METHOD (ADAPTED FROM INCORPERA ET AL. (2007))

Nature of Cross-flow:	Relation:
1. Both fluids unmixed	$\varepsilon = 1 - \exp\left[\left(\frac{(\dot{m}c_p)_{max}}{(\dot{m}c_p)_{min}}\right) NTU^{0.22}. \left(\exp\left(-\frac{(\dot{m}c_p)_{min}}{(\dot{m}c_p)_{max}} NTU^{0.78}\right) - 1\right)\right]$
2. $(\dot{m}c_p)_{max}$ **mixed** $(\dot{m}c_p)_{min}$ **unmixed**	$\varepsilon = \left(\frac{(\dot{m}c_p)_{max}}{(\dot{m}c_p)_{min}}\right). \left(1 - \exp\left(-\left(\frac{(\dot{m}c_p)_{min}}{(\dot{m}c_p)_{max}}\right)(1 - \exp(-NTU))\right)\right)$
3. $(\dot{m}c_p)_{min}$ **mixed** $(\dot{m}c_p)_{max}$ **unmixed**	$\varepsilon = 1 - \exp\left[-\frac{(\dot{m}c_p)_{max}}{(\dot{m}c_p)_{min}}. \left(1 - \exp\left(-\frac{(\dot{m}c_p)_{min}}{(\dot{m}c_p)_{max}} NTU\right)\right)\right]$

$\dot{Q}_{max}$ is the maximum theoretical heat transfer possible under the physical circumstances, which is calculated between the inlet temperatures of both hot and cold fluids, and with the minimum heat capacity. The NTU is the number of transfer units.

Having chosen the correct formula for ε from Table 9 with a specially written procedure in EES, and using the previously calculated values for all the variables required, a value is calculated for ε (the heat exchanger effectiveness) and the actual amount of heat transferred ($\dot{Q}$) can be calculated using the following formula:

$$\dot{Q} = \varepsilon \cdot \dot{Q}_{max}$$

[4 - 21]

The amount of heat transferred will be the same for both the hot and the cold fluids. With this important parameter known, the new preliminary temperatures for both fluids arecalculated with the following energy equations:

$$\dot{Q} = \dot{m}_{cf} cp_{cf} (T_{cf,out,prelim} - T_{cf,in})$$

[4 - 22]

$$-\dot{Q} = \dot{m}_{hf} (h_{hf,out,prelim} - h_{hf,in})$$

[4 - 23]

Using the outlet enthalpy ($h_{hf,out,prelim}$) calculated for the hot fluid (aqua-ammonia mixture outside the cylinders), the outlet temperature is determined using the EES NH_3H_2O function. It will be explained later why enthalpy, and not temperature was used for the hot fluid calculations. Furthermore, it should be noticed that these outlet conditions are the preliminary outlet conditions obtained, before any absorption has taken place. For the first top row of the cylinders in the absorber component, these properties will serve as the outlet properties, since it is assumed that no absorption takes place around this row. However, for the remaining rows of tubes below it, further calculations remains to be done.

4.4.5 CONCENTRATION CALCULATIONS

Having done the preliminary heat transfer calculations, basic calculations can now be done which will determine the new concentration of the aqua-ammonia mixture after absorption. Let x_{in} be the concentration (in weight percent) of the incoming solution and the subscripts be of further explanation, so that:

$$NH_{3\ in\ solution} = x_{in} \cdot \dot{m}_{hf,tot}$$

[4 - 24]

$$H_2O_{in\ solution} = (1 - x_{in}) \cdot \dot{m}_{hf,tot}$$

[4 - 25]

$$NH_{3,tot} = NH_{3,in\ solution} + \dot{m}_{NH_3}$$

[4 - 26]

where $\dot{m}_{NH_3}$ is the mass flow of ammonia gas entering the absorber and $\dot{m}_{hf,tot}$ be the total incoming mass flow of the weak solution. Let $\dot{m}_{hf,abs,tot}$ be the new total mass flow of the solution *after* absorption:

$$\dot{m}_{hf,abs,tot} = NH_{3,tot} + H_2O_{in\ solution}$$

[4 - 27]

The new concentration (if all ammonia gas has been absorbed) will then be:

$$x_2 = \frac{NH_{3,tot}}{\dot{m}_{hf,abs,tot}}$$

[4 - 28]

The new concentration calculated above is then correlated with the maximum concentration possible at the given temperature and pressure using the *correlation* developed in Chapter 3. This is to make sure that an unrealistic concentration is not worked with. If a too high mass flow of ammonia gas was introduced in the absorber, this would be the case. The following calculations are done to make sure that the concentration calculated in Eq. 4-26 is below the maximum concentration possible.

The Henry's law constant at the given outlet preliminary temperature is next calculated:

$$k_{HK} = 0.0341 \cdot \exp(0.0296 \cdot T_{hf,out,prelim})$$

[4 - 29]

Next, the maximum concentration in $[NH_3/H_2O]_{kg}$ is calculated using Henry's law:

$$c = \frac{P_{NH_3}}{k_{HK}}$$

[4 - 30]

The maximum concentration is converted back to the standard 'weigh percent' measure, via the method that was derived earlier in Chapter 3. This is done primarily because the NH_3H_2O procedure of EES works in weight percent. Thus:

$$x_{max} = c \cdot \left[\frac{1}{c+1}\right]$$

[4 - 31]

The final outlet concentration is determined by taking the minimum of the two concentrations calculated thus far. Thus, should the concentration calculated in Eq. 4-28 go over the maximum possible concentration, only the maximum concentration will be chosen as the final outlet concentration:

$$x_{out} = \min(x_2; x_{max})$$

[4 - 32]

The above thus calculates the outlet concentration of the strong solution of aqua-ammonia fluid exiting the absorber, for any given inlet mass flows of weak solution and ammonia gas. The heat generated in this absorption process needs to be dealt with next.

4.4.6 CALCULATION OF THE AMOUNT OF HEAT GENERATED DUE TO THE EXOTHERMIC ABSORPTION PROCESS

A mass-energy balance has carefully been constructed in order to calculate the amount of heat generated. The EES procedure NH_3H_2O also needed to be used correctly and carefully in order to make this possible. Consider briefly the following portion of EES program code:

```
CALL NH3H2O(123; T_hw[i]; P_b; x_in : xza[i]; xzb[i]; xzc[i]; h[i];
s[i]; u[i]; v[i]; q[i])

CALL NH3H2O(123; T_hw[i]; P_b; x_out[i] : xza[i+7]; xzb[i+7];
xzc[i+7]; h[i+7]; s[i+7]; u[I+7]; v[i+7]; q[i+7])
```

In the above program code, the EES procedure was asked to calculate the enthalpies of the hot aqua-ammonia mixture just *before* and just *after* the absorption process. This is in order to be capable of calculating the heat generated in the mass-energy balance. There are three degrees of freedom in this binary system for aqua-ammonia. The desired results were obtained by keeping all the inlet parameters constant except the concentration. The inlet concentration is that which came into the absorber, and the outlet concentration is that which was calculated above. By keeping the temperature constant in the procedure, the mass-energy balance can tell *how much heat needs to be removed in order to keep the temperature constant*. This amount of heat is equal to the heat generated during the absorption process.

The mass-energy balance is given below. It is based on the First Law of Thermodynamics, which implies that the total amount of energy before absorption is equal to the total amount of energy after absorption. Note that some of the mass flows in the mass-energy balance are divided by seven. This is due to the fact that the hot stream is divided into seven streams due to seven columns of absorber cooling cylinders. Refer to the figure below to see the vertical divisions of the cylinders:

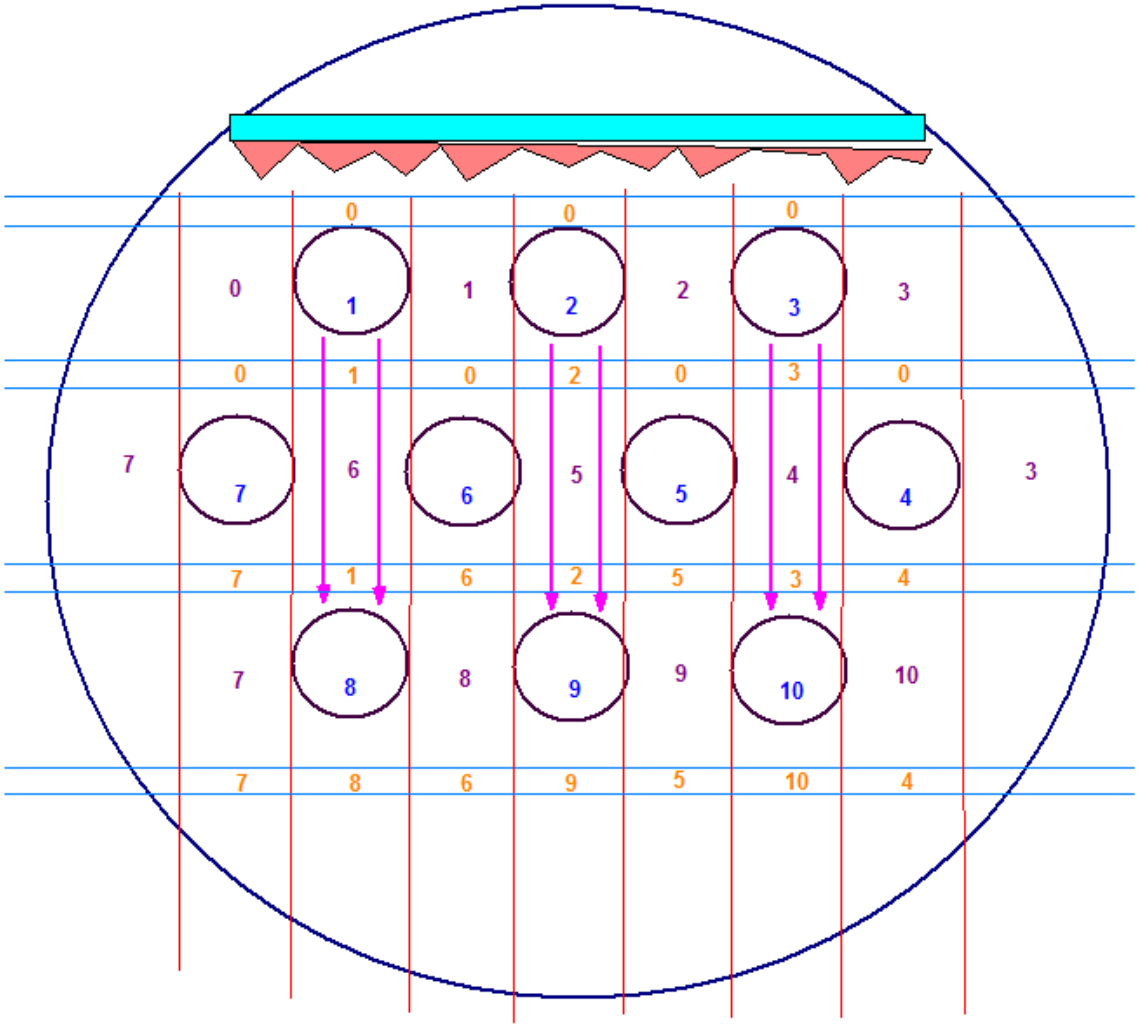

FIGURE 4.3: SCHEMATIC ILLUSTRATION OF THE CYLINDERS IN THE ABSORBER

The numbers in the illustration above were used as an aid in the programming of the EES model (and are not indicative of the number of columns of tubes). Where the mass flow is not divided in the balance, a separate parameter has already been created earlier which divides the mass flow according to the physical geometry. The amount of heat generated in each stream is calculated separately. The mass-energy balance is:

$$\frac{\dot{m}_{NH_3}}{7} \cdot h_{NH_3} + \dot{m}_{hf} \cdot h_{hf,pre-absorption} = \frac{\dot{m}_{hf,abs,tot}}{7} \cdot h_{hf,post-absorption} + \dot{Q}_{gen}$$

[4 - 33]

where *h* indicates the various enthalpies and $\dot{Q}_{gen}$ the amount of heat generated in the process.

Alternatively, Herold *et al*. (1996:73) gives another method to calculate the heat generated ($\dot{q}_{gen}$), in specific units:

$$\dot{q}_{gen} = h_{NH_3} - h_{weak-solution} + f(h_{weak-solution} - h_{strong-solution})$$

[4 - 34]

where *f* is defined as a mass ratio:

$$f = \frac{\dot{m}_{strong-solution}}{\dot{m}_{NH_3-gas}}$$

[4 - 35]

These two methods of calculating the heat generated were tested in a separate EES-program. It was found that the answers calculated yielded exactly the same value, if the specific heat calculated in Eq. 4-34 was multiplied by the correct mass flow in order to obtain the answer in kW. However, the method of Eq. 4-33 was preferred and used in the EES models, since the program was sometimes tested by setting the ammonia vapour mass flow to zero in order to test the program. This testing method resulted in division by zero Eq. 4-35 when the second method was used. Nonetheless, it is satisfying to see that both these methods yield the same results, and the latter method validates the former.

4.4.7 INCORPORATING THE HEAT GENERATED INTO THE Ɛ-NTU METHOD

Seeing the fact that the heat has been generated in the already hot solution of aqua-ammonia, the heat generated is now incorporated into this stream of fluid. A new enthalpy and temperature is calculated, as this stream of fluid heats up even further due to the heat generated. The properties obtained will be named 'transitional', since these are not the final outlet properties as yet.

$$\dot{Q}_{gen} = \frac{\dot{m}_{hf,abs,tot}}{7} \cdot (h_{hf,transitional} - h_{hf,out,preliminary})$$

[4 - 36]

Having calculated the transitional enthalpy, the corresponding *transitional temperature* is obtained by calling the NH_3H_2O procedure of EES.

Next, the ε-NTU method is applied 'halfway', now working with the preliminary outlet properties of the cold stream cooling water, and the transitional properties of the hot stream of aqua-ammonia. The new properties are denoted with a subscript '2'.

$$C_{hf,2} = \frac{\dot{m}_{hf,abs,tot}}{7} \cdot cp_{NH3H2O}$$

[4 - 37]

In the above equation, a correct mass flow needs to be used, due to the fact that the ammonia gas has now been absorbed into the aqua-ammonia solution.

$$C_{cf,2} = \dot{m}_{cf} \cdot cp_{cf}$$

[4 - 38]

$$C_{min,2} = \min\left(C_{cf,2}; C_{hf,2}\right)$$

[4 - 39]

Finally, a new theoretically possible maximum heat transfer rate of heat transfer between the hot and the cold fluids can be calculated, which takes the absorption heat into account. This new maximum is calculated once more between the *preliminary* outlet temperature of the cold stream, and the *transitional* temperature of the hot stream. The transitional temperature is what has taken the heat generated into account. Thus:

$$\dot{Q}_{max,2} = C_{min,2}\,(T_{hf,transitional} - T_{cf,preliminary})$$

[4 - 40]

Next, the new *actual* heat transfer rate that will take place is calculated. This heat transfer rate takes thermal resistance into account and works with the effectiveness of the heat exchanger:

$$\dot{Q}_2 = \varepsilon \cdot \dot{Q}_{max,2}$$

[4 - 41]

With the new heat transfer rate known, the new temperatures for each stream after absorption is calculated.

For the cold stream:

$$\dot{Q}_2 = \dot{m}_{cf} \cdot cp_{cf}(T_{cf,abs} - T_{cf,preliminary})$$

[4 - 42]

where $T_{cf,abs}$ is now the temperature of the cold fluid after absorption.

For the hot stream, the generated heat surfaces again in the energy balance. The net amount, which the hot stream will heat up, will be due to the difference between heat generated and the heat that can actually be removed again in the heat exchanger and will go to the cold stream of fluid. This calculation is done between the preliminary outlet enthalpies of the hot fluid, and the final outlet enthalpy after absorption. The transitional temperature does not surface here again. This can be mathematically expressed as:

$$\dot{Q}_{gen} - \dot{Q}_2 = \frac{\dot{m}_{hf,abs,tot}}{7} \cdot (h_{hf,abs} - h_{hf,out,preliminary})$$

[4 - 43]

Having calculated the outlet enthalpy of the hot fluid, the corresponding outlet temperature can be obtained via the NH_3H_2O procedure in EES.

Finally, the seven streams of hot fluid are brought together again at the bottom of the absorber component. The final temperature of the combined stream is then calculated by adding up the product of the mass and temperature (of each stream), and dividing it by the total mass of the hot fluid. The final cold fluid temperature will be calculated according to the configuration in which the cooling tubes are connected to each other. In the case of connection in series, the cold stream's outlet temperature will be that already calculated in Eq. 4-42. In the case where the cooling tubes are connected in parallel, the temperature will be calculated in principle as has been done with the hot stream. Elaboration on the seven models for the different configurations will be done in a subsequent chapter.

4.4.8 THE CONSERVATION OF MASS AND ENERGY IN THE SYSTEM

As with any thermodynamic system, the laws of conservation of mass and energy also need to be satisfied for the model presented. The total mass and energy that enter the system boundary must be equal to the total mass and energy leaving the system. The following equations give the method with which the mass and energy entering and leaving the system were calculated. Let the subscripts explain each parameter further.
For the energy balance:

$$E_{in} = \dot{m}_{hf,tot,in} \cdot h_{hf,in} + \dot{m}_{cf,in} \cdot h_{cf,in} + \dot{m}_{NH_3} \cdot h_{NH_3}$$

[4 - 44]

$$E_{out} = \dot{m}_{hf,abs,tot} \cdot h_{hf,abs,out} + \dot{m}_{cf,out} \cdot h_{cf,out}$$

[4 - 45]

For the mass balance:

$$\dot{m}_{in} = \dot{m}_{hf,tot,in} + \dot{m}_{cf,in} + \dot{m}_{NH_3}$$

[4 - 46]

$$\dot{m}_{out} = \dot{m}_{hf,abs,tot} + \dot{m}_{cf,out}$$

[4 - 47]

The results of the mass and energy balances will be explained in the chapter giving the results of the model.

4.4.9 OBSERVATIONS SURROUNDING THE THEORETICAL MODEL

A few general observations around the theoretical model need to be made, which are significant. The observations are divided in the categories that follow.

4.4.10 HEAT CAPACITY VERSUS ENTHALPY VALUES FOR CALCULATIONS

The careful observer reading through the equations given, would have noticed something different about the energy equations (for example Eq. 4-23) dealing with the hot stream of fluid. Throughout the mathematical model, using the *specific heat capacity* (at constant pressure) of aqua-ammonia was avoided as far as possible. It was discovered during the development of the model, that using the *specific heat capacity* does not always yield realistic outlet temperatures.

The heat capacities of thermodynamic mixtures can usually be calculated by using weighted averages (see Eastop & McConkey (1978)). However, for aqua-ammonia, Herold *et al*. (1996:66) gives the following equation (just with slightly different notation) for the specific heat capacity (at constant pressure):

$$cp_{NH3H2O} = x \cdot cp_{NH_3} + (1 - x) \cdot cp_{H_2O} - \left[\frac{dq}{dT}\right]_{P,x}$$

[4 - 48]

As can be seen in Eq. 4-48, the heat capacity of the mixture is indeed a weighted average, but there is an additional term involved (the last term in the equation). This is a so called mixing term (Herold *et al*., 1996:67). This term appears to be non-zero when additional ammonia gas is absorbed into the aqua-ammonia solution, and is the possible reason for the discrepancies observed. This likely implies that when aqua-ammonia mixtures undergo phase or state change, calculating specific heat values become more cumbersome. Thus, enthalpy values were used as far as possible for calculations surrounding the hot fluid.

Where it was not possible to use enthalpy values, the cp-values were employed as a last resort.

4.4.11 POSSIBLE IMPROVEMENT ON THE METHOD FOR THE INCORPORATION OF GENERATED HEAT IN THE Ɛ-NTU-METHOD

At the heart of the ε-NTU method, is the calculation of how effective the heat exchanger actually is for transfer heat. This effectiveness is dependent on a number of parameters, including the thermal resistance, which in turn is dependent on the convection heat transfer coefficient.

A possible theoretical improvement to the method outlined in section 4.4.12 would be to calculate a new effectiveness (ε) for the heat exchanger using the preliminary conditions for the cold fluid, and the transitional conditions for the hot fluid. This *new* effectiveness could then be used to calculate the actual heat transfer rate. Time did not permit this improvement to be made to all seven programs or simulations developed, since the simulation program architecture became reasonably complex. However, one simulation was indeed adapted with the above-mentioned improvement, and the outlet temperature of the strong solution (the hot stream) was used as a measure to see what the actual difference is. Keeping all the input parameters constant, it was found that the outlet temperatures differed by only 1.5% (if the temperature is taken in degrees Celsius). This means that the difference is negligible in this case. This is probably due to the fact that the thermodynamic properties involved in calculating the convection heat transfer coefficients did not vary much with the differences in temperature that occurred. The same would likely not be the case if the hot and cold fluid streams were gases.

Thus, in summary: there is theoretically an improvement that can be made to the method already developed in this study. However, it was found that in this context, the improvement is negligible and it was not worth spending the time to change the complex architecture of the models. The improvement is recommended when one or two gases are used as a fluid, which exchanges heat, however.

4.4.12 OTHER THERMODYNAMIC PROPERTIES AND EES 2016

In order to eventually calculate the *convection heat transfer coefficient*, a number of fluid properties are needed. These properties include the *conductivity*, *density*, *viscosity* and the

Prandtl number. EES had a separate function under its 'Brines' library for calculating these properties for aqua-ammonia mixtures. These properties were not part of the standard NH_3H_2O-procedure which was commonly used throughout the program (even though the density could have been calculated via taking the inverse of specific volume). Thus, it was attempted to use the Brines-library function.

However, it was soon discovered that the Brines-function could only go to a concentration of 30%, with a temperature limit as well. Higher concentrations and certain temperatures were not defined, and out of range for the function, which prevented the program to solve. The strategy used to overcome this problem, was to call the properties of pure liquid water, when the concentration and temperature exceeded the range.

When EES 2016 was published in late 2015, it was discovered that the EES-developers had created yet a new function for ammonia-water mixtures (in addition to the existing Brines-function and NH_3H_2O procedure). This new function was indeed capable of calculating properties for higher concentrations and temperatures, which was good news. The function was immediately incorporated into all the programs. Nonetheless, the accuracy of the previous strategy was tested by drawing comparisons even before the new EES 2016-function saw the light. This was done because the new function in EES is not perfected yet, and future modellers might be interested to know how accurate the results obtained are, should a similar problem be encountered in the future. The strong solution outlet temperature was once again used as a 'litmus test' to calculate the effect of the approximation of using water's properties. The following table gives the differences for each of the seven configurations. The inlet concentration of the weak solution was set to 29% (weight percent), which was still in range for the Brines-function. One set of programs used the Brine-function, and the other set used liquid water. The numerical value varies somewhat between choosing degrees Celsius or Kelvin as reference to do the difference calculation, thus both temperature units were used. The results were as follows:

TABLE 4.2: OUTLET TEMPERATURE DIFFERENCE DUE TO WATER VS BRINES PROPERTIES

Heat Exchanger (Absorber) Configuration	Outlet temperature difference [K]	Outlet temperature difference [˚C]
	[%]	[%]
1 Cylinder	1,78	8,67

10 cylinders 3 rows in *series*	0,32	1,21
10 cylinders 3 rows *series-parallel*	0,32	1,20
10 cylinders 3 rows *parallel*	0,32	1,20
14 cylinders 4 rows *series*	0,27	1,01
14 cylinders 4 rows *series-parallel*	0,27	1,01
14 cylinders 4 rows *parallel*	0,27	1,01
Average difference:	0,51	2,19

It can clearly be observed that the difference in the strong solution outlet temperature is within a reasonable range, with the averages of 0.51% and 2.19% respectively, and with one outlier value, which gave differences of 1.75% and 8.67% respectively.

Thus, should the modeller of an aqua-ammonia system find lacking the previously mentioned properties for calculating the convection heat transfer coefficient, a reasonable approximation can be made by using the properties of liquid for water.

In order to minimize errors however, the new 2016 EES function was nonetheless fully incorporated into the simulations developed. It is also suspected that at higher concentrations for the incoming weak solution, the error might become more significant, but no testing was done for higher concentrations to confirm this.

4.5 CONCLUDING REMARKS

In this chapter, the theoretical model developed has been discussed in detail. Not only was the theoretical model presented mathematically, but also important surrounding issues discussed. Motivations were given for this particular layout and architecture, assumptions made stated and the general approach followed was carefully outlined. Strategies followed to overcome certain challenges were also briefly discussed. This chapter should thus enable the reader to understand the most important principles surrounding the theoretical model developed for the absorber component in this study. The theoretical model in return, offers special insight into the behaviour of the absorber component, which enables predictability and design.

5. RESULTS

5.1 INTRODUCTION

The fundamentals of the theoretical model(s) and the handling of the problems have been set forth in Chapter 4. In this chapter, the absorber component in this study will be characterised using the simulation models developed in EES. Indeed, characterization is one of the main purposes for developing these models. This in turn saves the designer costs, as a portion of the behaviour can be established before any component has been physically built. In the case of this study, this is particularly important, as many of the components have to be manufactured from stainless steel, which can turn out to be expensive. Characterization and simulation can also potentially be of aid to the designers of other components in the larger heat pump cycle. Simulations are, for example, capable of predicting outlet parameters and conditions if they are correctly designed. In this chapter, the influences of various parameters on the performance will be studied using the models developed. An optimization attempt will be explained, as well as verification and validation done.

5.2 SEVEN SIMULATIONS DEVELOPED AND OPTIMIZED

It has been briefly mentioned in Chapter 4 that seven different configurations for the absorber component have been simulated. Details on the exact differences between these configurations were not discussed yet. In this chapter, the seven simulations for the seven configurations will be explained and then used for the purpose they were developed.

5.2.1 EXPLANATION OF THE SEVEN SIMULATION MODELS

The main differences between the seven simulations lie in the way the cooling water tubes are arranged. Six of the seven simulation models follow the *basic* architecture given in Chapter 4, and specifically Figure 4.1. The differences lie in the way these cooling tubes are connected to each other.

One of the seven configurations is a single cylinder. Hot, warm weak solution flows on the outside, while cooling water flows in the inside. The following picture illustrates the basic principle:

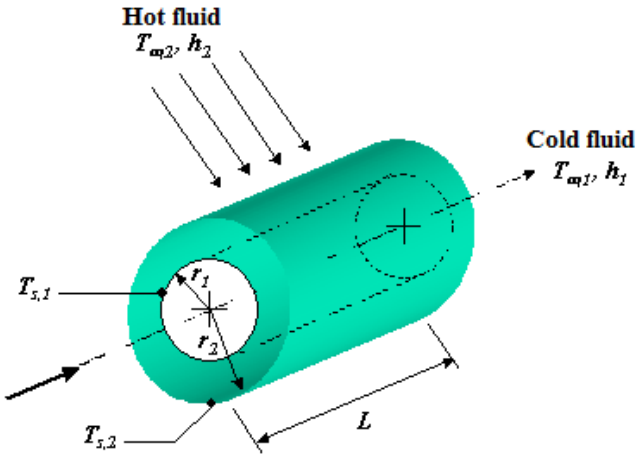

FIGURE 5.1: BASIC ILLUSTRATION OF THE SINGLE CYLINDER MODEL (FROM INCROPERA ET AL., 2007).

This configuration and model was programmed mainly for the purpose of having a reference model. Indeed, this model is much simpler than the remaining six models, and comparing the more complex models to the simple one, gave an indication of possible errors (in the remaining more complex models). It was also easier to test and implement the basic principles developed by starting with a simpler model and program.

As for the heat exchanger configuration performance, it was possible to draw up a graph for the single cylinder configuration. The graph divides the process the same way the problem is solved. First, the pre-absorption process is displayed (as pre-cooling), with absorption following. Upon considering the graph in Figure 5.2 carefully, it can be seen that the single cylinder heat exchanger follows a parallel-configuration trend in the pre-absorption region, even though the configuration is technically a cross-flow configuration. Next, with absorption taking place and the heat generated *in situ*, both the hot and the cold streams end up at higher temperatures than with which they entered. Indeed, Cerezo et al. (2009:1007) observed this phenomenon as well, as mentioned in Chapter 4. Due to the program architecture of the six more complex simulations, similar graphs could not be compiled for them. Thus, in this case as well, the single cylinder configuration serves as a reference.

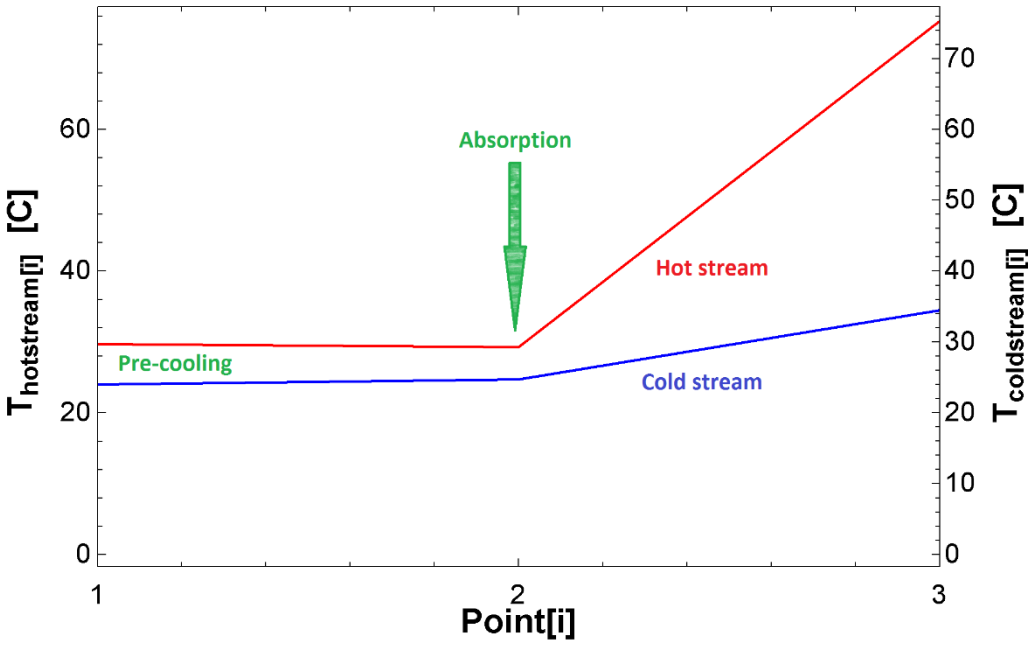

FIGURE 5.2: SINGLE CYLINDER HEAT EXCHANGER PERFORMANCE WITH ABSORPTION

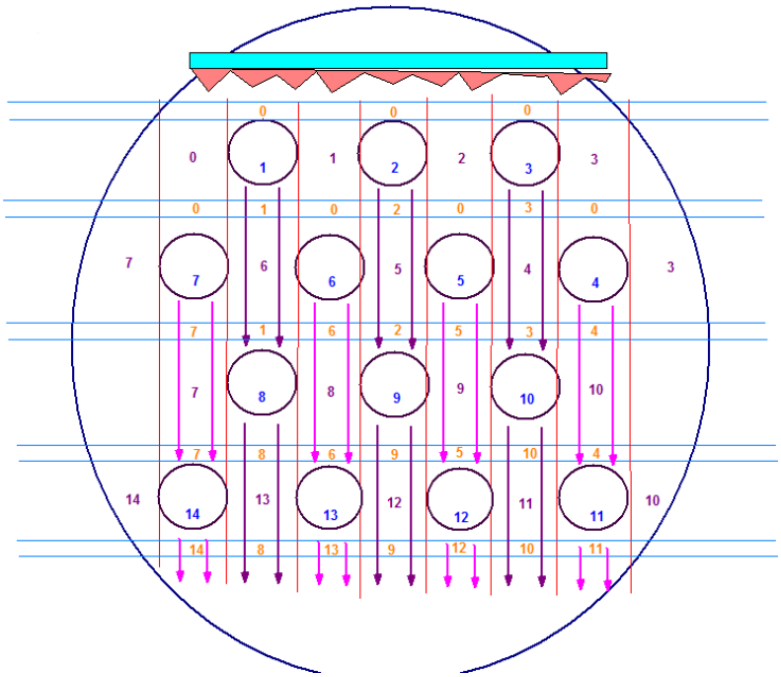

FIGURE 5.3: ABSORBER CONFIGURATION WITH 4 ROWS OF COOLING TUBES

The remaining six configurations (and simulations) fall into two categories. Each category has three variations. The first category has 10 cooling tubes arranged into 3 rows (Figure

4.1), and the second variation has 14 cooling tubes arranged into 4 rows. The latter is illustrated in Figure 5.3 above. Each of these two categories has three variations, these are named *series*, *parallel* and *series-parallel*. This nomenclature refers to *the way* that the individual cylinders are connected to one another. The following table gives a more exact explanation of what this means:

TABLE 5.1: EXPLANATION OF THE CONFIGURATION NOMENCLATURE

Nomenclature	Explanation
SERIES	Cooling water enters the absorber and enters one cooling tube in the top row. Each cooling tube is connected to the next, such that the outlet of one cooling tube is the inlet of the next cooling tube in the row. The last cooling tube in a row is connected to the first cooling tube in the next row below it. The final cooling water outlet comes from the last cooling tube in the bottom row.
PARALLEL	Cooling water enters the absorber, and then splits up into 10 or 14 streams via a manifold (depending on the variation at hand), so that each cooling tube receives fresh cold water, which has not exchanged heat anywhere yet. The outlets of all the cooling tubes come together again to form a main stream. No cooling tube's outlet is connected to another cooling tube's inlet.
SERIES - PARALLEL	This configuration is a combination of the above two configurations. Cooling water enters the absorber and splits up into 3 or 4 streams, depending on the number of rows. Each row's cooling tubes are connected in series, meaning the outlet of one tube is the inlet of the next in the row. However, all the rows of tubes are connected in parallel, meaning one row does not receive cooling water from another adjacent row, but directly from the main cooling water inlet, which has not exchanged heat yet. All the final outlets of the rows eventually come together again to form the final outlet stream. No heat is exchanged after this step.

Having two categories of absorber cooling tube layouts, gives six configurations in total, with the above configurations. For each of these configurations, a simulation was developed in EES. The purpose of developing these different variations, was to attempt *optimization* thereof. It was hoped that one of these variations will perform better than the others, while using the same *amount* of cooling tubes and cooling medium (in one particular category). The category of 4 rows of cooling tubes was added to see whether it would be worthwhile to add a fourth row in terms of the strong solution outlet temperature.

The idea to develop models with different cooling water circuitry, comes from an old computer program from the National Institute of Science and Technology (NIST) in the USA, named EVAP-COND (which presumably stands for 'evaporator' and 'condenser'). One of the features of EVAP-COND, is to attempt optimization via trying different circuit configurations. EVAP-COND can unfortunately not be used in the context of aqua-ammonia, but the idea is worth testing via developing programs in EES.

5.2.2 RESULTS FROM THE SEVEN CONFIGURATIONS

In this section, the results from the optimization attempt are given. The performance of the six different variations is set forth and compared. Besides the process of absorption itself, one of the purposes of the absorber component is to remove generated heat from the aqua-ammonia mixture. For this reason, the strong solution outlet temperature is selected as the parameter on which the different configurations will be judged. Other parameters will also be studied, where necessary. Parametric studies were done on all the models, where the strong solution outlet temperature is calculated and plotted as a function of the cooling water mass flow rate. The following conditions were input parameters for the graphs that were drawn up, unless otherwise stated.

TABLE 5.2: INPUT VALUES FOR COMPARISON BETWEEN DIFFERENT ABSORBER CONFIGURATIONS

Inputs		
	[K]	**[°C]**
Warm weak solution (NH_3H_2O) inlet temperature	302,85	29,7
	[kg/s]	**[g/s]**
Warm weak solution (NH_3H_2O) mass flow	0,003006	3,006
	[NH_3/(NH_3 + H_2O)]kg	
Warm weak solution inlet (NH_3H_2O) concentration	0,3427	

	[kPa]	[Bar]
System Pressure	700	7
	[K]	[°C]
Cold water inlet temperature	297,15	24
	[kg/s]	[g/s]
Cold water mass flow	0,03239	32,39
	[K]	[°C]
Ammonia-gas inlet temperature	288,26	15,11
	[kg/s]	[g/s]
Ammonia-gas inlet mass flow	0,0005986	0,5986
	[kPa]	[Bar]
Ammonia-gas partial pressure	236.2	2,36
	[m]	[cm]
Cooling pipes length	0,096	9,6
	[m]	[cm]
Cooling pipes outside diameter	0,012	1,2

In the comparative graphs that follow, the cooling water mass flow was varied, in order to see what the effect would be on the strong solution outlet temperature.

The graphs are marked with numbers 1, 2 and 3, where:

- 1 = series configuration.
- 2 = parallel configuration.
- 3 = series-parallel configuration.

The graph for the variation with 3 rows and 10 cooling cylinders is given first, with the 4 rows and 14 cooling cylinders following. The results are as follows:

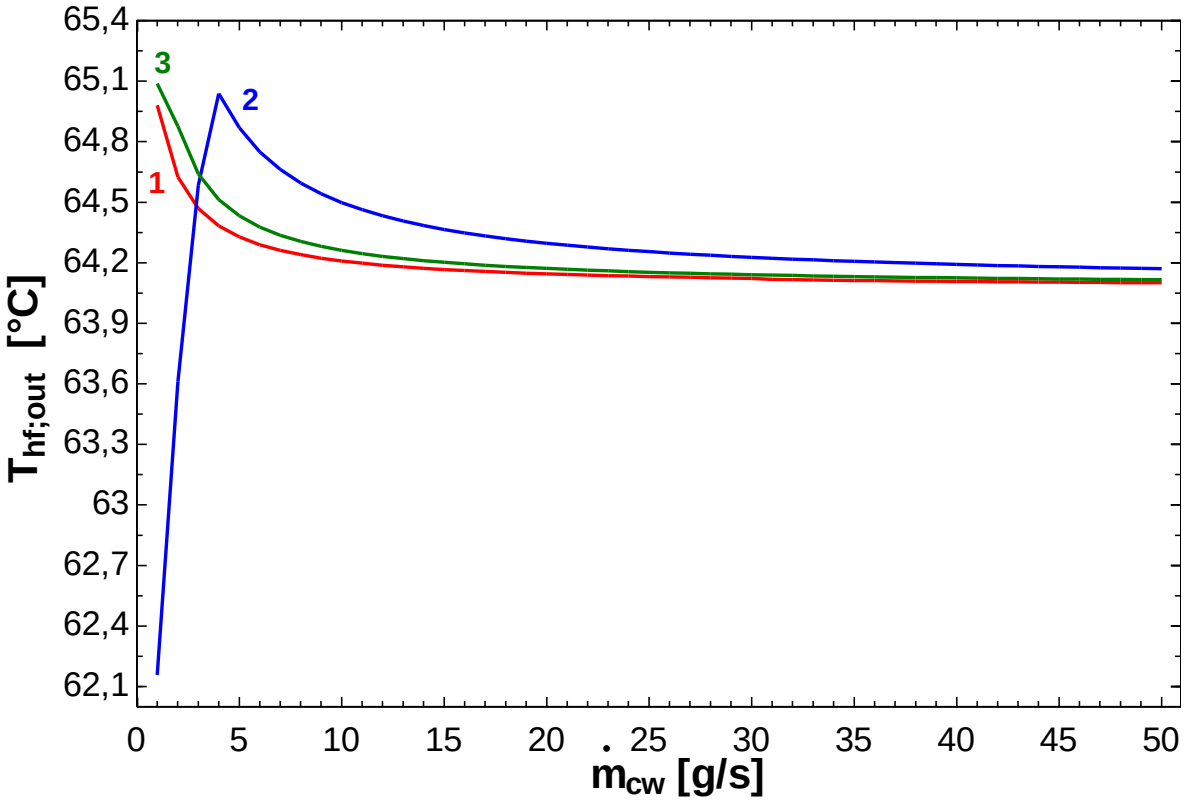

FIGURE 5.4: STRONG SOLUTION OUTLET TEMPERATURE VS COOLING WATER MASS FLOW FOR 3 ROWS AND 10 CYLINDERS

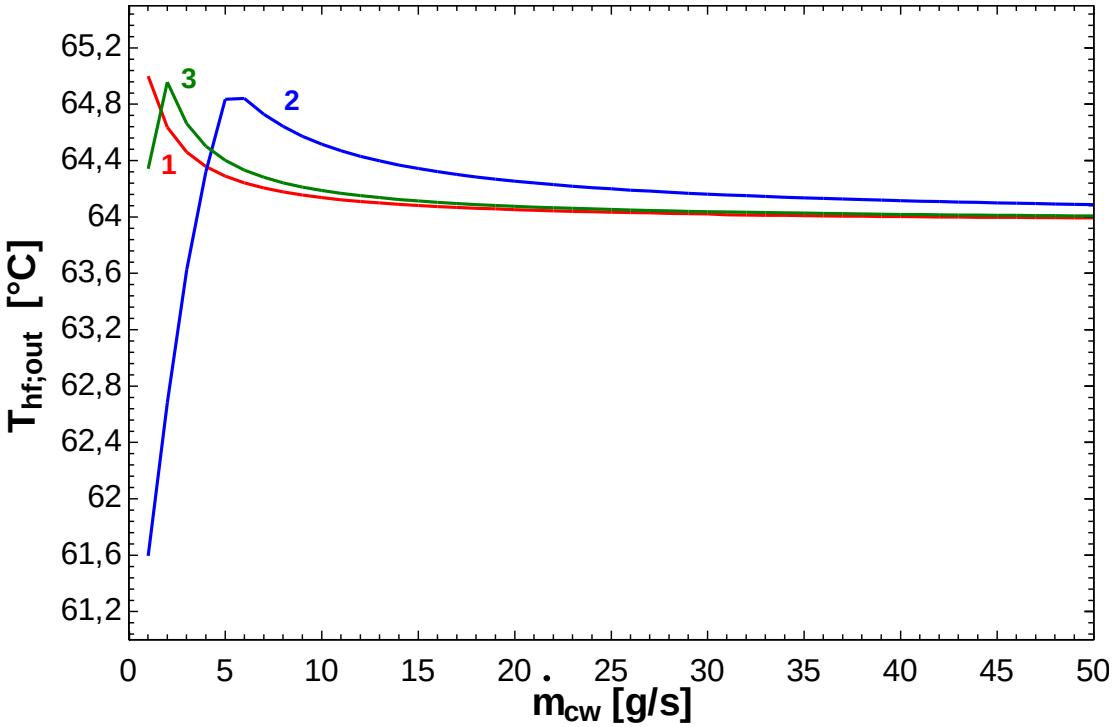

FIGURE 5.5: STRONG SOLUTION OUTLET TEMPERATURE VS COOLING WATER MASS FLOW FOR 4 ROWS AND 14 CYLINDERS

The following conclusions are made from the above graphs:

- The optimization attempt is only meaningful at low cooling water mass flows. It can be clearly seen that a certain value or range for cooling water mass flow exists where after all three configurations converge to the same outlet temperature for the strong solution (within a small range).
- In addition to the above, it is thus seen that simply keeping on increasing the cooling water mass flow beyond a certain point, would not lead to better cooling ability.
- The parallel flow configuration gives both the best and the worst performance in the low cooling water mass flow range between 1 to 6 g/s.
- The series-parallel configuration shows the same behaviour as the series configuration in the variation with 3 rows and 10 cylinders, but the addition of a 4th row and 4 more cylinders introduces parallel behaviour in the low mass flow range.

5.2.3 OBSERVATIONS REGARDINGTHE PARALLEL CONFIGURATION.

The behaviour of the parallel flow configuration seems puzzling at first, but can likely be explained by the following hypotheses:

- When the total cooling water mass flow is low, for example 1 g/s, the parallel configuration brakes the mass flow up even further into 10 and 14 streams, respectively. This means that for a cooling water mass flow of 1 g/s, the mass flow in each individual cylinder would be 100 and 71 mg/s, respectively. This is a very low mass flow, which likely allows residence time for more heat to be transferred to the cooling water.
- At approximately 3 to 5 g/s of cooling water mass flow, there is no longer the same amount of residence time which allows as much heat transfer to the cooling water, but here the flow is very laminar. After the apex, the Reynolds number of the cooling water starts to increase enough to allow better heat transfer once more, and the strong solution outlet temperature start to drop again.

The above explanations may also explain why the ‘parallel behaviour’ starts to manifest in the *series-parallel* configuration with 4 rows and 14 cooling cylinders. In this case, the cooling water mass flow is divided into 4 streams instead of 3.

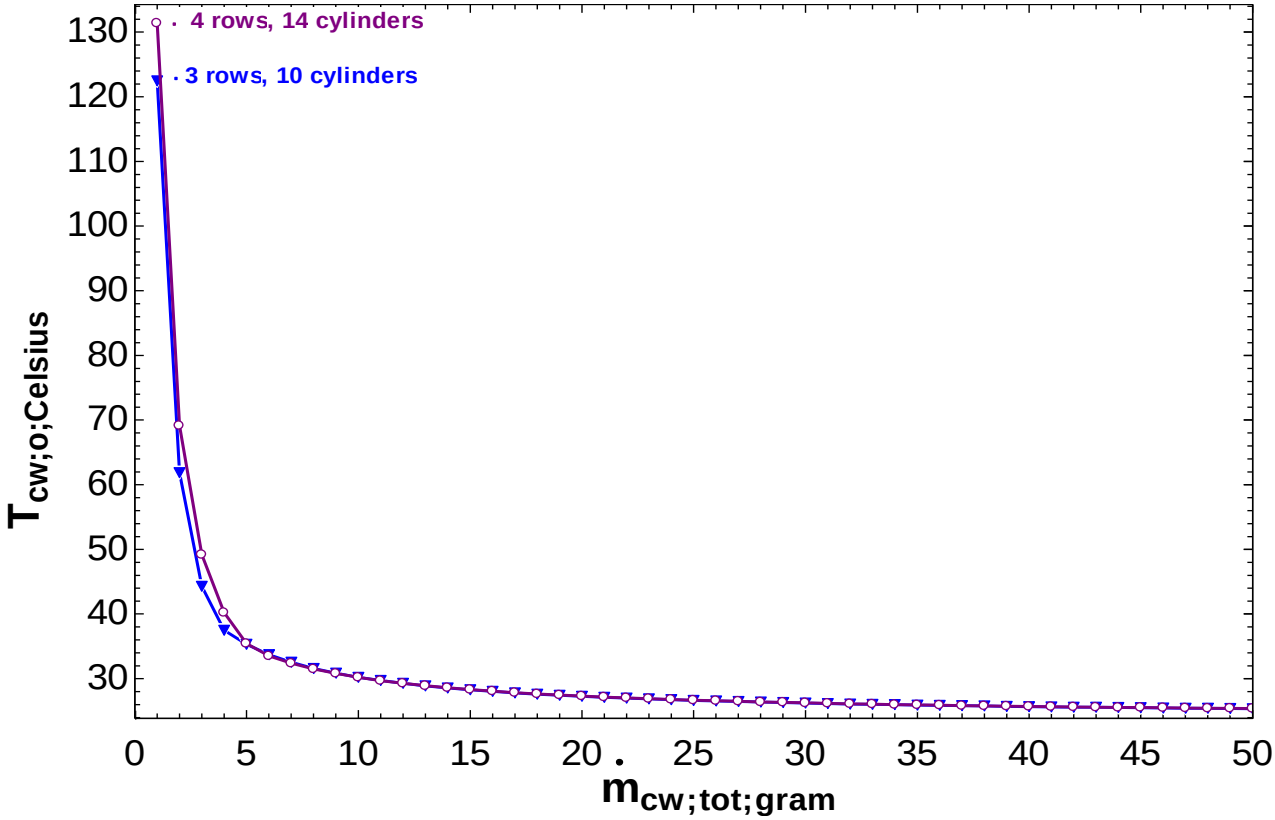

FIGURE 5.6: COOLING WATER OUTLET TEMPERATURE VS COOLING WATER MASS FLOW

In the light of the above explanations, the cooling water outlet temperature is now considered via the graph above (Fig. 5.6) as a function of cooling water mass flow, where the cooling water is at 150 kPa pressure. The graph above does tend to lend support to the hypotheses set forth as explanation for the parallel-flow behaviour. It can be clearly seen that for the lowest mass flow (1 g/s), the outlet temperature is exceptionally high. Similar graphs for the other configurations show much lower cooling water outlet temperatures for 1g/s cooling water mass flow. The *series* configuration (3 as well as 4 rows) give an outlet temperature of about 35°C, while the *series-parallel* configuration yield outlet temperatures of 35°C and 45°C for 3 and 4 rows, respectively.

The above observations and graph have important practical implications. Should relatively hot cooling water be desired at the outlet of the absorber, the parallel configuration may be the best configuration to use. However, care will need to be taken, in order to make sure that the outlet temperature does not come close to a 100°C if the cooling water is at 100 kPa. This will cause the cooling water to boil, which has ramifications of its own. On the theoretical side, the models for the absorber are not written to incorporate two-phase flow for

the cooling water, as two-phase flow is no simple matter to model. On the practical side, the boiling will cause massive volumetric expansion of the cooling water, as it turns into gas/steam. The aqua-ammonia system will likely not be able to handle this, as it is not designed as such. The steam will also need to be condensed somewhere in the sytem, if the cooling water is to be recycled.

5.2.4 FURTHER GENERAL OBSERVATIONS SURROUNDING THE DIFFERENT CONFIGURATIONS.

Besides the above points discussed, a few more comparisons can be made. In the graphs below, each configuration (as listed in Table 12) is compared for 3 and 4 rows, respectively. This is once again done by using the strong solution outlet temperature as a function of cooling water mass flow. It can be clearly seen that although the 4 row variation performs slightly better than the 3 row variation, the improvement by adding a 4th row is only minimal, and would be practically negligible.

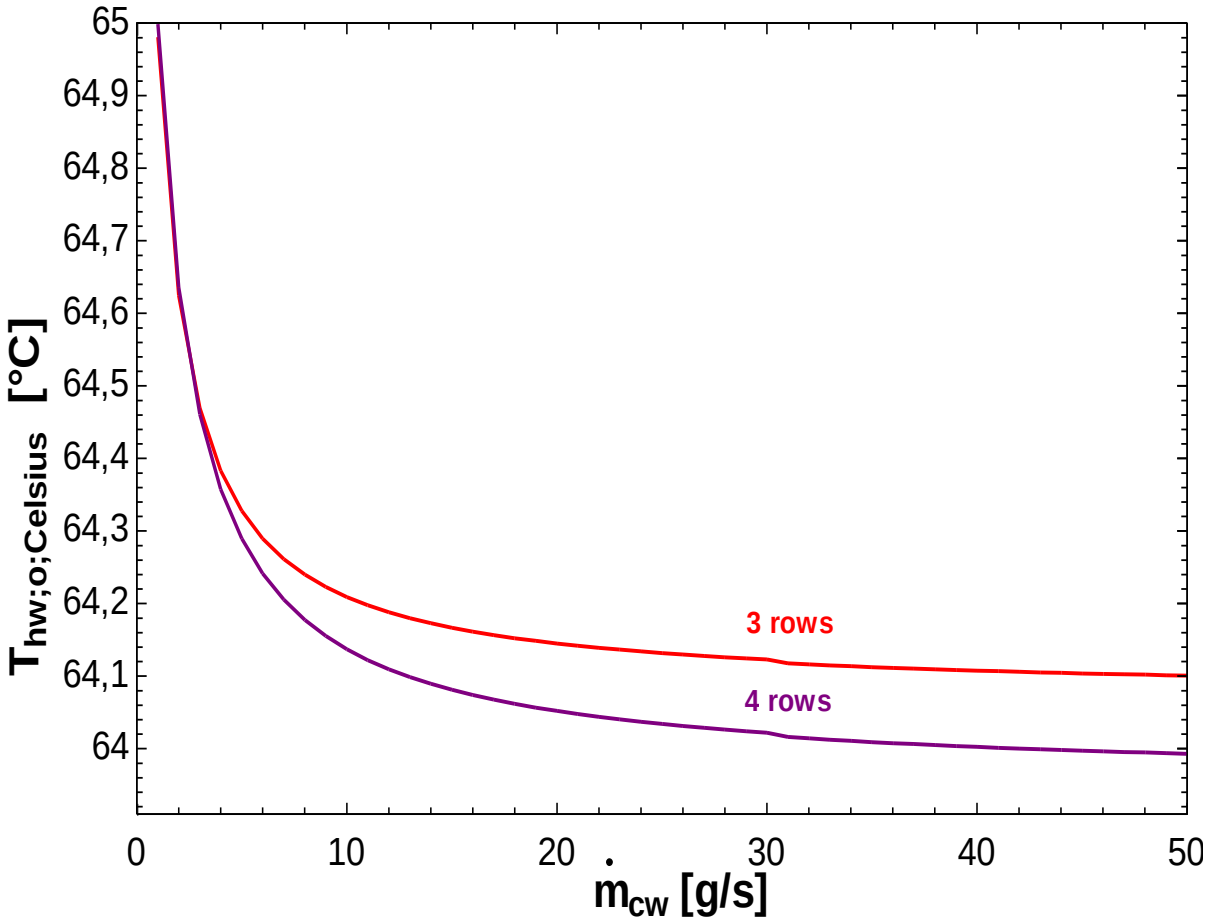

FIGURE 5.7: STRONG SOLUTION OUTLET TEMPERATURE FOR A SERIES CIRCUIT WITH 3 AND 4 ROWS, RESPECTIVELY.

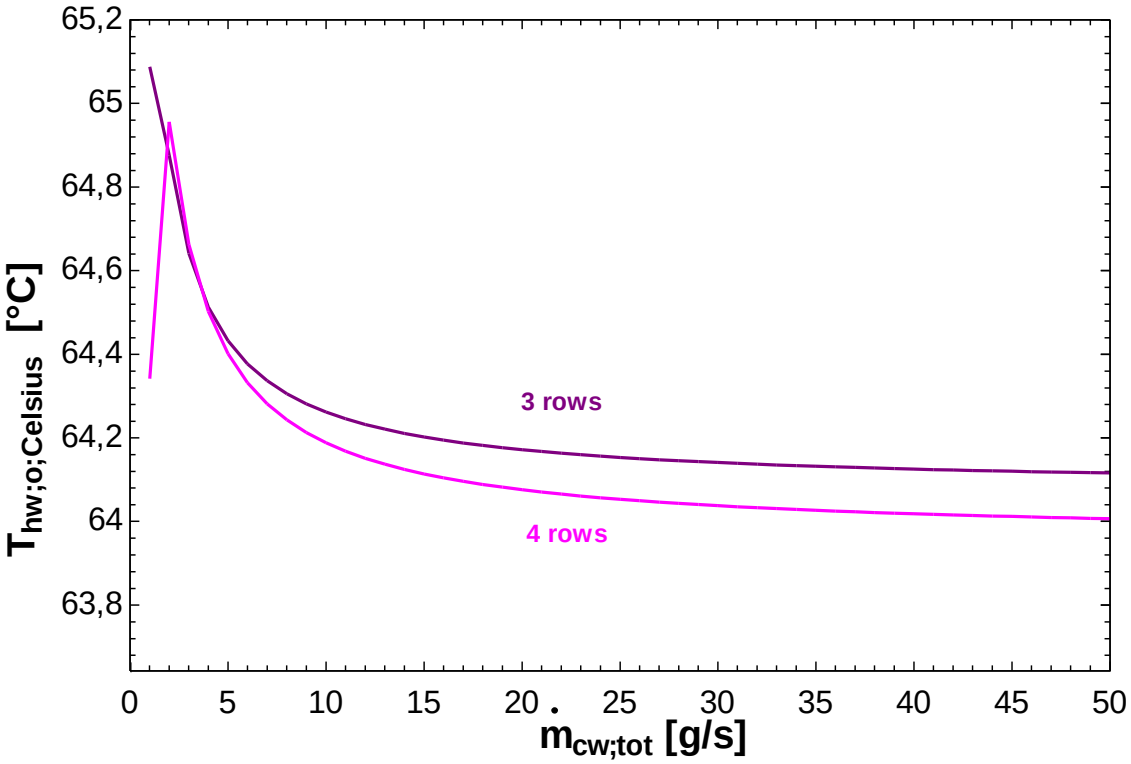

FIGURE 5.9: STRONG SOLUTION OUTLET TEMPERATURE FOR A SERIES-PARALLEL CIRCUIT WITH 3 AND 4 ROWS, RESPECTIVELY.

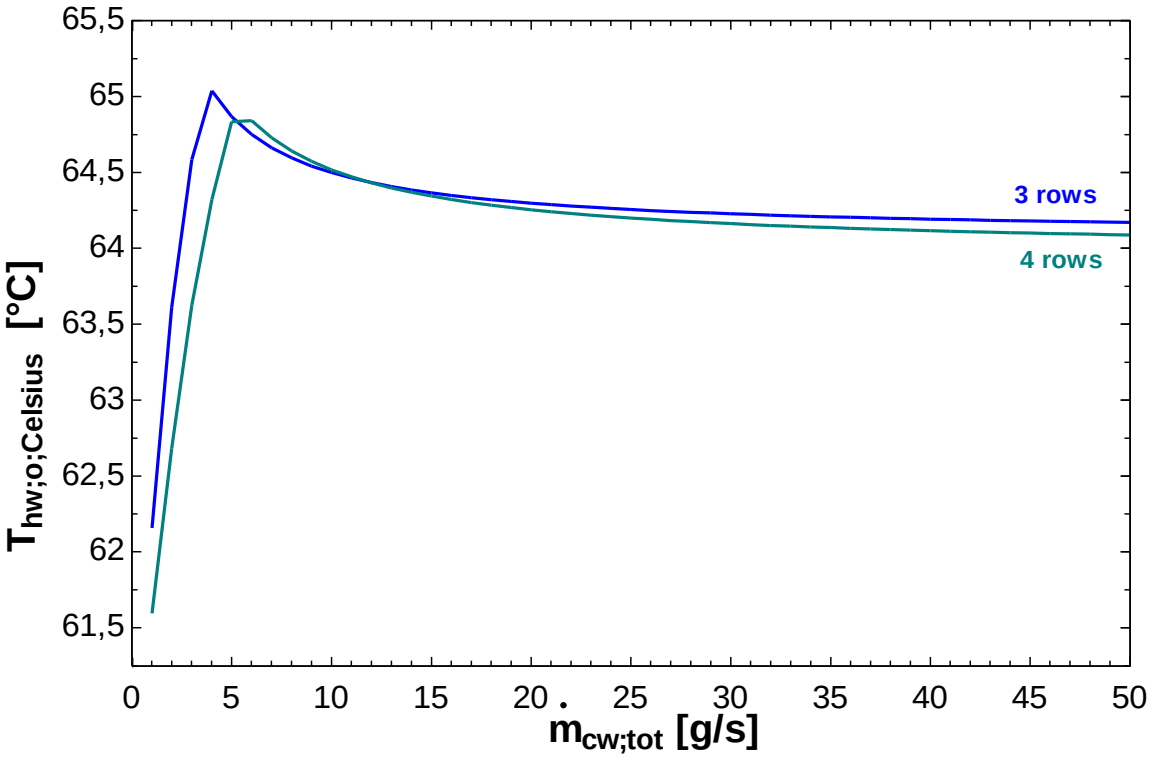

FIGURE 5.8: STRONG SOLUTION OUTLET TEMPERATURE FOR A PARALLEL CIRCUIT WITH 3 AND 4 ROWS, RESPECTIVELY.

From the above two graphs of the remaining configurations, it can clearly be seen that the same general conclusion can be reached than with the series configuration. As the cooling water increases, the strong solution outlet temperature converges to a certain specific temperature. The 4 rows variation performs slightly better than the 3 rows variation. However, the improvement is only very slight (a fraction of a degree Celsius), and would practically thus not be worthwhile.

The above mentioned observation is important, as it has cost implications. Adding a fourth row would increase the cost of the absorber, since the components have to be manufactured from stainless steel, but the gain in terms of temperature is not enough to justify the addition. Furthermore, the text of Incropera *et al*. (2007:441) points out that in the context of a tube bank, there is little change in the convection heat transfer coefficient (and subsequently outlet temperature) from approximately the fifth row in the tube bank. (It has already been explained that the absorber component in this problem is not exactly the same as a tube bank, but certain similarities do occur, hence the observation). In the context of the absorber, it can be seen that no significant change in temperature occurs even after the third row of cooling tubes, for all the configurations.

5.3 CONFIGURATION CHOSEN

Since the absorber component is part of a bigger project and of a total system (the aqua-ammonia heat pump), a choice had to be made with regards to a configuration for the absorber. This is because an under-graduate student was commissioned to build this component as a final year project. At the time the choice had to be made, not all the above information was available or known yet, and the student could not wait until each detail was finished. The configuration chosen at that time, was the *series*-configuration with 3 rows and 10 cooling tubes. The main motivation at the time for this choice was manufacturability. It is believed that the series-configuration would be the easiest to manufacture, as it would not need distributors for the cooling water tubes. The models were indeed well enough developed at the time to show that adding a 4^{th} row of cooling tubes would not be worthwhile in terms of cooling ability and cost. Thus, the three-row variation was chosen.

In retrospect, looking at Figures 5.4 and 5.5, it can be concluded that the choice was a good one, since the difference in strong solution outlet temperature among the different configurations is small, for most of the cooling water mass flow range. Thus, manufacturability was a reasonable criterion.

Although the parallel-flow configuration could theoretically give the best cooling ability at very low mass flow rates, it is noted that the cooling water mass flow will then have to be very accurately and carefully controlled, and at 1 g/s need to be above 100 kPa in order to avoid possible boiling. The reason for the need for careful control is that the parallel-configuration gives both its best and worst performance within the small cooling water range of 1 to 6 g/s. The series-configuration is thus much more stable in this regard. It is believed that the above optimization excercise is not in vain, however, since useful information was generated and characterization done, which can help future designers and operators of the absorber component. The above research and work also leaves a lot of options to choose from, which is a positive contribution. Should different needs arise, or the opportunity presents itself, it is even possible that another variation of the absorber can be built and tested.

5.4 FURTHER CHARACTERIZATIONS OF THE ABSORBER COMPONENT

Since the series-configuration has been chosen for reasons of physical manufacturing, the rest of the characteristics discussed further will be based on this configuration.

5.4.1 THE INFLUENCE OF THE GAS PRESSURE ON THE ABSORBER PERFORMANCE.

A variable which seems to have an influence of importance, is the pressure of the gas which is to be found on the aqua-ammonia side of the absorber. The influence can be observed by nothing that the gas pressure has a direct effect on the warm strong solution outlet temperature. This effect has been studied in two ways:

- The first assumes a constant partial pressure of the ammonia-gas of 200 kPa, and varying the system pressure between 200 kPa and 1000 kPa. Such variation is practically possible by the fact that there is an unreactive auxiliary gas in the system.
- The second approach assumes that there is no auxiliary gas in the absorber component, and the ammonia gas pressure is varied between 200 kPa and 700 kPa.

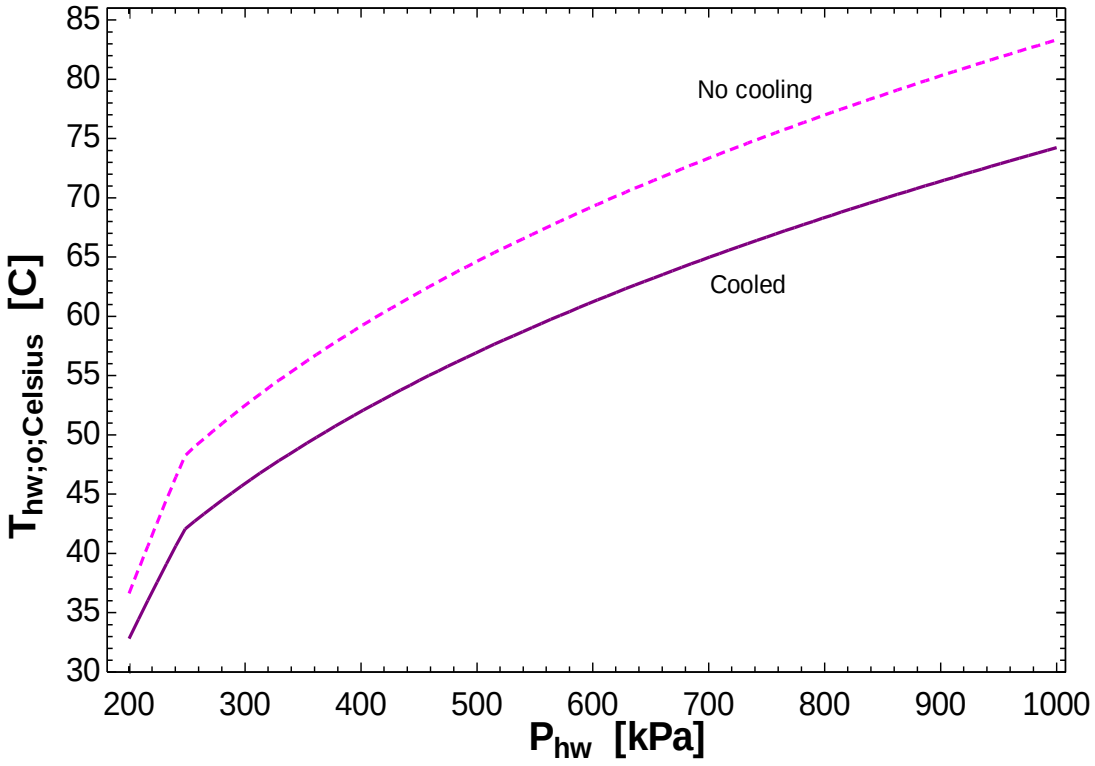

FIGURE 5.10: THE EFFECT OF SYSTEM PRESSURE ON WARM STRONG SOLUTION OUTLET TEMPERATURE.

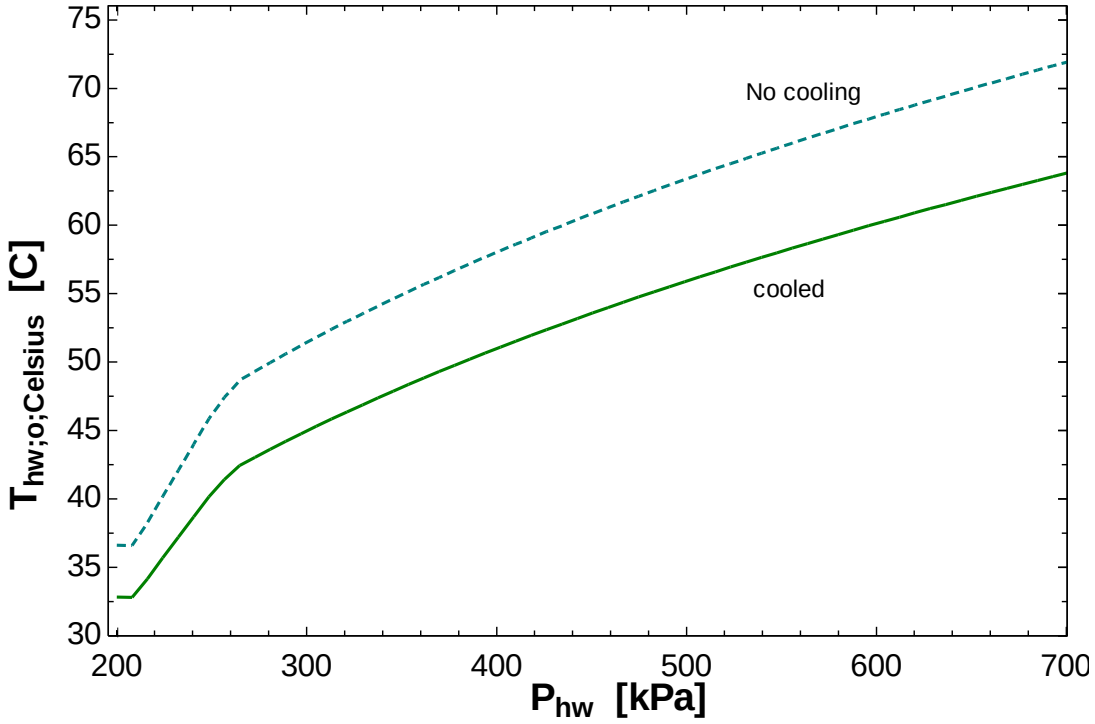

FIGURE 5.11: THE EFFECT OF AMMONIA PRESSURE ON WARM STRONG SOLUTION OUTLET TEMPERATURE.

The results of the pressure variations are given in the two graphs above (Figs. 5.10 and 5.11). It can clearly be seen that the pressure has a significant influence on the outlet temperature of the strong solution. For the system pressure, the outlet temperature more than doubles between pressures of 200 kPa and 1000 kPa. The same general trend is observed when the pressure is only that of the ammonia gas. This is practically important once more, since the system pressure of the aqua-ammonia heat pump will vary significantly between winter and summer conditions. According to the data received from the Ph.D. candidate, the typical *winter* system pressure will vary between 441 kPa and 510 kPa respectively, while typical *summer* system pressure vary between 822 kPa and 933 kPa, respectively. The highest system pressure found in the data set is 1155 kPa and the lowest is 441 kPa.

It should be mentioned, however, that in reality, the partial pressure of the ammonia gas may also vary as the system pressure varies. However, it was not possible to vary the ammonia partial pressure together with the system pressure, for the parametric study done above. Nor was there data, which gave specific values for the ammonia partial pressure, which could be used, at the time of writing. Thus, an important observation to make, is that the outlet temperatures of the strong solution will vary throughout the year.

Also displayed in the above graphs, is the cooling effect, and what the outlet temperature of the strong solution would have been, had there been no cooling at all. The question may be asked as to why there is not more cooling done to the strong solution. The answer lies in the fact that the absorption of ammonia gas in water is much like phase change of pure substances, with important similarities as well as differences. One of the important similarities, is that there is latent energy involved which does not manifest itself in terms of temperature, while one important difference is that the aqua-ammonia phase change does *not* happen on a constant temperature line, but a *temperature glide*, unlike pure water, for example (Herold *et al*., 1996:49).

The latent effects can easily be demonstrated by using the same input values into a similar EES program, where the aqua-ammonia has been replaced by pure water, and the heat generated due to absorption replaced by an electric heating element. For the same input values as given in Table 13 and 1.05 kW of heat either added or generated, the full aqua-ammonia program gives an *un-cooled strong solution* outlet temperature of 72°C, and a *cooled* strong solution outlet temperature of 64°C. This is only an 8°C difference. The

water/water program, in contrast, gives an *un-cooled water* outlet temperature of 113°C, and a cooled water outlet temperature of 62°C. This is a temperature difference of 51°C. Clearly, for the program that is not in the phase change region, the cooling effect is more dominant in terms of temperature, since the latent effects are absent.

The subject of phase change can also give an explanation as to why the pressure on the side of the aqua-ammonia has such a big influence on the strong solution outlet temperature. Again, for easy reference, refer to pure water in a Rankine cycle in the diagram below, where steam is bled off at different pressures, for regenerative feedheaters.

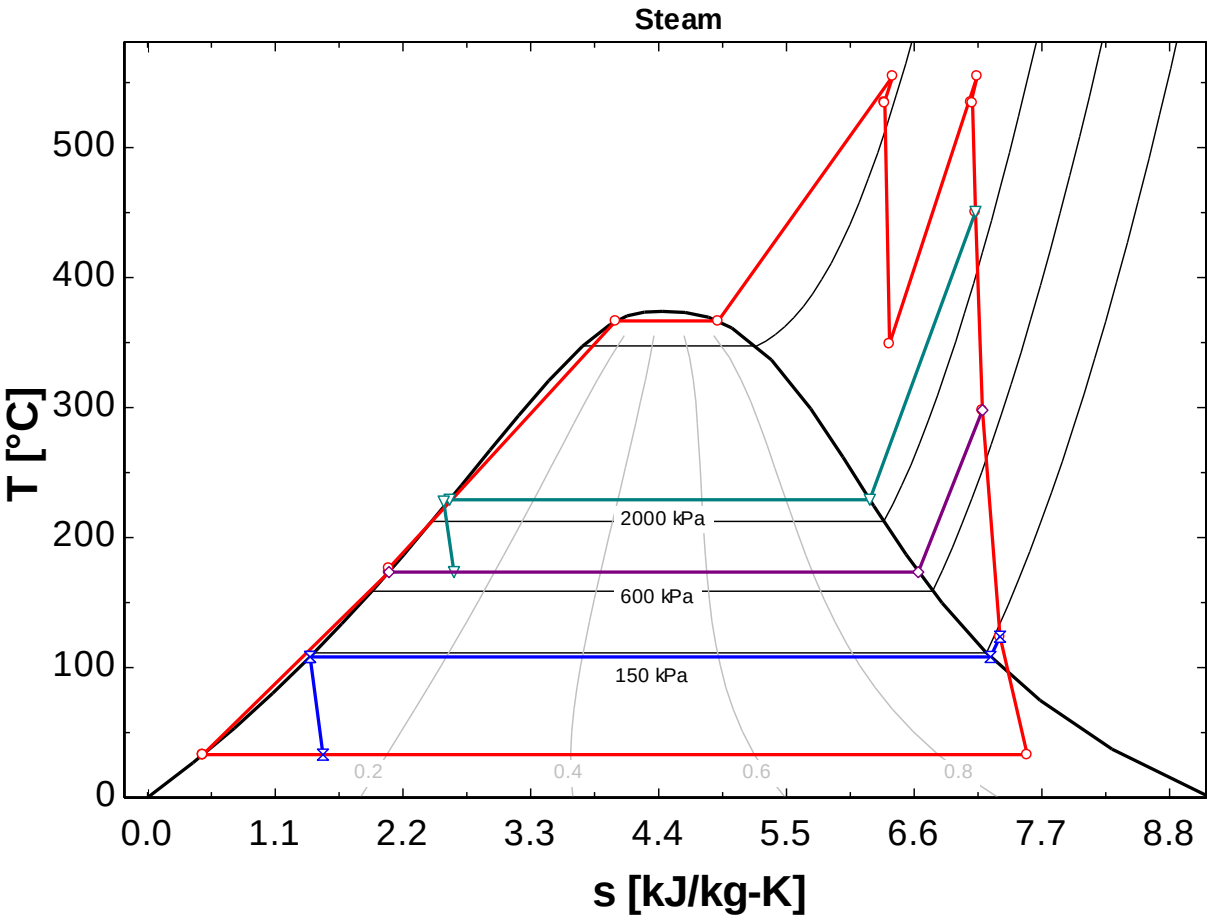

FIGURE 5.12: T-Δs DIAGRAM DEMONSTRATING STEAM BEING BLED OFF AT DIFFERENT PRESSURES IN A RANKINE CYCLE.

It can clearly be seen from studying the above temperature-entropy diagram, that the higher the pressure at which the steam is being bled off (the non-red lines on the graph), the higher the temperature at which the phase change takes place. The aqua-ammonia system also displays this behaviour, (which explains why higher system pressure yields higher outlet temperatures) with the exception that the temperature does not stay constant, as has already

been mentioned. The above section explains another behavioural aspect of the absorber component, which provided useful insight.

5.4.2 THE INFLUENCE OF THE COOLING WATER INLET TEMPERATURE

The effect of the cooling water inlet temperature on the strong solution has also been considered. The cooling water inlet temperature was varied between -10°C and 30°C. The cooling water will have some form of antifreeze added (such as ethylene glycol) in order to enable operation sub-zero temperatures. The influence is shown by the following graph:

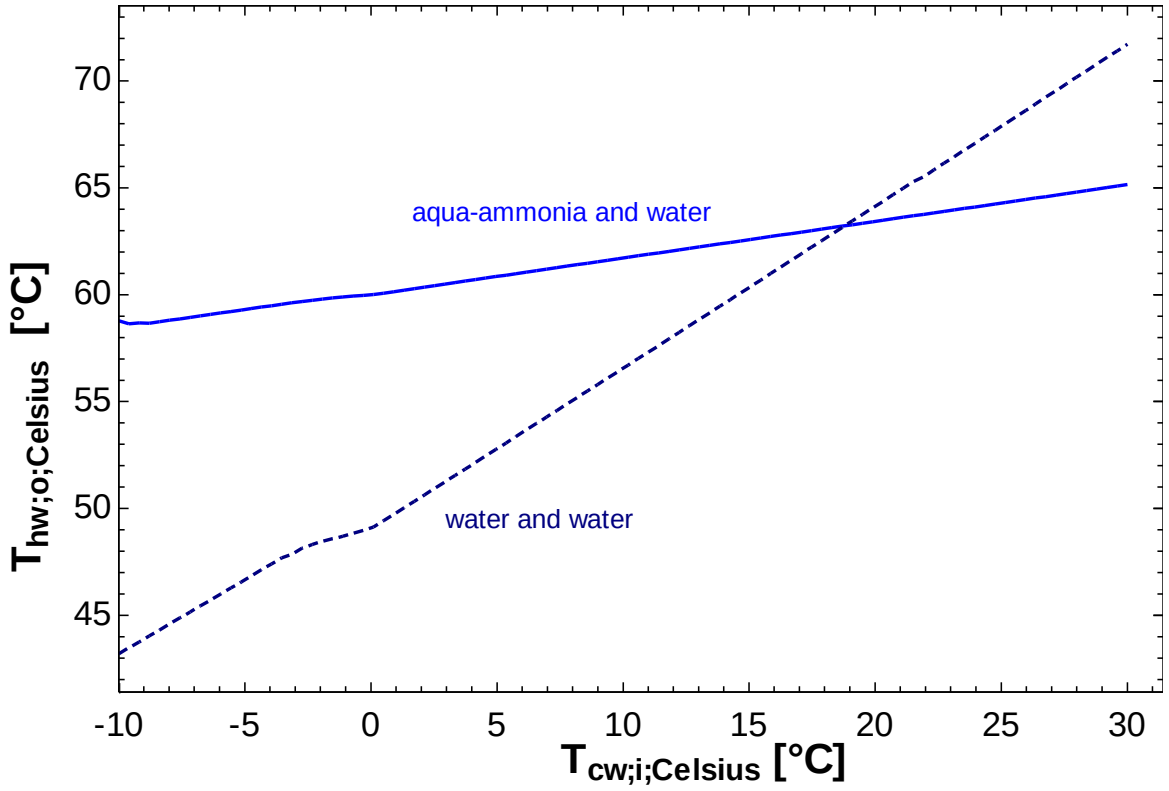

FIGURE 5.13: THE EFFECT OF COOLING WATER INLET TEMPERATURE ON THE STRONG SOLUTION OUTLET TEMPERATURE.

Once again, it was expected that the low cooling water temperatures would yield much lower strong solution outlet temperatures. By comparing the aqua-ammonia model to the water/water model (in Fig. 5.13) as before, it can be seen that there must be some latent effects, which prevent lower temperatures, since the water/water model (which has the same program architecture in handling the heat added) gives much lower temperatures. The important point must also be made that the cooling water temperature should be kept as far below the inlet temperature of the warm weak solution as possible, in order to facilitate pre-cooling. Never should the inlet cooling water temperature be above the weak solution inlet

temperature, as this will pre-heat the weak solution before absorption, which is very undesirable.

5.5 RESULTS FOR GIVEN INPUT VALUES FROM A SIMULATED CYCLE

In this section, specific results are given for input values obtained from an overall simulation of the *cycle* by the Ph.D. candidate mentioned earlier. The desired specific output parameter values (of the absorber) are obtained by using the simulation programs (in EES) developed in this study.

The overall simulation for the heat pump cycle done, fall into two categories, namely 'Clear Sky' and 'Global Data'. This has to do with the fact that solar energy is incorporated into the simulations of this project, which is ongoing at the North West University on the aqua-ammonia heat pump.

The cycle simulations were done for conditions throughout the year in the South African town of Potchefstroom . However, the winter and summer conditions will be considered below, since it is believed that these represent best and worst case scenarios. Average values from the 'winter' and 'summer' values were calculated, and used as input values for the absorber. The input values from the Ph.D. cycle simulations with the corresponding output values from the model developed, are given in the table below:

TABLE 5.3: INPUT AND OUTPUT VALUES FOR THE ABSORBER COMPONENT FOR SIMULATED RESULTS

		Inputs (received)			
		Winter		Summer	
		Global	Clear Sky	Global	Clear Sky
Warm weak solution (NH_3H_2O) mass flow	[kg/s]	0,00245	0,003991	0,002456	0,003057
Warm weak solution (NH_3H_2O) inlet temperature	[°C]	5,4274	5,4274	22,746	22,746
Warm weak solution inlet concentration	[NH_3/(NH_3 + H_2O)]kg	0,3792	0,3792	0,34948	0,34948
Ammonia-gas inlet mass flow	[kg/s]	0,000318	0,000518	0,000475	0,000591
Ammonia-gas inlet temperature	[°C]	3	3	21	21
Ammonia-gas partial pressure	[kPa]	238,076	238,076	236,174	236,174
System Pressure	[kPa]	475,6	475,6	877,06	877,06

Cold water inlet temperature	[°C]	-4,5726	-4,5726	12,746	12,746
		Outputs (calculated)			
Strong solution outlet concentration	[NH_3/(NH_3 + H_2O)]kg	0,4506	0,4506	0,4549	0,4549
Amount of heat generated	[kW]	0,5872	0,954	0,8635	1,072
Cooling water outlet temperature	[°C]	-3,253	-2,783	13,462	13,533
Warm strong solution outlet enthalpy	[kJ/kg.K]	-98,55	-79,8	65,27	74,33
Warm strong solution outlet temperature	[°C]	**31,014**	**35,143**	**66,954**	**67,435**
WSS Outlet temperature without cooling	[°C]	49,89	49,86	76,86	76,83

Three remarks need to be made before the results are briefly discussed. They are:

- Input values which are not stated in Table 5.3 above, are the same as those given in Table 5.2.
- The cooling water temperature was not given in the overall cycle simulation for obvious reasons. Thus, it was decided to choose the cooling water temperature 10 °C below the warm, weak solution inlet temperature for each scenario (since pre-cooling is desired)
- It was discovered that in the cycle simulation results, a very small amount of ammonia is bled from the evaporator into the absorber. Time did not permit working this into the absorber models, but it is believed that the effect will be minimal.

The results (as presented in Table 5.3) are satisfying in more than one way. It can be clearly seen that the strong solution outlet temperature is significantly lower in the winter than in the summer (about 54% lower for the 'Global' data and 52% for the 'Clear Sky' data). This is naturally also due to the nature of the simulated input values.

The cycle simulations by the Ph.D. candidate from global considerations also estimated the heat that will be generated. These estimations are relatively close to the calculated heat generated with mass energy balances as has been explained in Chapter 4. For example, in the 'Global' winter conditions, the amount of heat generated as reported by the received values is 0.5464 kW while the calculated generated heat is 0.5872 kW, which represents a 6.9% difference. For the 'Clear Sky' summer conditions, the amount of heat generated is reported by the received values as 0.9668 kW and the calculated amount of heat generated

by the model and mass-energy balance, is 1.072 kW, which represents a 9.8% difference. Seeing the fact that these two sets of simulations are working from very different angles, the results are within a quite acceptable range. The models developed in this study can thus be used for further predictions of output parameters, with any given set of input values (on the condition that they are realistic), which is one of the major purposes of the models.

5.6 MASS AND ENERGY BALANCES

Naturally, the developed model must obey the conservation laws, as has already been explained in Section 4.5.6. For all the models, the total incoming and outgoing energy as well as the total incoming and outgoing mass flow rates have been calculated, with the differences between incoming and outgoing expressed as percentages. For all the models developed, there is a 0% difference between incoming and outgoing mass flow rate. For the series configuration and the set of input values given in Table 5.2, there exists a small difference of 3.15% between the incoming energy (of 3.93 kW) and outgoing energy (3.80 kW), with the other models giving values that closely resemble the above.

The observed difference can likely be explained by the fact that EES uses interpolation and extrapolation to obtain the thermodynamic properties of the aqua-ammonia mixture. The program makes use of these properties all the time, in order to solve the heat transfer problem. Using exactly the same program and different (but realistic) input values can sometimes yield an even lower difference, or sometimes higher.

5.7 GENERAL OBSERVATIONS ABOUT THE EES-MODELS OR PROGRAMS

A few general observations need to be stated regarding the complex models coded in EES:

- The models need realistic input values. Unrealistic values can result either in non-meaningful answers, or the program not solving. This is especially true of the amount of ammonia gas which is going to be absorbed. Should an unrealistically high value be given, the model will either not solve, and give error messages, or actually give a negative answer for the amount of heat generated. The latter likely shows that the mixture needs to be cooled down in order to absorb the higher amount of heat. Very low amounts of ammonia gas as input (relatively speaking) does not provide a problem, however.

- Some of the model variations give an error when solving for the first time after opening the program. This is not due to error in the programing by the user, but was first found with the introduction of EES 2016' latest aqua-ammonia brines' properties. The EES software likely needs some refining for its latest aqua-ammonia procedure. The problem can easily be overcome by simply solving the program for a second time, in which case the error does not reappear.
- It is safer to solve the EES programs two or three times after opening them for the first time. This is likely due to the fact that the 'guess values' need to be updated due to the complex nature of the architecture of the program. Also, with the error which appears in some programs, as mentioned in the previous point, it was noticed that when the program actually solves (without error) for the first time, the values are questionable (likely due to the fact that the error introduced wrong guess values). Solving a third time gives the correct values.

Thus, although the models are automated (only basic input values need to be given), the user needs to use these programs with knowledge and basic insight into the problem that is being solved, as well as the programs.

5.8 VERIFICATION

Basic verification of the EES program for the series-configuration was done by comparing the results from this program, to the results generated by a set of Microsoft Excel spreadsheets in one workbook. The same heat transfer and absorption problem was solved manually in Microsoft Excel, for the series-configuration. Naturally, the Excel spreadsheets cannot be as automated as the programs developed in EES, so only one set of input values was used for testing. The following table gives the input values which was used for both the Excel and EES models:

TABLE 5.4: INPUT VALUES USED FOR VERIFICATION WITH MICROSOFT EXCEL

Parameter	Unit	Value
Warm weak solution (NH_3H_2O) inlet temperature	**[C]**	23
Warm weak solution (NH_3H_2O) mass flow	**[kg/s]**	0,005411
Warm weak solution (NH_3H_2O) concentration	**[NH_3/(NH_3 + H_2O)]kg**	0,347
System Pressure	**[kPa]**	904,5
Cold water inlet temperature	**[C]**	18
Cold water mass flow	**[kg/s]**	0,02

Ammonia-gas inlet temperature	**[C]**	22
Ammonia-gas inlet mass flow	**[kg/s]**	0,001077
Ammonia gas partial pressure	**[kPa]**	250
Cooling pipes *effective* length (wetted length)	**[mm]**	96
Cooling pipes inside diameter	**[mm]**	10
Cooling pipe wall thickness	**[mm]**	1
Cooling pipes outside diameter	**[mm]**	12

The following table gives the basic output values of the EES program and the Microsoft Excel spreadsheet set which solves for the absorber. The difference is expressed as a percentage with the Excel spreadsheet as reference:

TABLE 5.5: COMPARISON OF RESULTS YIELDED BY EXCEL AND EES FOR SOLVING THE ABSORBER PROBLEM

FINAL OUTPUT PARAMETERS		EXCEL	EES	% Diff.
Total heat generated in absorption process	**[kW]**	1,939	1,939	0,011
Outlet concentration of strong solution	**[NH_3/(NH_3 + H_2O)]kg**	0,4554	0,4554	0,001
Preliminary outlet temperature of NH_3H_2O	**[˚C]**	22,679	21,107	6,932
Preliminary outlet temperature of cooling water	**[˚C]**	18,576	18,534	0,226
Final outlet temperature of NH_3H_2O	**[˚C]**	69,521	69,510	0,016
Final outlet temperature of cooling water	**[˚C]**	19,432	19,931	2,568

As can be seen in the table of results above, the differences between the results of the Excel spreadsheets and the EES program are minimal, and within an acceptable range. The biggest difference is 6.9% for the preliminary aqua-ammonia mixture outlet temperature, and the smallest difference 0.001% for the outlet concentration of the strong solution. The most important results are the outlet temperatures of each stream of fluid. These results correspond very well to one another. The Excel workbook and accompanying EES program can be found in Appendix C on the CD.

5.9 VALIDATION

This absorber development is one project and component of the heat pump and can only physically be tested once the entire system is completed. This project is thus also

dependent on other projects, which are still in progress. Due to the hazardous nature of ammonia and the safety regulations attached thereto, testing of this nature is not possible at this point in time. However, validation of these results is done against findings and results of other researchers' equivalent studies:

- Cardenas & Narayanan (2010:1795) noticed that at their highest coolant temperature, the temperature of their solution still increases at certain parts of their absorber channel, despite the removal of heat. This is observed in this study as well, as the net temperature of the aqua-ammonia solution always turn out higher than the inlet temperature of the solution, if absorption takes place. This is despite the cooling water presence. It has been shown in this study however, that the cooling water still has an important cooling effect, as the solution outlet temperature would be even higher when no cooling by the water takes place (see Figures 5.10 and 5.11).
- Cerezo et al. (2009:1010) notice that the effect of simply increasing the cooling water flow rate had a less pronounced effect on the heat transfer coefficient. By considering Figures 5.4 to 5.9, it can clearly be seen that increasing the cooling water flow rate eventually has a smaller and smaller effect on the strong solution outlet temperature (the heat transfer coefficient and the outlet temperature are directly related via Newton's law of cooling). An exponential decay is observed. In this regard, the results of this study correspond to this particular finding of Cerezo *et al*.

The selected design parameters of cooling water tube diameters, dripping, rate of dripping, droplet splash diameter, height of dripping, etc. were determined by physical experiments indeed, as can be found in Chapter 6.

---

6. DROPLET EXPERIMENTS

6.1 INTRODUCTION

In this chapter, very basic but helpful experiments which were done with droplets, are set forth. These experiments aided in the overall understanding of the behaviour of the dripping fluid over the cooling tubes. They also showed additional potential problems which may occur, what the absorber component will likely be sensitive for, etc. Certain important parameters were experimentally determined as well.

6.2 PURPOSE

The purpose of these experiments was to determine physical parameters and conditions which could not easily have been predicted theoretically, but easily be observed physically. These include:

- The *volume* of fluid per droplet formed.
- The diameter or *width* of the film formed on the tube by the falling droplet.
- The *influence* of the *height* of the droplet outlet medium on the film width mentioned above.
- To test whether the *diameter* of the cooling tubes would have any influence on the thin film width on the cooling tubes.
- The *size* of the holes needed for a specific rate of droplet flow.
- The ideal *height of the fluid level above the feed tubes,* in the absorber component. This is to know which pressure head will be needed, which will be found in the bubble pump.

In order to understand the 2nd and 3rd bullets above, refer to the following illustration below (Fig. 6.1):

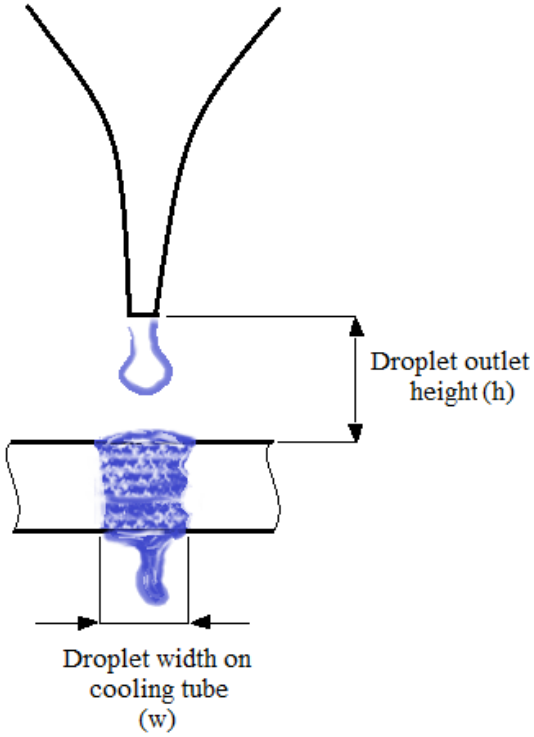

FIGURE 6.1: SCHEMATIC ILLUSTRATION OF THE DROPLET FALLING HEIGHT AND WIDTH ON TUBE (ILLUSTRATION BY THE AUTHOR).

The purpose for determining the width of the thin film on the cooling tube was to establish which length of cooling tube would be needed for a given mass flow of hot, weak solution. The width of the thin film was suspected to be dependent on the droplet outlet height to some extent. In the experimental setup, this outlet was a burette, and in the absorber component, this outlet will be tubes containing the weak solution.

The *volume per droplet* was determined, together with a *flow rate* for a given *hole-size* and *pressure head*, so that the amount of holes needed could be determined per given mass flow of the warm weak solution entering the absorber component.

6.3 EXPERIMENTAL METHODOLOGY

In order to establish all the desired parameters, three experiments were performed separately.

6.3.1 EXPERIMENT NO. 1

Experiment no. 1 was done in order to determine the volume per droplet. This simple experiment consisted of a burette and thermometer. The temperature of the fluid was measured, and a certain volume of fluid was allowed to drip into a beaker. The number of droplets were counted and the total volume which flowed through the burette was divided by the number of droplets counted. This experiment was done with water as well as commercially available ammonia-water solution of 8% (weight percent).

6.3.2 EXPERIMENT NO. 2

Experiment no. 2 was done in order to determine the width of the thin film on the cooling tubes. This experiment consisted of a burette, aluminium cylinders of various diameters, a stopwatch and a thermometer plus basic instruments to grip the main components. Each aluminium cylinder was given a piece of coloured surface by a brown coloured permanent marker, after the surfaces were given a finish and polished. On this coloured surface area, marks notating millimetres were made in order to establish a way to measure the width of the collapsed droplet. This is illustrated in the photograph below.

FIGURE 6.2: PHOTOGRAPH SHOWING THE MILLIMETRE MARKS ON AN ALUMINIUM CYLINDER.

The burette was slowly opened so that droplets dripped on the aluminium cylinders at such a rate, which allowed observation. The height of the burette outlet nozzle was varied somewhat, and effects on the thin film width noted. The width of thin film was often observable by the naked eye. However, in cases where this was not possible, the dripping process on the aluminium tube was recorded using a phone camera, which allowed playback in slow motion and giving some magnification.

The following parameters were noted: the *droplet width* on the tube, the *outlet nozzle height*, the *time interval,* and the *amount of droplets per time interval*. Formation and dripping of droplets at the bottom of the cylinder was also observed, and notations of the time interval were made where possible. This is illustrated in the photograph below (Fig. 6.3). Five diameters of cylinders were tested. These are diameters of 8 mm, 12 mm, 16 mm, 20 mm and 22 mm respectively.

FIGURE 6.3: PHOTOGRAPH SHOWING A DROPLET FALLING ON THE CYLINDER

6.3.3 EXPERIMENT NO. 3

For Experiment no. 3, a special but simple component needed to be manufactured. A transparent plastic tube with an outer diameter of 8 mm was selected for the task. A series

of holes was drilled in the tube along the length, with diameters ranging from 0.3 to 1.0 mm respectively, increasing with 0.1 mm increments. The drilling of these holes was done by specialists, due to the small sizes. The concept is illustrated below (Fig. 6.4):

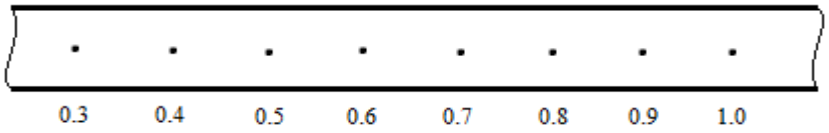

FIGURE 6.4: PLASTIC TUBE WITH SERIES OF HOLES

The drilled plastic tube was next connected to a small water tank via a flexible connection pipe, and clamped in a vertical position hanging in the air. One end was connected to the pipe, while the other end was stopped with rubber. A metal ruler was introduced to the setup, in order to be capable of observing the water level and the subsequent pressure head. The clamp holding the tube vertically in the air, was capable of adjusting its height. This helped with adjustment in order to test different pressure heads. The following three photographs show the setup (Figs. 6.5, 6.6 and 6.7). The adjustable clamp is illustrated in first the photograph. The second photograph shows how the water level and pressure height was observed, using the ruler, as well as the vertical position of the tube with holes in the clamp. The third photograph shows the holes at the bottom of the plastic tube, before water was introduced into the tube. The holes faced downwards. In the background of all three photographs, the water tank can be seen.

FIGURE 6.5: ADJUSTABLE CLAMP USED FOR THE TUBE WITH HOLES IN EXPERIMENT NO. 3.

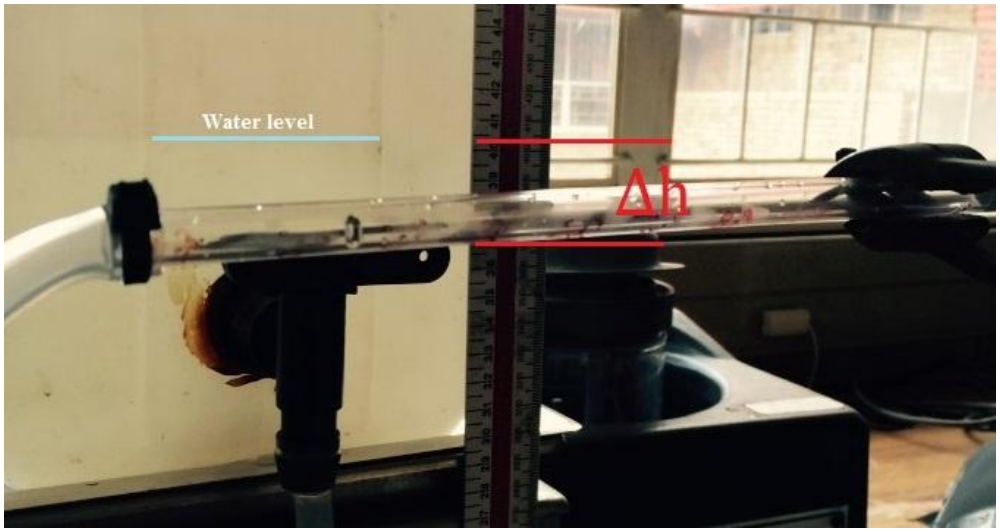

FIGURE 6.6: HORISONTAL TUBE WITH HOLES AND THE PRESSURE HEIGHT IN EXPERIMENT 3

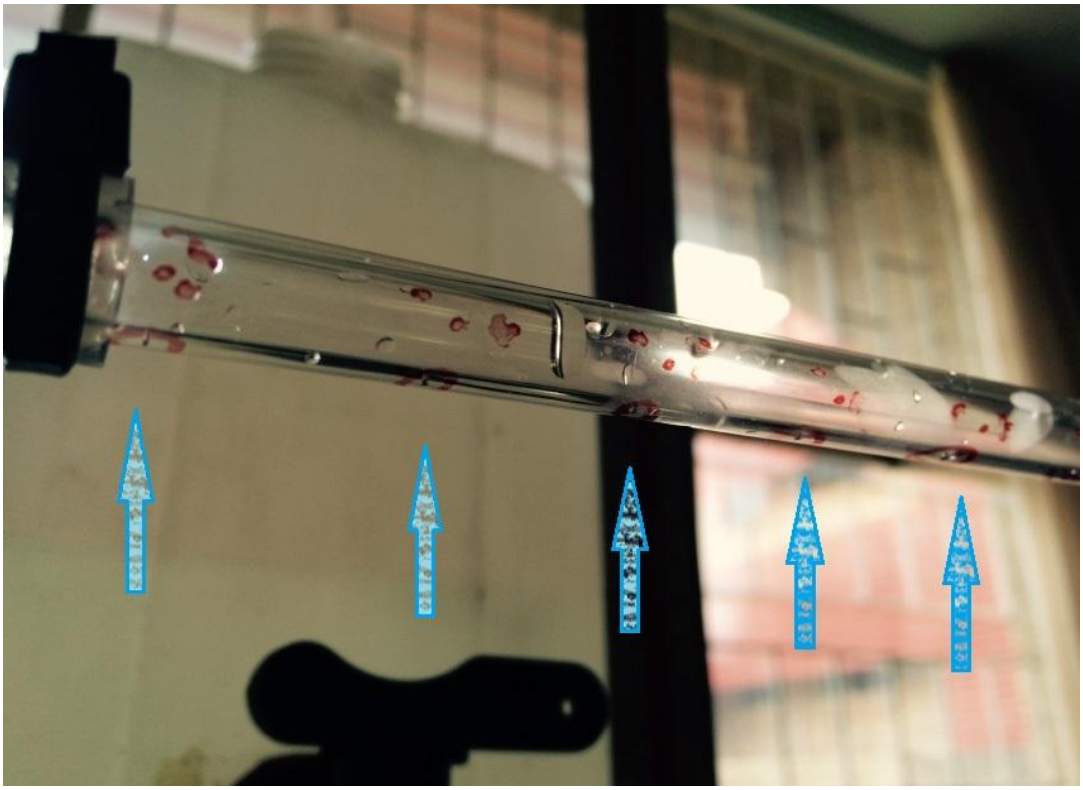

FIGURE 6.7: THE DIFFERENT SIZES OF HOLES IN THE PLASTIC TUBE

When the tap of the water tank was opened, the water started flowing through the holes, and observations could be made for the different sizes of the holes. The results will be discussed in a separate section.

6.4 RESULTS

The results of the three experiments described, are given in this section.

6.4.1 EXPERIMENT NO. 1

For this simple experiment, several measurements were taken with both water and an aqueous-ammonia solution on 8%. The temperature of the water was varied from 16 to 38 °C, while the aqua-ammonia solution was kept at a constant temperature of 20.6 °C. It was found that the variance was low for the water even within the temperature range. It was undesirable to heat up the aqua-ammonia, due to the inevitable fumes, which would develop. The results of the measurement show that the average volume of a water droplet was **0.054 ml** while the average volume of the ammonia-water mixture was **0.036 ml**. This represents a

difference of **33.3%** when water is used as reference. For obvious reasons, the value for ammonia-water droplets will be used in further calculations.

6.4.2 EXPERIMENT NO. 2

The following general observations were made during Experiment no. 2:

Different diameters of cylinders indeed showed different behaviour for dripping. For example, with the thickest diameter tested, the fluid would often only flow on *one side* of the cylinder, which is undesirable. Also, with the thickest diameter, the water droplets did not always role off the cylinder until another droplet falls on it. This is undesirable for heat transfer. Constant movement is preferable. The film-width on the cylinder is indeed to a reasonable extent dependent on the height of the outlet medium, from which the droplet is dropped. At a certain height, the fluid starts to splash, which is once more undesirable. The following table gives the data collected for this experiment:

TABLE 6.1: RESULTS OBTAINED IN DROPLET EXPERIMENT 2

			TOP		BOTTOM		TOP	BOTTOM	TOP	BOTTOM
Tube outside Diameter	Droplet Diameter on tube	Height of tip	Amount of Droplets	Time	Amount of Droplets	Time	Time per droplet	Time per droplet	Droplets per second	Droplets per second
[mm]	[mm]	[mm]	[-]	[s]	[-]	[s]	[s/drop]	[s/drop]	[drop/s]	[drop/s]
8	5	6,35	10	4,78	-	-	0,478	-	2,092	-
8	6	6,35	10	3,66	-	-	0,366	-	2,732	-
8	4,5	4,5	10	7,93	-	-	0,793	-	1,261	-
8	4,55	4,5	10	3,08	-	-	0,308	-	3,247	-
Av. 8	***5,013***	***5,43***	***10***	***4,863***	***-***	***-***	***0,486***	***-***	***2,333***	***-***
12	6	5,9	10	6,53	-	-	0,653	-	1,531	-
12	4,5	5,9	10	2,95	10	6,98	0,295	0,698	3,390	1,433
12	5,5	8,6	10	8,1	-	-	0,81	-	1,235	-
12	6	8,6	10	4,36	10	4,68	0,43600	0,468	2,294	2,137
Av. 12	***5,500***	***7,25***	***10***	***5,485***	***10***	***5,83***	***0,549***	***0,583***	***2,112***	***1,785***
16	5,5	7,31	10	5,76	-	-	0,576	-	1,736	-
16	6	7,31	10	2,8	-	-	0,28	-	3,571	-
16	6,5	9,97	10	3,51	-	-	0,351	-	2,849	-
16	7	9,97	10	2,36	-	-	0,236	-	4,237	-
Av. 16	***6,250***	***8,64***	***10***	***3,608***	***-***	***-***	***0,361***	***-***	***3,098***	***-***
20	4,5	5,7	10	4,98	10	10,1	0,498	1,011	2,008	0,989
20	5	5,7	10	4,05	10	8	0,405	0,8	2,469	1,250

20	7,5	10,0	10	5,54	10	9,35	0,554	0,935	1,805	1,070
20	8	10,0	10	2,73	10	5,4	0,273	0,54	3,663	1,852
Av. 20	***6,25***	***7,89***	***10***	***4,325***	***10***	***8,21***	***0,4325***	***0,822***	***2,486***	***1,290***
22	5,5	6,52	10	8,63	-		0,863	-	1,159	-
22	5,5	6,52	10	4,93	10	5,48	0,493	0,548	2,028	1,825
22	7	8,1	10	3,56	10	8,93	0,356	0,893	2,809	1,120
22	7	8,1	10	2,46	10	3,06	0,246	0,306	4,065	3,268
Av. 22	***6,25***	***7,31***	***10***	***4,895***	***10***	***5,82***	***0,4895***	***0,582***	***2,515***	***2,071***

As can be seen from the table above (Table 6.1), a wide variety of conditions were tested, and different observations were made. The 'top' and 'bottom' conditions refer to observations regarding the top and bottom of the cylinder, which the fluid dripped on. The designation 'Av.' refers to average values for a particular cylinder diameter. As can be seen, dripping frequency was also recorded in order to aid with design later.

A set of desirable conditions were selected from the above data set. From this data set, the outside diameter of the cooling tube will be **12 mm**, the width of the thin-film will be approximately **6 mm** when the fluid outlet medium is approximately **8.6 mm** from the cooling tube. The dripping frequency on top of the cylinder was observed to be **2.3** droplets per second, and at the bottom of the cylinder, droplets dripped at **2.1** droplets per second. Indeed, one reason why this set of data was selected, is because the top and the bottom dripping frequencies are quite close to one another. Recall the architecture of the absorber set forth in Chapter 4, and Figure 4.1. In this figure, it is clearly seen that the fluid of the first row of cooling tubes eventually drips on the third row of cooling tubes. For this reason, it was convenient to find a data set where the drip frequencies on the top and bottom of the cylinder was close to one another.

6.4.3 EXPERIMENT NO. 3

The methodology of Experiment no. 3 has already been explained previously. The adjustable clamp was first set in such a manner that a pressure head (Δh) of **36 cm** via the water level was introduced. After opening the tap of the water tank, it was soon realised that this pressure head was way too high, as water flowed out of the all the holes in a continuous stream, thus not dripping. This was undesirable. The Δh was decreased to **9 cm** and the tap opened. Upon opening the tap, the overall behaviour was already different. The smallest three holes (of 0.3, 0.4 and 0.5 mm diameter) showed dripping at different rates, while the rest of the holes still had continuous streams of water flowing. The Δh was decreased to **6 cm** and the tap opened. In this scenario, the smallest five holes (0.3 to 0.7 mm) showed

dripping at different rates while the remaining three showed continuous flow. Next, the Δh was decreased to **3.5 cm** and **3 cm** respectively. The following tables give the results in numerical form:

TABLE 6.2: RESULTS FOR A PRESSURE HEAD OF 3.5 CM

		Δ Height = 3,5 [cm]							
		Diameter of holes							
		0,3	**0,4**	**0,5**	**0,6**	**0,7**	**0,8**	**0,9**	**1,0**
		[mm]	[mm]	[mm]	[mm]	[mm]	[mm]	[mm]	[mm]
Number of droplets	[#]	5	5	10	10	10	10	10	Cont.
Time lapse	[s]	13,68	7,3	8,75	6,06	4,83	3,45	1,81	N/A
Time per Droplet	[s/droplet]	2,736	1,46	0,875	0,606	0,483	0,345	0,181	N/A
Droplets per second	[droplets/s]	0,365	0,685	1,143	1,650	2,070	2,899	5,525	**N/A**

TABLE 6.3: RESULTS FOR A PRESSURE HEAD OF 3 CM

		Δ Height = 3 [cm]							
		Diameter of holes							
		0,3	**0,4**	**0,5**	**0,6**	**0,7**	**0,8**	**0,9**	**1,0**
		[mm]	[mm]	[mm]	[mm]	[mm]	[mm]	[mm]	[mm]
Number of droplets	[#]	5	5	10	10	10	10	10	Cont.
Time lapse	[s]	17,39	55,5	7,65	5,35	4,88	4,78	2,60	N/A
Time per Droplet	[s/droplet]	3,478	11,1	0,765	0,535	0,488	0,478	0,26	N/A
Droplets per second	[droplets/s]	0,288	0,090	1,307	1,869	2,049	2,092	3,846	**N/A**

Looking at the results above, it can be concluded that the overall behaviour of the holes is much more useful already. In both these scenarios, only the hole with the biggest diameter (1.0mm) shows continuous flow (denoted as 'Cont.' in the above tables), while the rest drips at different rates. These rates have been measured, notated, calculated and are displayed in the tables above. It is clear from the general behaviour, that a pressure head between **3.0** and **3.5 cm** is preferable. Furthermore, a dripping rate of just over **2** droplets per second is

preferred, due to the results obtained in Experiment no. 2. Indeed, such conditions were found in the range of experiments done in Experiment no. 3. From the data, the holes with diameters of **0.7** to **0.8 mm** were found to give this desired rate of dripping, at a pressure head of **3.0** to **3.5 cm** respectively. A diameter of **0.7 mm** was selected for the absorber design.

Should key parameters change, new values can be looked up in the tables above, and new hole-sizes selected.

6.5 CONCLUSIONS DRAWN FROM THE EXPERIMENTS

There are several important practical conclusions that are to be drawn from having done these simple, yet helpful experiments, due to the observations:

- The flow through the holes was very sensitive to the pressure head in the water tank. This means that the pressure head in the bubble pump will need to be carefully controlled.
- Different sizes of holes drip at different rates. When the hole-size exceeds a certain critical diameter (for a particular pressure height), a continuous stream of water flows, rather than dripping.
- The centres of the warm, weak solution feed tubes will have to be very well vertically aligned to the centres of the cooling tubes. Subsequently, the centres of the first row of cooling tubes will need to be well aligned to that of the third row of cooling tubes. It was observed that misalignment interfered with the flow pattern on the cooling tubes, and often had undesirable effects.
- Bubbles which entered the vertical plastic tube in Experiment 3, obstructed the flow. Thus, bubbles will need to be kept out of the weak solution feed tubes as far as possible. However, to make provision for bubbles which may occasionally enter the feed tubes, one option would be to drill some of the holes on top of the feed tube. It was found in the experiment that gas bubbles could in some cases be forced out of the plastic tube, by turning the plastic tube upside down, so that the holes face upwards. This pushed the gas bubbles out at the top.
- The holes need to be drilled correctly and very carefully. One of the holes did not function normally like the others, and it is suspected that this is due to the surface inside the hole, or likely some very fine burr remaining in the hole after drilling. Due to the small size of these holes, however, it was not possible to make an exact observation with the naked eye. This also means that after manufacturing, it would

be best to test the feed tubes with water, in order to make sure all the holes are correctly drilled. The feed tubes will, after all, be much like the test plastic tube used in Experiment 3, with the main difference being that all the holes will all be the same size, and the feed tubes will be made from some kind of stainless steel.

6.6 SUMMARY OF THE DATA OBTAINED FROM THE EXPERIMENTS

As has been explained earlier, part of the purpose of these experiments was to determine certain parameters which could not be so easily calculated theoretically. Following is a table, which summarizes the parameter values determined from the experiments:

TABLE 6.4: SUMMARY OF PARAMETER VALUES OBTAINED FROM DROPLET EXPERIMENTS

Parameter	Value	Unit
Volume per NH3H2O [8%] droplet	0.036	[ml]
Cooling tube outside diameter	12	[mm]
Thin film width (diameter) on cooling tube	6	[mm]
Outlet medium height from cooling tube	8.6	[mm]
Dripping frequency at top of cooling tube	2.294	[droplets/s]
Dripping frequency at bottom of cooling tube	2.137	[droplets/s]
Pressure head (Δh) between fluid level and feed tube holes	3.0 to 3.5	[cm]
Diameter of holes in warm, weak solution feed tubes	0.7	[mm]

The above information was entered into an Excel spreadsheet, and which was used to calculate finer details used by the under-graduate student. The minimum length of the cooling tubes and amount of holes needed could for example easily been calculated, as a function of mass flow of the warm weak solution. The mass flow which was received from the Ph.D student varied as iteration and revision took place. The amount of holes was naturally based on the maximum mass flow of warm, weak solution, which the absorber component will have to handle. The spreadsheet containing this more detailed information can be found in Appendix D.

7. CONCLUSIONS AND RECOMMENDATIONS

7.1 INTRODUCTION

It is clear from Chapter 1 that there are good reasons why an alternative refrigeration method should be investigated, as problems are starting to surface both nationally and internationally. For the South African citizen, there is a reasonable chance that hard times may be coming in regards to the national electricity provision, which is under strain. The need to become more independent from the Eskom grid is real, as refrigeration is an absolute necessity for food preservation. It can be seen from Chapter 2 that the aqua-ammonia heat pump, like other conventional heat pumps, also have a condenser where heat is rejected. The condenser can thus be utilized in the average household to heat water or air.

The absorber component is a key component of the aqua-ammonia heat pump. Thus, it was necessary to do a proper study on the absorber, in order to model the absorber component for predictive purposes, as well enable a careful absorber design. The absorber architecture and layout in this study are somewhat unique, compared to other absorber models and layouts. This needed to be the case, since the other absorber components considered in the literature survey all had undesirable entities present. These entities vary from pressurised gas bottles in the test bench, pumps, pressure heads against which the ammonia gas would need to be introduced and characteristics which would introduce significant pressure drops (such as having to press the ammonia gas through a porous wall, and through a micro channel).

7.2 CONTRIBUTIONS OF THIS STUDY

This study accomplished several goals, of which the most important are:

- Heat transfer models were developed which can solve the heat transfer problem, for the particular absorber architecture presented in this study. Many of the principles used to solve the problem, would also be useable in other types of absorbers. These models were turned into computer models, which have the ability to predict outlet parameters with only the minimal set of inlet parameters given to the program. This was not a mediocre task. These computer models enable the cycle designers and

designers of other components to obtain predictions, while characterization of the absorber component was also done.

- The work done in this study facilitated a first design for the absorber component, as can be seen. The drawings for the design can be found in Appendix B, and was done by an under-graduate student. Although the development of the models were the primary objective, surrounding issues were also addressed, which aided the design of the component.
- The layout and absorber design presented in this study will be able to function without pumps or pressurized bottles of ammonia gas. Thus, it should fulfil the need of a system, which has the objective of operating using mainly thermal syphoning, density differences and gravity. The ammonia gas in the system would also be recycled, instead of coming from an outside source.
- The development of several variations of the model leaves the designer with several options available to choose from.

7.3 RECOMMENDATIONS FROM THIS STUDY

The following recommendations are made, which are a result of this study:

- The general input parameters for the EES models, should be realistic, as discussed in Chapter 5.
- The EES programs should be solved more than once before the results are recorded. It is recommended that all designs following from this study attempt to stick to the experimental parameters set forth in Chapter 6, as it was found that these were the optimal conditions. It was also found that certain aspects of the absorber are quite sensitive, hence this recommendation.
- It is strongly recommended that pure water be used with the commissioning of the aqua-ammonia heat pump cycle in general. Together with pure water, it is recommended that this pure water should be rid of any carbon dioxide gas (for reasons set forth in Chapter 2). This could possibly be achieved by heating the water almost to the point of boiling, prior to introduction to the system, as the solubility of all gases in water would decrease with increasing temperature. This would 'boil off' most of the dissolved gases.

- In future manufacturing of the absorber component, manufacturers should not be allowed to use nickel brazing on the component. The nickel is not compatible with the concentrations of aqua-ammonia solutions used in this heat pump.
- It is recommended that the pressure head and weak solution level should be very carefully monitored and controlled, in order to get the desired flow rates and patterns in the absorber component. It would be worthwhile to install *sight glasses* or any other means in the relevant components, which could help technicians or engineers establishing the correct liquid levels and pressure height.
- The cooling water inlet temperature should be as low as possible, in order to establish pre-cooling in the first row of tubes. Never should the cooling water inlet temperature be close to, equal to, or especially higher than the weak solution inlet temperature. At the worst-case scenario, it is recommended that the cooling water inlet temperature be at least 10°C below the weak solution inlet temperature.
- In the manufacturing process of the absorber, the component and its sub-components must be tested first before the component is sealed permanently. The testing should specifically focus on the holes in the weak solution feed tubes, and the subsequent flow of fluid. It was seen in the experiments in Chapter 6, that there were an individual hole or two, which did not function correctly.
- The absorber component must be kept perfectly horizontally at all times, when operating in the heat pump cycle. It should also be handled carefully, since hard knocks can upset the fluid flow in the component.
- Each absorber component should be tested for leaks prior to use, especially since ammonia gas has a pungent smell. It was observed by others that the general method of using water with soap, in order to form bubbles, does not work when ammonia gas is involved. This is because the ammonia gas readily absorbs into the water and prohibits bubble formation. If ammonia gas has already been introduced into the system, water with a chemical basic indicator can be used, as ammonia in water forms a base.

---

8. REFERENCES AND BIBLIOGRAPHY

REFERENCES

Agency for Toxic Substances and Disease Registry (ATSDR). 2004. Toxicological profile for Ammonia. Atlanta, GA: U.S. Department of Health and Human Services, Public Health Service. http://www.atsdr.cdc.gov/toxprofiles/tp126-c4.pdf Date of access: 26 October 2015.

Airgas Speciality Products. 2010. Appendix A - Charts, Graphs and Tables. www.airgasspecialtyproducts.com/Libraries/Aqua_Ammonia_Technical_Data_Manual/Appendix_A_-_Charts_Graphs_and_Tables.sflb.ashx Date of access: 27 October 2015.

Areff, A. Over 50% chance of total blackout, Nersa hears. News24. http://www.fin24.com/Economy/Eskom/Over-50-chance-of-grid-meltdown-energy-analyst-20150624 Date of access: 2 December 2015.

Bogart, M.J.P. 1981. Ammonia absorption refrigeration in industrial Processes. Houston TX: Gulf Publishing Company.

Calm, J.M. 2008.The next generation of refrigerants-historical review, considerations, and outlook. *International Journal of Refrigeration*, 31(7), 1123-1133.

Cardenas, R. 2009. *Study of a constrained-film bubble absorber under cycle operating conditions*. Corvallis: Oregon State University (Thesis – M.Sc).

Cardenas, R., & Narayanan, V. 2010. A numerical model for ammonia-water absorption into a constrained microscale film. *International Journal of Thermal Sciences,* 49 (2010), 1787–1798.

Craig, B.D., & Anderson, D.S., *eds.* 2002. Handbook of corrosion data. 2nd ed. ASM International.

Çengel, A., & Boles, M. A. 2002. Thermodynamics: an engineering approach. 4th ed. McGraw-Hill Higher Education.

Cerezo, J., Bourouis, M., Vallès, M. Coronas, A., Best, R. 2009. Experimental study of an ammonia-water bubble absorber using a plate heat exchanger for absorption refrigeration machines. *Applied Thermal Engineering,* 29(2009), 1005–1011.

De Lange, J. 2014. 600 MW minder krag vir dié winter. http://152.111.11.6/argief/berigte/volksblad/2014/04/08/11/janduvha_30_0_479331506.html Date of access: 2 November 2015.

Eastop, T.D., & McConkey, A. 1978. Applied Thermodynamics for Engineering Technologists. 3rd ed. London: Longman Group Limited.

Engineering ToolBox. 2014. Solubility of gases in water. http://www.engineeringtoolbox.com/gases-solubility-water-d_1148.html Date of access: 17 March 2014.

Engineering ToolBox. 2015. Gases – Critical temperatures and pressures. http://www.engineeringtoolbox.com/gas-critical-temperature-pressure-d_161.html Date of access: 14 Oct. 2015.

Fernandez-Seara, J., Sieres, J., Rodriguez, C., Vazquez, M. 2005. Ammonia-water in verticular tubular absorbers. *International Journal of Thermal Sciences*, 44(2005), 277-288.

Fin24. 2014a. Eskom gets nod to increase prices. http://www.fin24.com/Economy/Eskom-gets-nod-to-increase-prices-20140730 Date of access: 30 June 2014.

Fin24. 2014b. More gloom amid bigger electricity hikes. http://www.fin24.com/Economy/More-gloom-amid-bigger-electricity-hikes-20140801 Date of access: 5 August 2014.

Fin24. 2014c. Eskom welcomes decision. http://www.fin24.com/Economy/Eskom-welcomes-decision-20140730 Date of access: 5 August 2014.

Fin24. 2014d. Switch off and save electricity – Eskom. http://www.fin24.com/Economy/Switch-off-and-save-electricity-Eskom-20140715 Date of access: 5 August 2014.

Fin24. 2014e. Eskom warns of tight electricity system. http://www.fin24.com/Economy/Eskom-warns-of-tigh-electricity-system-20140626 Date of access: 5 August 2014.

Fin24. 2014f. Strike puts brakes on Medupi, Kusile. http://www.fin24.com/Economy/Labour/News/Numsa-trike-puts-brakes-on-Medupi-Kusile-20140701 Date of access: 5 August 2014.

Fin24. 2014g. Eskom: Load shedding a must to avoid blackout. http://www.fin24.com/Economy/Eskom-Load-shedding-a-must-to-avoid-blackout-20141102 Date of access: 2 November 2014.

Fin24. 2014h. Power disruptions in Joburg after pylon theft. http://www.news24.com/SouthAfrica/News/Power-disruptions-in-Joburg-after-pylon-theft-20140605 Date of access: 5 August 2014.

Fin24. 2014i. Eskom rebuilds collapsed pylons. http://www.news24.com/SouthAfrica/News/Eskom-rebuilds-collapsed-pylons-20140731 Date of access: 5 August 2014.

Hales, J.M., & Drewes, D.R. 1979. Solubility of ammonia in water at low concentrations. *Atmospheric Environment*, 13(1979), 1133-1147.

Herold, E., Rademacher, R., & Klein, S.A. 1996. Absorption chillers and heat pumps. Boca Raton, FL: CRC Press.

Incropera, F.P., Dewitt, D.P., Bergman, T.L., Lavine, A.S. 2007. Fundamentals of Heat and Mass Transfer. 6th Edition. New York: John Wiley & Sons.

Kotz, J.C., Treichel, P.M., & Townsend, J.R. 2009. Chemistry & chemical reactivity. 7th ed. Belmont, CA: Thomson Brooks/Cole.

Matrix Process Solutions. 2015. Brazed Heat Exchangers. http://www.matrixps.com/products/alfalaval/heatex/PD_Leaflets/82_83_PHE_NB14_76_gb.pdf Date of access: 19 October 2015.

McGreal, C., 2008. Mines shut as South Africa faces electricity 'emergency'. http://www.theguardian.com/world/2008/jan/25/southafrica.business Date of access: 30 June 2014.

News24. 2014a. Power disruptions in Joburg after pylon theft. http://www.news24.com/SouthAfrica/News/Power-disruptions-in-Joburg-after-pylon-theft-20140605 Date of access: 5 August 2014.

News24. 2014b. Eskom rebuilds collapsed pylons. http://www.news24.com/SouthAfrica/News/Eskom-rebuilds-collapsed-pylons-20140731 Date of access: 5 August 2014.

NC State University. 2015. Ammonia Fountain. http://ncsu.edu/project/chemistrydemos/GasLaw/Ammonia%20Fountain.pdf Date of access: 22 October 2015.

Penn State. 2015. Fully thermally activated refrigeration. http://sites.psu.edu/mtfe/fully-thermally-activated-refrigeration/ Date of access: 21 October 2015.

Potgieter, M.C. 2013. *The evaluation of a solar-driven aqua-ammonia diffusion heating and cooling cycle*. Potchefstroom: NWU (Dissertation - M.Eng).

Pressly, D. 2014. Municipalities owe Eskom R10bn. Fin24. http://www.fin24.com/Companies/Industrial/Municipalities-owe-Eskom-R10bn-20140812 Date of access: 14 August 2014.

Sapa. 2013. Municipalities owe Eskom R1.4bn. Fin24. http://www.fin24.com/Economy/Municipalities-owe-Eskom-R14bn-20131125 Date of access: 5 August 2014.

Schmidt-Nielsen, K. 2010. Animal physiology – Adaptation and environment. 5th ed. New York, NY: Cambridge University Press.

Selim, A.M., & Elsayed, M.M. 1999. Performance of a packed bed absorber for aqua ammonia absorption refrigeration system. *International Journal of Refrigeration*. 22 (1999), 238 – 292.

Smith, F.L. & Harvey, A.H. 2007. Avoid common pitfalls when using Henry's Law. CEP Magazine. http://www.aiche.org/resources/publications/cep/2007/september/avoid-common-pitfalls-when-using-henrys-law Date of access: 26 October 2015.

Srikhirin, P., & Aphornratana, S. 2002. Investigation of a diffusion absorption refrigerator. *Applied Thermal Engineering*, 22(2002), 1811-1193.

Stoecker, W.F. 1998. Industrial Refrigeration Handbook. McGraw-Hill Professional.

Stoecker, W.F., & Jones, J.F. 1982. Refrigeration & air conditioning. 2nd ed. McGraw-Hill.

University of California, Berkeley. 2012. Ammonia Fountain. https://www.youtube.com/watch?v=-z4liRirdv0 Date of Access: 22 October 2015.

Theunissen, R. 2011. *Investigation of a radiative cooling system with natural circulation for regulating a heat sink*. Potchefstroom: NWU (Dissertation - M.Eng).

Van Eldik, M. 2012. Course Notes: INGM 412 - Heat transfer. Potchefstroom: North-West University.

Van der Walt, S. 2012. *The design and optimisation of a bubble pump for an aqua-ammonia diffusion absorption heat pump*. Potchefstroom: NWU (Dissertation - M.Eng).

Van Niekerk, E. 2013. A Study of the Evaporator Coil in a Super-Critical CO_2 Heat Pump Test Bench. Potchefstroom: NWU (Mini-Dissertation - B.Eng).

Zohar, A., Jelinek, M., Levy, A. & Borde, I. 2008. The influence of the generator and bubble pump configuration on the performance of diffusion absorption refrigeration (DAR) system. *International Journal of Refrigeration*,31(2008), 962-969.

BIBLIOGRAPHY

Alefeld, G., & Radermacher, R. 1994. Heat conversion systems. Boca Raton, FL: CRC Press.

Henley, E.J. & Seader, J.D. 1981.Equilibrium-Stage Separation Operations in Chemical Engineering. John Wiley & Sons.

Pearson, A. 2005.Carbon dioxide—new uses for an old refrigerant. *International Journal of Refrigeration*, 28(8), 1140-1148.

Royal Society of Chemistry. 2015. Ammonia fountain experiment. http://www.rsc.org/learn-chemistry/resource/res00000979/ammonia-fountain-experiment?cmpid=CMP00004758 Date of access: 22 October 2015.

9. APPENDICES

APPENDIX A

This appendix contains the EES program code for the absorber configuration of 3 rows and 10 cooling tubes in *series*. It should be kept in mind that the program must be solved three times (see main text) when it is opened the first time. Initially, EES would throw out an error, but the program should just be solved again.

```
"Eleana van Niekerk"
"21840458 NWU Potchefstroom"
"2015"
"Hitte Oordrag Model"
"Vir die absorbeerder"
"Warmer Aqua-Ammoniak mengsel drup op verskeie pype van bo af op die siliners, wat self met koue water gevul is"
"Ammoniak-gas word van onder af ingespuit"
"Alle verkoelingspypies is in serie geskakel"
"Reynolds getalle buite om silinders gedefinieer in terme van massavloei, en nie snelheid nie"

"Berekening van die konveksie h vir eksterne vloei van die warm water"

PROCEDURE H_EXT(T_hw;  P_hw; m_dot_hw; D_o; x_in : C_in; k_hw; rho_hw; mu_hw; Pr_hw; Re_hw; Nu_hw; alpha_hw)

C_in =  x_in*100

k_hw = Conductivity(NH3H2O;T=T_hw;x=x_in;P=P_hw)/1000

rho_hw = Density(NH3H2O;T=T_hw;x=x_in;P=P_hw)

mu_hw = Viscosity(NH3H2O;T=T_hw;x=x_in;P=P_hw)


    IF (T_hw<303,15) AND (C_in<30) THEN

    Pr_hw = Prandtl(NH3W;T=T_hw;C=C_in)

    ELSE

    Pr_hw =Prandtl(Water;T=T_hw;P=P_hw)

    ENDIF

Re_hw = (4*m_dot_hw)/(pi*D_o*mu_hw)

Nu_hw = 0,3 + (0,62*(Re_hw^0,5)*(Pr_hw^(1/3)))/((1 + (0,4/Pr_hw)^(2/3))^0,25)*((1 + (Re_hw/282000)^(5/8))^(4/5))

alpha_hw = (Nu_hw*k_hw)/D_o

END
```

```
"Berekening van die konveksie h vir die interne vloei van die koue water"

PROCEDURE H_INT(D_i; T_cw; T_hw; m_dot_cw; C_EG : A_i; k_cw; rho_cw; V_cw; mu_cw; Re_cw; Pr_cw; Nu_cw; alpha_cw)

 A_i = pi*((D_i/2)^2)

IF (C_EG<=60) THEN

    rho_cw = Density(EG;T=T_cw;C=C_EG)

    mu_cw = Viscosity(EG;T=T_cw;C=C_EG)

    k_cw = Conductivity(EG;T=T_cw;C=C_EG)

    Pr_cw = Prandtl(EG;T=T_cw;C=C_EG)

    ELSE

    rho_cw = Density(Water;T=T_cw;P=101)

    mu_cw=Viscosity(Water;T=T_cw;P=101)

    k_cw = Conductivity(Water;T=T_cw;P=101)/1000

    Pr_cw=Prandtl(Water;T=T_cw;P=101)

    ENDIF

V_cw = (m_dot_cw)/(rho_cw*A_i)

Re_cw = (rho_cw*V_cw*D_i)/Mu_cw


    IF (Re_cw<2300) THEN

    Nu_cw = 4,36

    ELSE

    IF (T_hw > T_cw) THEN

    Nu_cw = 0,023*(Re_cw^(4/5))*(Pr_cw^0,4)          "Dittus-Boelter korrelasie, Verhitting van water vind plaas dus n = 0,4"

    ELSE

    Nu_cw = 0,023*(Re_cw^(4/5))*(Pr_cw^0,3)          "Dittus-Boelter korrelasie, Verkoeling van water vind plaas dus n = 0,3"

    ENDIF

    ENDIF

alpha_cw = (Nu_cw*k_cw)/D_i

END

"Berekening van die hitte kapasiteit van Aqua-Ammoniak"
```

```
PROCEDURE cp_NH3H2O(x ; T ; P_hw : C_AqAm; cp_H2O ; cp_NH3 ; cp_AqAm)

C_AqAm = x*100

cp_H2O=Cp(Water;T=T;P=P_hw)

cp_NH3=Cp(Ammonia;T=T ;P=P_hw)

    IF (T<303,15) AND (C_AqAm<30) THEN

    cp_AqAm=Cp(NH3W;T=T;C=C_AqAm)

    ELSE

    cp_AqAm = x*cp_NH3 + (1 - x)*cp_H2O

    ENDIF

END
"Kies van die regte Epsilon-verwantskap:"

PROCEDURE Relation(C_hw;C_cw;C_min;C_max;C_r;NTU : Epsilon)

    IF (C_hw=C_min) THEN

     Epsilon = 1 - exp(-C_r  ^(-1)*(1-exp(-C_r*(NTU))))

   ELSE
    IF (C_cw=C_min) THEN

          Epsilon = (1/C_r)*(1-exp(-C_r*(1-exp(-NTU))))

    ENDIF

   ENDIF

{Epsilon = 1 - exp(-NTU)}

END

"Inset Parameters:"

"Aqua-Ammoniak mengsel - buite, warm:"

T_hw_i = 29,7 + 273,15                          [K]

m_dot_hw_tot = 0,003006                         [kg/s]

P_hw = 700

x_in = 0,3472                                   "Die konsentrasie van die Aqua-Ammoniak
wat inkom"

"Verkoelingswater - binne, koud:"

T_cw_i_Celsius = 24

T_cw_i = T_cw_i_Celsius + 273,15                [K]
```

m_dot_cw_gram = 32,39

m_dot_cw = m_dot_cw_gram/1000 [kg/s]

P_cw = 101 [kPa]

C_EG = 25 "Konsentrasie van die Ethylene Glycol/Water mengsel"

"Ammoniak- gas wat inkom"

m_dot_NH3 = 0,0005986 [kg/s]

T_Am_i = 15,11 + 273,15 [K]

P_NH3 = 236,2 [kPa] "Parsiële druk van die ammoniak-gas wat inkom"

"Algemeen:"

L_pyp_mm = 96 [mm]

L_pyp = L_pyp_mm/1000 "Pypies se effektiewe lengte"

wt = 1/1000 [m] "Wanddikte van die pypies"

D_i_mm = 10 "Binne diameter in milimeter"

D_i = D_i_mm/1000 [m] "Binne diameter"

D_o = (D_i + 2*wt) "Buite diameter"

"Berekeninge:"

m_dot_hw = m_dot_hw_tot/7 "Die massavloei van water oor een enkele silinder - funksie van hoeveelheid silinder kolome, sien skets"

P_b = P_hw/100

CALL NH3H2O(123; T_hw_i; P_b; x_in : xza_hw_i; xzb_hw_i; xzc_hw_i; h_hw_i; s_hw_i; u_hw_i; v_hw_i; q_hw_i) "Berekening van inlaat entalpie van die Aqua-Ammoniak mengsel"

h_cw_i = Enthalpy(Water;T=T_cw_i;P=P_cw)

h_NH3_i = Enthalpy(Ammonia;T=T_Am_i;P=P_NH3)

T_hw[0] = T_hw_i

T_cw[0] = T_cw_i

h_hw[0] = h_hw_i

"_____ DEEL I _____"

"Eerste 7 pype se berekeninge word hier gedoen "

"Berekening van die UA-waarde"

Duplicate i = 1;7

CALL H_INT(D_i; T_cw[i-1]; T_hw[0]; m_dot_cw; C_EG : A_i[i]; k_cw[i]; rho_cw[i]; V_cw[i]; mu_cw[i]; Re_cw[i]; Pr_cw[i]; Nu_cw[i]; alpha_cw[i])

CALL H_EXT(T_hw[0]; P_hw; m_dot_hw; D_o; x_in : C_in[i] ;k_hw[i]; rho_hw[i]; mu_hw[i]; Pr_hw[i]; Re_hw[i]; Nu_hw[i]; alpha_hw[i])

Tav[i] = (T_cw[i-1]+T_hw[0])/2

k_SSteel[i] =Conductivity(Stainless_AISI304; T=Tav[i])/1000

R_tot[i] = 1/(alpha_hw[i]*pi*D_o*L_pyp) + (ln(D_o/D_i))/(2*pi*k_SSteel[i]*L_pyp) + 1/(alpha_cw[i]*pi*D_i*L_pyp) "Eerste term begin by die water buite, dan die VV staal pyp, en dan die water binne in die pyp"

UA[i] = 1/R_tot[i]

"Effektiwiteits NTU-metode"

T[i] = T_hw[0]

x[i] = x_in

CALL cp_NH3H2O(x[i] ; T[i] ; P_hw : C_AqAm[i] ; cp_H2O[i] ; cp_NH3[i] ; cp_AqAm[i])

Cp_cw[i] = Cp(Water;T=T_cw[i-1];P=101) "T_hw[0] moet vir die eeste 7 rye by 0 bly, uit geometrie van die probleem"

C_cw[i] = m_dot_cw*Cp_cw[i]

C_hw[i] = m_dot_hw*Cp_AqAm[i]

C_min[i] = min(C_hw[i]; C_cw[i])

C_max[i] = max(C_hw[i]; C_cw[i])

C_r[i] = C_min[i]/C_max[i]

Q_dot_max[i] = C_min[i]*(T_hw[0] - T_cw[i-1])

NTU[i] = UA[i]/C_min[i]

CALL Relation(C_hw[i];C_cw[i];C_min[i];C_max[i];C_r[i];NTU[i] : Epsilon[i]) "Ons neem aan geen fase verandering vind plaas nie, en dat die water buite om wel gemeng word"

Epsilon[i] = q_dot[i]/q_dot_max[i]

"Koue stroom"

Q_dot[i] = m_dot_cw*Cp_cw[i]*(T_cw[i] - T_cw[i-1])

"Warm stroom"

-Q_dot[i] = m_dot_hw*(h_hw[i] - h_hw[0]) "h_hw[0] moet vir die eeste 7 rye by 0 bly, uit geometrie van die probleem"

CALL NH3H2O(123; T_hw[i]; P_b; x_in : xza_hw[i]; xzb_hw[i]; xzc_hw[i]; h_hw[i]; s_hw[i]; u_hw[i]; v_hw[i]; q_hw[i])

END

"_____ DEEL II_____"

"Pypies 8 tot 10"

Duplicate i = 8;10

CALL H_INT(D_i; T_cw[i-1]; T_hw[i-7]; m_dot_cw; C_EG : A_i[i]; k_cw[i]; rho_cw[i]; V_cw[i]; mu_cw[i]; Re_cw[i]; Pr_cw[i]; Nu_cw[i]; alpha_cw[i])

CALL H_EXT(T_hw[i-7]; P_hw; m_dot_hw; D_o; x_in : C_in[i] ;k_hw[i]; rho_hw[i]; mu_hw[i]; Pr_hw[i]; Re_hw[i]; Nu_hw[i]; alpha_hw[i])

Tav[i] = (T_cw[i-1]+T_hw[i-7])/2

k_SSteel[i] =Conductivity(Stainless_AISI304; T=Tav[i])/1000

R_tot[i] = 1/(alpha_hw[i]*pi*D_o*L_pyp) + (ln(D_o/D_i))/(2*pi*k_SSteel[i]*L_pyp) + 1/(alpha_cw[i]*pi*D_i*L_pyp) "Eerste term begin by die water buite, dan die VV staal pyp, en dan die water binne in die pyp"

UA[i] = 1/R_tot[i]

"Effektiwiteits NTU-metode"

T[i] = T_hw[i-7] "Hierdie twee parameters is gestel vir die Cp-waarde algoritme vir die Aqua-Ammoniak"

x[i] = x_in

CALL Cp_NH3H2O(x[i] ; T[i] ; P_hw : C_AqAm[i] ; cp_H2O[i] ; cp_NH3[i] ; Cp_AqAm[i])

Cp_cw[i] = Cp(Water;T=T_cw[i-1];P=101)

C_cw[i] = m_dot_cw*Cp_cw[i]

C_hw[i] = m_dot_hw*Cp_AqAm[i]

C_min[i] = min(C_hw[i]; C_cw[i])

C_max[i] = max(C_hw[i]; C_cw[i])

C_r[i] = C_min[i]/C_max[i]

q_dot_max[i] = C_min[i]*(T_hw[i-7] - T_cw[i-1])

NTU[i] = UA[i]/C_min[i]

CALL Relation(C_hw[i];C_cw[i];C_min[i];C_max[i];C_r[i];NTU[i] : Epsilon[i]) "Ons neem aan geen fase verandering vind plaas nie, en dat die water buite om wel gemeng word"

Epsilon[i] = q_dot[i]/q_dot_max[i]

"Koue stroom"

```
Q_dot[i] = m_dot_cw*Cp_cw[i]*(T_cw[i] - T_cw[i-1])

"Warm stroom"

-Q_dot[i] =  m_dot_hw*(h_hw[i] - h_hw[i-7])

CALL NH3H2O(123; T_hw[i]; P_b; x_in : xza_hw[i]; xzb_hw[i]; xzc_hw[i]; h_hw[i]; s_hw[i]; u_hw[i];
v_hw[i]; q_hw[i])

END

"Berekening van nuwe konsentrasie"

NH3_in = x_in*m_dot_hw_tot

H2O = (1-x_in)*m_dot_hw_tot

NH3_tot = NH3_in + m_dot_NH3

m_dot_hw_tot_abs = NH3_tot + H2O

x_2 = NH3_tot/m_dot_hw_tot_abs

"Korreleer dit met maksimum konsentrasie"

Duplicate i = 4;10

"Korrelasie vir Henry se konstante, op gravimetriese basis. Korrelasie werk met Kelvin"

k_HK[i] =  0,0341*(exp(0,0296*T_hw[i]))

"Maksimum konsentrasie met korrelasie en Henry se Konstante, in kg NH3 per H2O:"

c[i]= P_NH3/k_HK[i]

"Maksimum konsentrasie, in kg NH3 per (NH3 + H2O):"

x_Max[i] = c[i]*(1/(c[i] +1))

"Kies die finale uitlaat konsentrasie"

x_out[i] = min(x_2;x_Max[i])

END

"Eienskappe van die NH3-gas wat inkom"

h_NH3 =Enthalpy(Ammonia;T=T_Am_i;P=P_NH3)

"Berekening van nuwe temperature met die absorpsie-proses in ag geneem"

"Belangerik: Ons neem aan die absorpsie van ammoniak in water vind slegs plaas in die laaste
onderste gedeelte/strook en ry"

Duplicate i = 4;10

CALL NH3H2O(123; T_hw[i]; P_b; x_in : xza[i]; xzb[i]; xzc[i]; h[i]; s[i]; u[i]; v[i]; q[i])
```

CALL NH3H2O(123; T_hw[i]; P_b; x_out[i] : xza[i+7]; xzb[i+7]; xzc[i+7]; h[i+7]; s[i+7]; u[I+7]; v[i+7]; q[i+7]) "[i+7] word gebruik om nuwe indekse te vul"

"Massa-energie balans vir elke stroompie"

(m_dot_NH3/7)*h_NH3 + m_dot_hw*h[i] = (m_dot_hw_tot_abs/7)*h[i+7] + Q_dot_gen[i] "Sekere massas moet gedeel word in 7 gelyke dele. m_dot_hw is reeds vroeer opgedeel"

END

"Berekening van finale uitlaat temperature"

Duplicate i = 4;10

T[i+7] = T_hw_transitional[i]

x[i+7] = x_out[i]

"Berekening van nuwe Q_Max - halwe NTU effektiwiteitsmetode"

Q_dot_gen[i] =(m_dot_hw_tot_abs/7)*(h_hw_transitional[i] - h_hw[i])

CALL NH3H2O(123; T_hw_transitional[i]; P_b; x_out[i] : xza_hw_trans[i]; xzb_hw_trans[i]; xzc_hw_trans[i]; h_hw_transitional[i]; s_hw_trans[i]; u_hw_trans[i]; v_hw_trans[i]; q_hw_trans[i])

CALL Cp_NH3H2O(x[i+7] ; T[i+7] ; P_hw : C_AqAm[i+7] ; cp_H2O[i+7] ; cp_NH3[i+7] ; Cp_AqAm[i+7])

C_hw_2[i] = (m_dot_hw_tot_abs/7)*Cp_AqAm[i+7]

Cp_cw_2[i] = Cp(Water;T=T_cw[i];P=101)

C_cw_2[i] = m_dot_cw*Cp_cw_2[i]

C_min_2[i] = min(C_hw_2[i];Cp_cw_2[i])

Q_dot_max_2[i] = C_min_2[i]*(T_hw_transitional[i] - T_cw[i])

Q_dot_max_2[i]*Epsilon[i] = Q_dot_2[i]

"Die warm stroom"

Q_dot_gen[i] - Q_dot_2[i] = (m_dot_hw_tot_abs/7)*(h_hw_abs[i] - h_hw[i]) "Neem hier die massa van die ammoniak-gas in ag, sowel as nuwe konsentrasie vir cp-waarde"

CALL NH3H2O(123; T_hw_abs[i]; P_b; x_out[i] : xza_hw_abs[i]; xzb_hw_abs[i]; xzc_hw_abs[i]; h_hw_abs[i]; s_hw_abs[i]; u_hw_abs[i]; v_hw_abs[i]; q_hw_abs[i])

"Die koue stroom"

Q_dot_2[i] = m_dot_cw*Cp_cw_2[i]*(T_cw_abs[i] - T_cw[i])

END

"Uitlaat temperature sonder absorpsie prosess:"

T_cw_o_pre = T_cw[10]

m_dot_hw_tot*T_hw_o_pre = (m_dot_hw)*T_hw[4] + (m_dot_hw)*T_hw[5] + (m_dot_hw)*T_hw[6] + (m_dot_hw)*T_hw[7] + (m_dot_hw)*T_hw[8] + (m_dot_hw)*T_hw[9] + (m_dot_hw)*T_hw[10]

"Uitlaat temperature sonder verkoeling prosess:"

Q_dot_gen_total = m_dot_hw_tot*(h_hw_not_cooled - h_hw_i)

CALL NH3H2O(123;T_hw_not_cooled; P_b; x_out : xza_hw_not_cooled ; xzb_hw_not_cooled ; xzc_hw_not_cooled ; h_hw_not_cooled ; s_hw_not_cooled ; u_hw_not_cooled ; v_hw_not_cooled ; q_hw_not_cooled)

T_hw_not_cooled_Celsius = T_hw_not_cooled - 273,15

"Finale temperature"

T_cw_o = T_cw_abs[10]

h_cw_o=Enthalpy(Water;T=T_cw_o;P=P_cw)

m_dot_hw_tot_abs*h_hw_o = (m_dot_hw_tot_abs/7)*h_hw_abs[4] + (m_dot_hw_tot_abs/7)*h_hw_abs[5] + (m_dot_hw_tot_abs/7)*h_hw_abs[6] + (m_dot_hw_tot_abs/7)*h_hw_abs[7] + (m_dot_hw_tot_abs/7)*h_hw_abs[8] + (m_dot_hw_tot_abs/7)*h_hw_abs[9] + (m_dot_hw_tot_abs/7)*h_hw_abs[10]

x_out = Average(x_out[4];x_out[5];x_out[6];x_out[7];x_out[8];x_out[9];x_out[10])

CALL NH3H2O(123; T_hw_o; P_b; x_out : xza_hw_o; xzb_hw_o; xzc_hw_o; h_hw_o; s_hw_o; u_hw_o; v_hw_o; q_hw_o)

"Kontrole punte: Indien die koue stroom uitlaat warmer is as die warm stroom uitlaat, sal die hitte nie meer vloei in die rigting wat die program aan neem nie"

"Albei waardes moet positief bly"
"Funksie van lengte, inlaat temperature en massavloeie"
"Indien negatief, moet die inlaat temperature verder uit mekaar uit wees, en die lenge aangepas word"

Duplicate i = 1;10

CheckPoint_A_Pipe_[i] = T_hw[i] - T_cw[i]

END

Duplicate i = 4;10

CheckPoint_B_Pipe_[i] = T_hw_abs[i] - T_cw_abs[i]

END

"Totale hitte gegenereer"

Q_gen_total[3] = 0

Duplicate i = 4;10

Q_gen_total[i] = Q_gen_total[i-1] + Q_dot_gen[i]

END

Q_dot_gen_total = Q_gen_total[10]

"Temperature in grade Celsius"

T_hw_o_Celsius = T_hw_o - 273,15

T_hw_o_pre_Celsius = T_hw_o_pre - 273,15

T_cw_o_Celsius = T_cw_o - 273,15

"Energie-balans - algeheel"

E_in_overall = m_dot_hw_tot*h_hw_i + m_dot_cw*h_cw_i + m_dot_NH3*h_NH3_i

E_out_overall = m_dot_hw_tot_abs*h_hw_o + m_dot_cw*h_cw_o

DeltaE_overall = abs((E_in_overall - E_out_overall)/E_in_overall)*100

"Massa-balans"

m_dot_in = m_dot_hw_tot + m_dot_cw + m_dot_NH3

m_dot_out = m_dot_hw_tot_abs + m_dot_cw

Delta_m = (abs((m_dot_in - m_dot_out)/m_dot_in))*100

APPENDIX B

This section consists of drawings done by the under-graduate student Ané Janse van Rensburg. This design is the result of the work done in this study.

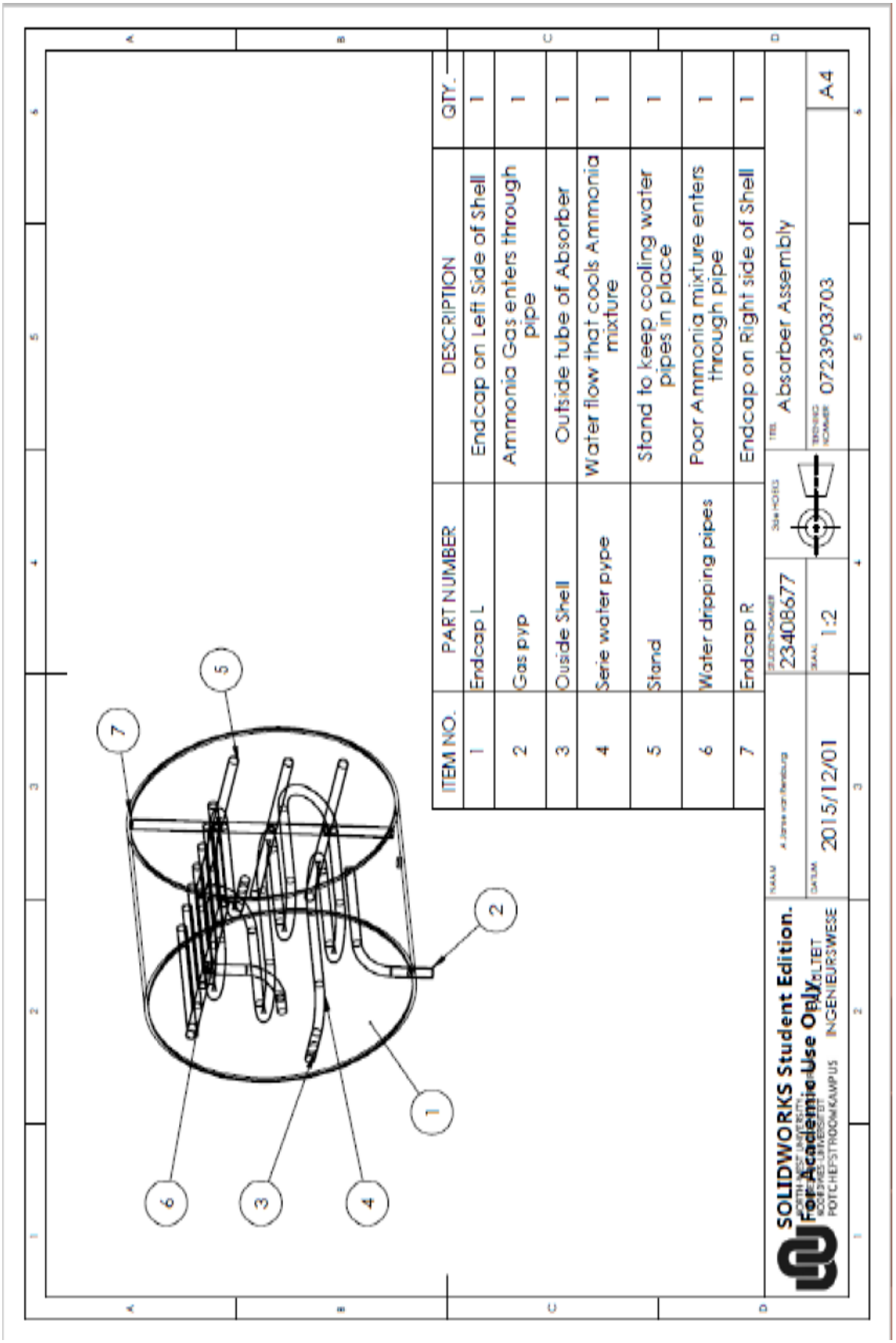
ITEM NO. | PART NUMBER | DESCRIPTION | QTY.
1 | Endcap L | Endcap on Left Side of Shell | 1
2 | Gas pyp | Ammonia Gas enters through pipe | 1
3 | Ouside Shell | Outside tube of Absorber | 1
4 | Serie water pype | Water flow that cools Ammonia mixture | 1
5 | Stand | Stand to keep cooling water pipes in place | 1
6 | Water dripping pipes | Poor Ammonia mixture enters through pipe | 1
7 | Endcap R | Endcap on Right side of Shell | 1
TITEL Absorber Assembly
TEKENINGNUMMER 0723903703
A4
SCHAAL 1:2
DATUM 2015/12/01
SOLIDWORKS Student Edition. For Academic Use Only
NORTH-WEST UNIVERSITY YUNIBESITI YA BOKONE-BOPHIRIMA NOORDWES-UNIVERSITEIT POTCHEFSTROOMKAMPUS
FAKULTEIT INGENIEURSWESE

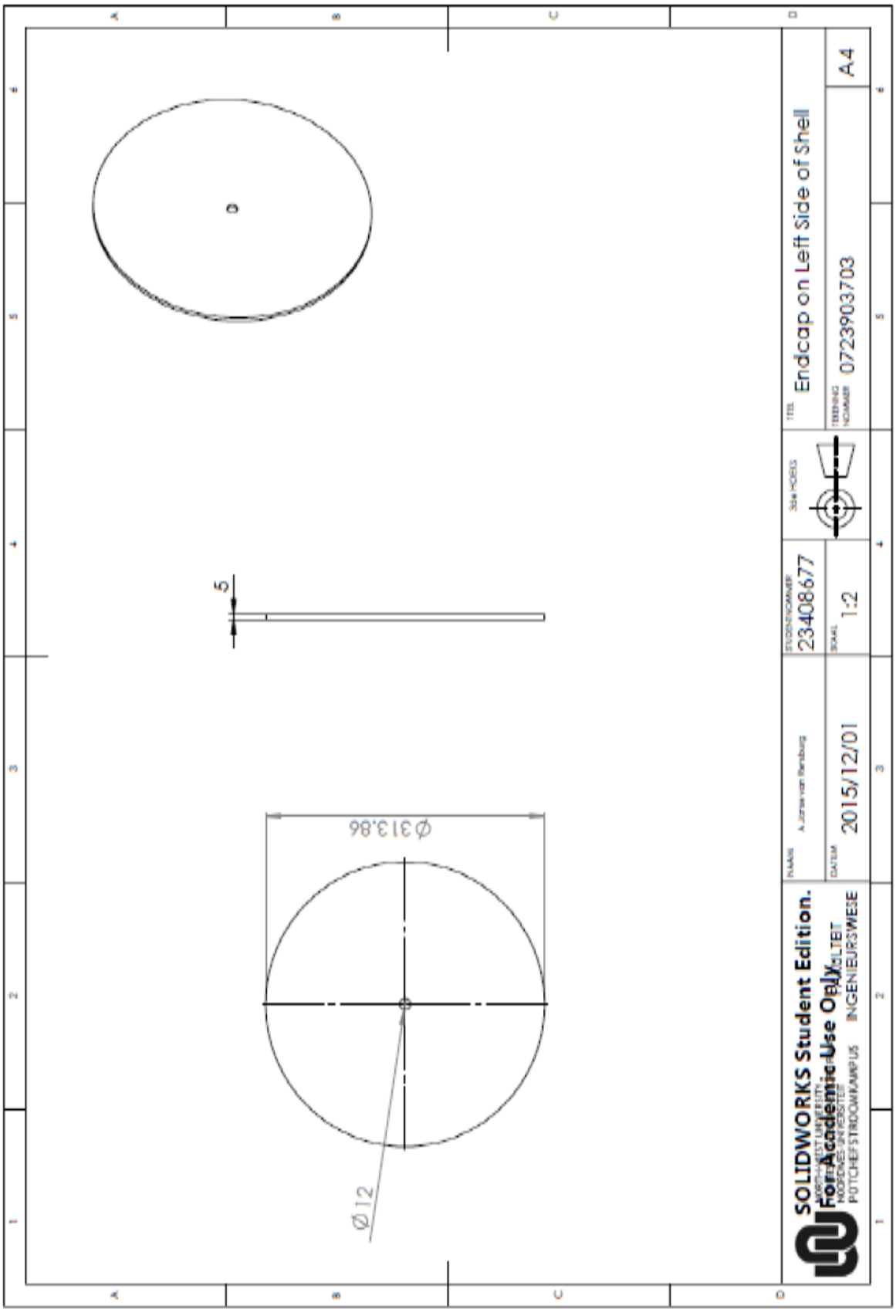
Endcap on Left Side of Shell
A4
0723903703
23408677
1:2
2015/12/01
SOLIDWORKS Student Edition.
For Academic Use Only.
5
Ø313.86
Ø12

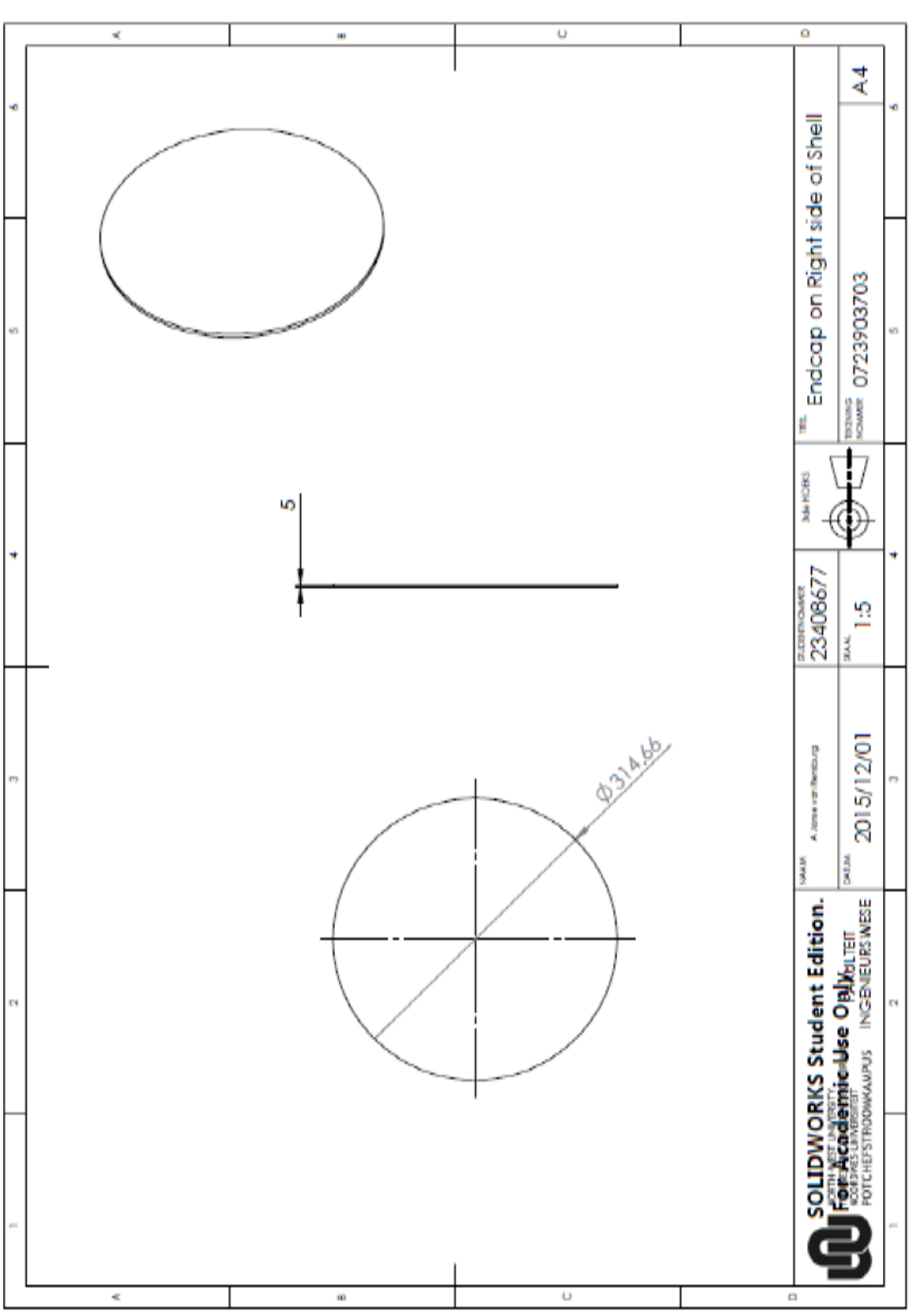
5
Ø314,66
Endcap on Right side of Shell
A4
07239033703
1:5
23408677
2015/12/01
SOLIDWORKS Student Edition.
For Academic Use Only.

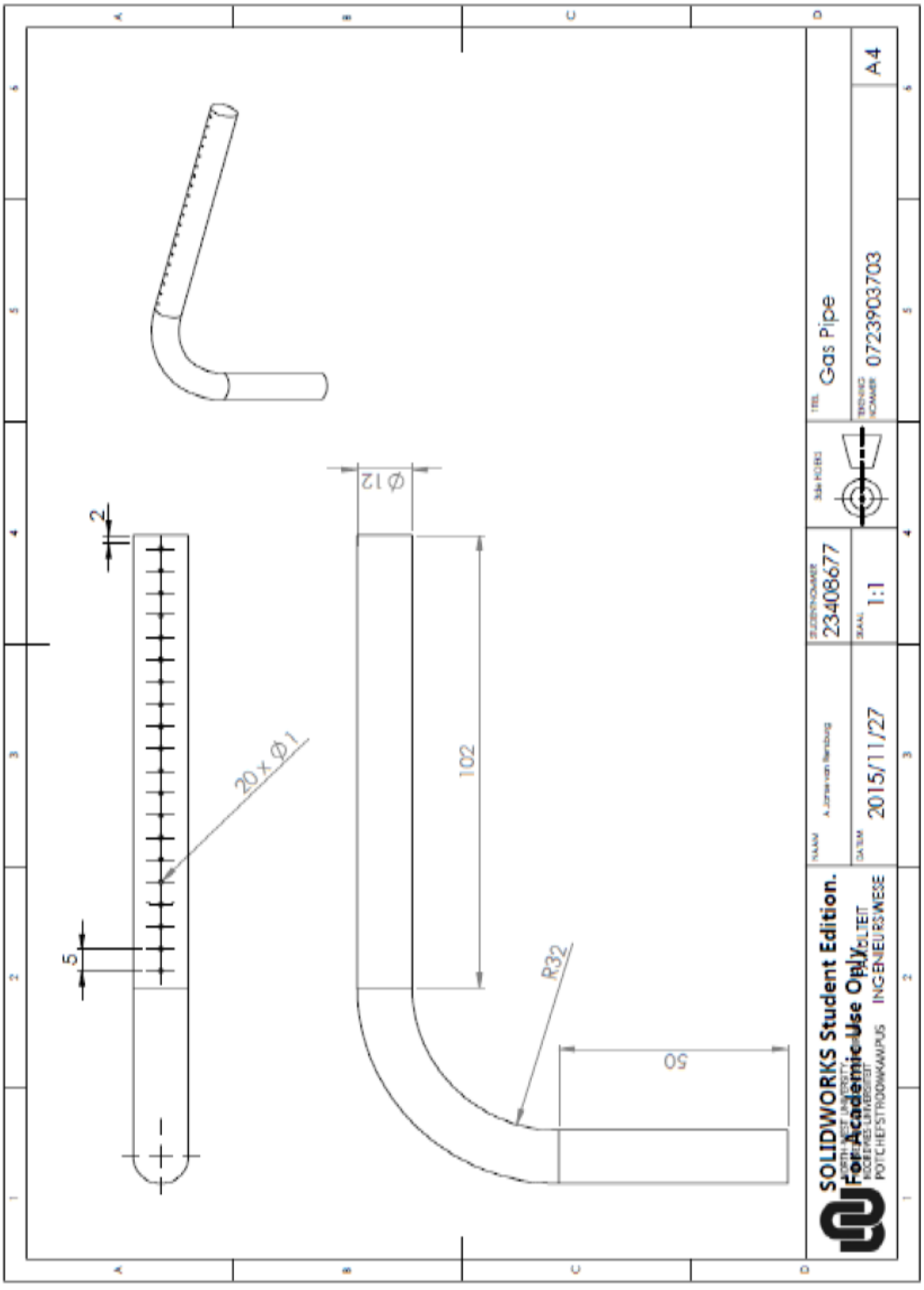
Gas Pipe
0723903703
A4
23408677
1:1
2015/11/27
SOLIDWORKS Student Edition.
For Academic Use Only.
NORTH-WEST UNIVERSITY
YUNIBESITI YA BOKONE-BOPHIRIMA
NOORDWES-UNIVERSITEIT
POTCHEFSTROOMKAMPUS
INGENIEURSWESE
Ø12
2
20 x Ø1
5
102
R32
50

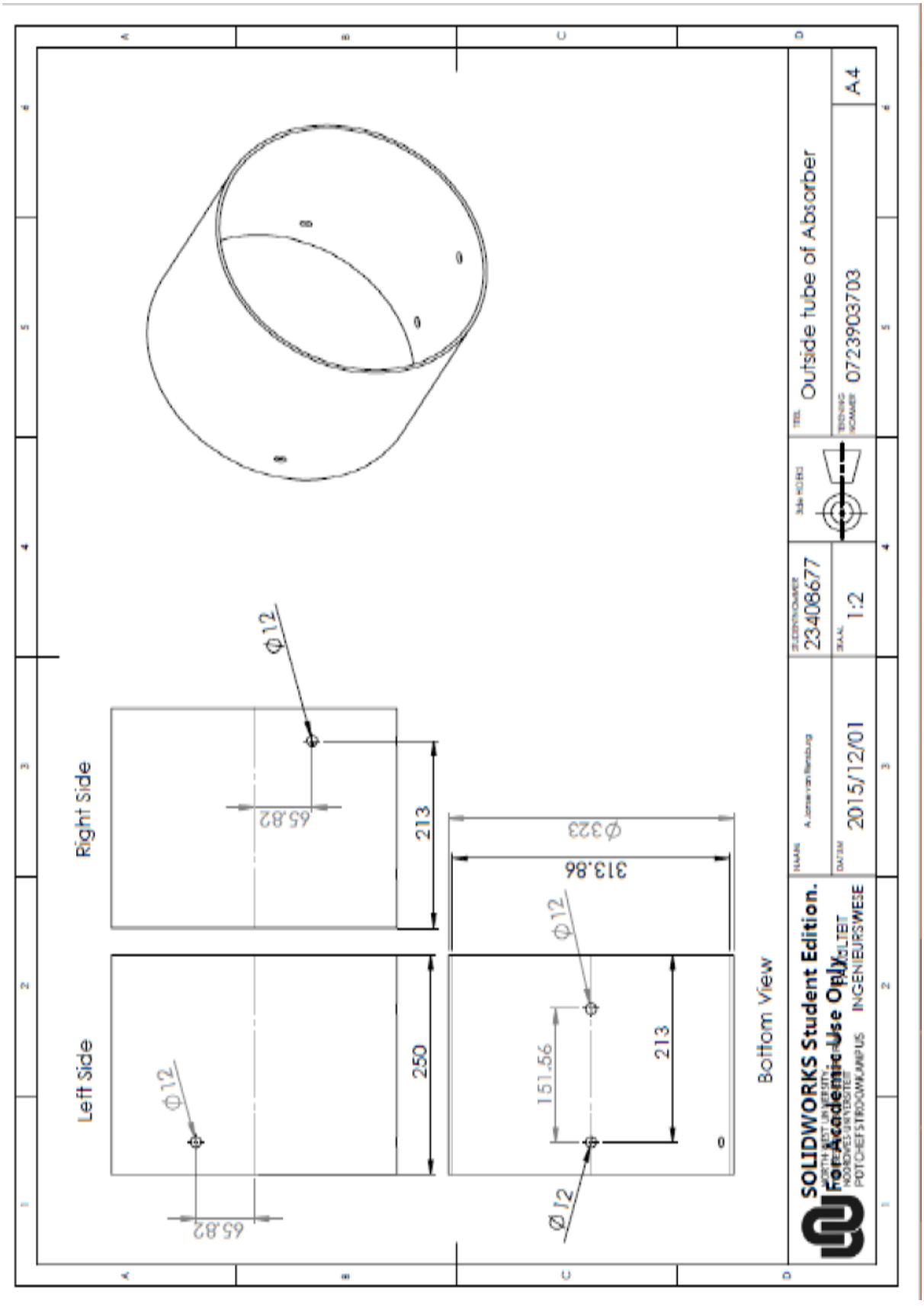
Outside tube of Absorber
0723903703
A4
23408677
1:2
2015/12/01
SOLIDWORKS Student Edition.
For Academic Use Only.
Right Side
Left Side
Bottom View
213
250
313.86
323
151.56
65.82
12

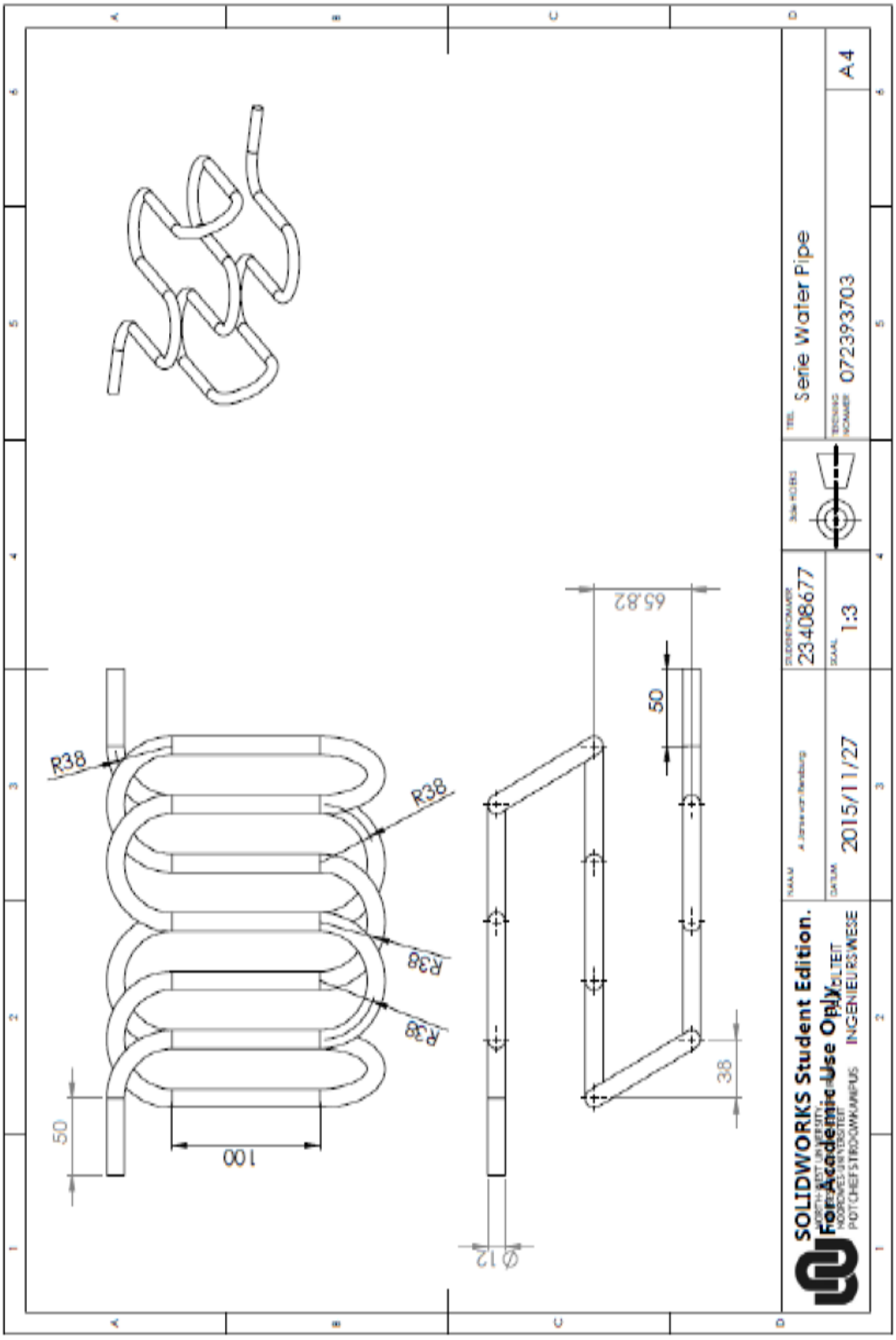
Serie Water Pipe
072393703
A4
1:3
234088677
2015/11/27
SOLIDWORKS Student Edition.
For Academic Use Only.
R38
R38
R38
R38
50
100
65.82
50
38
Ø12

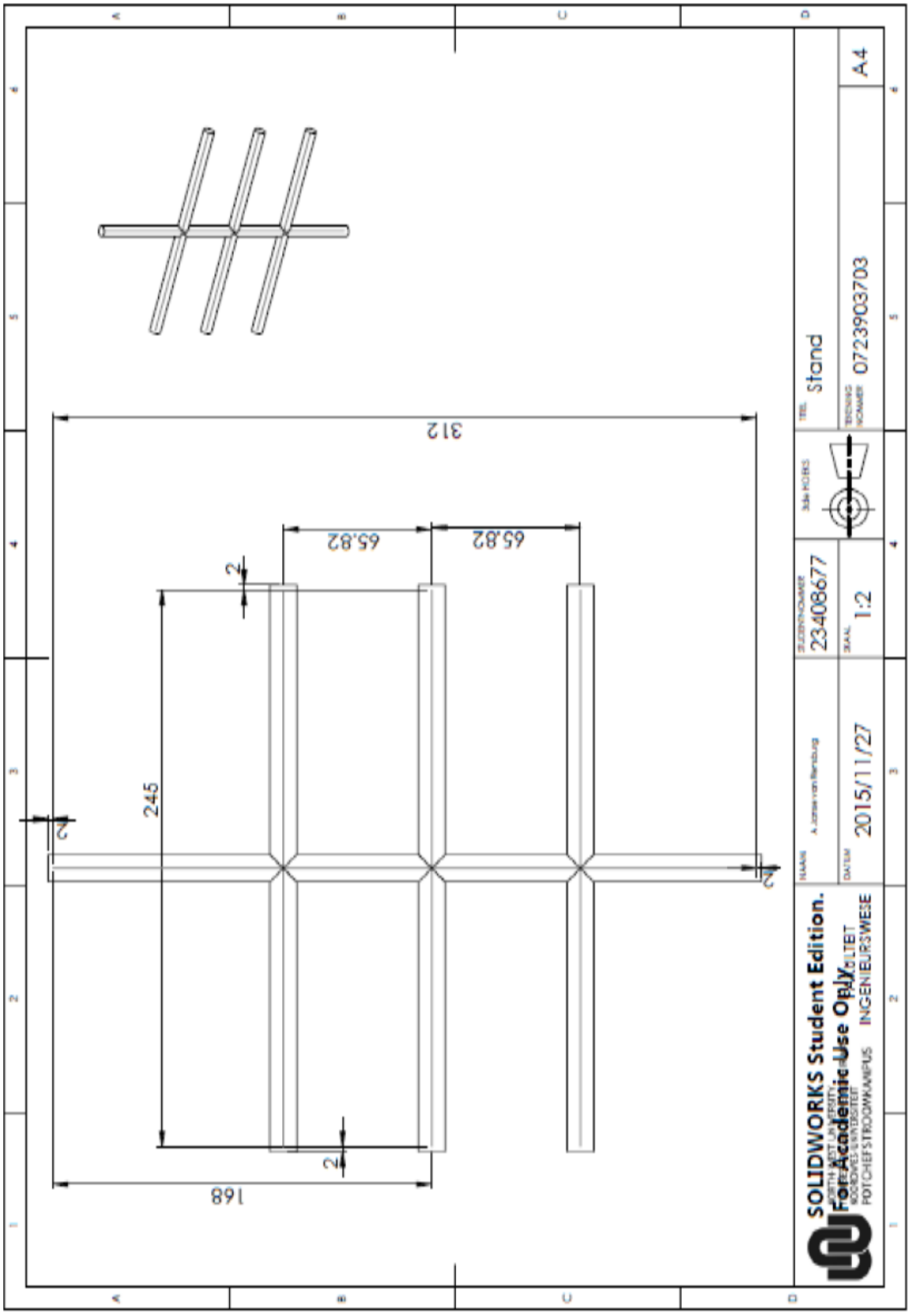
312
65.82
65.82
2
245
2
2
2
168
Stand
0723903703
A4
23408677
1:2
2015/11/27
SOLIDWORKS Student Edition.
For Academic Use Only.

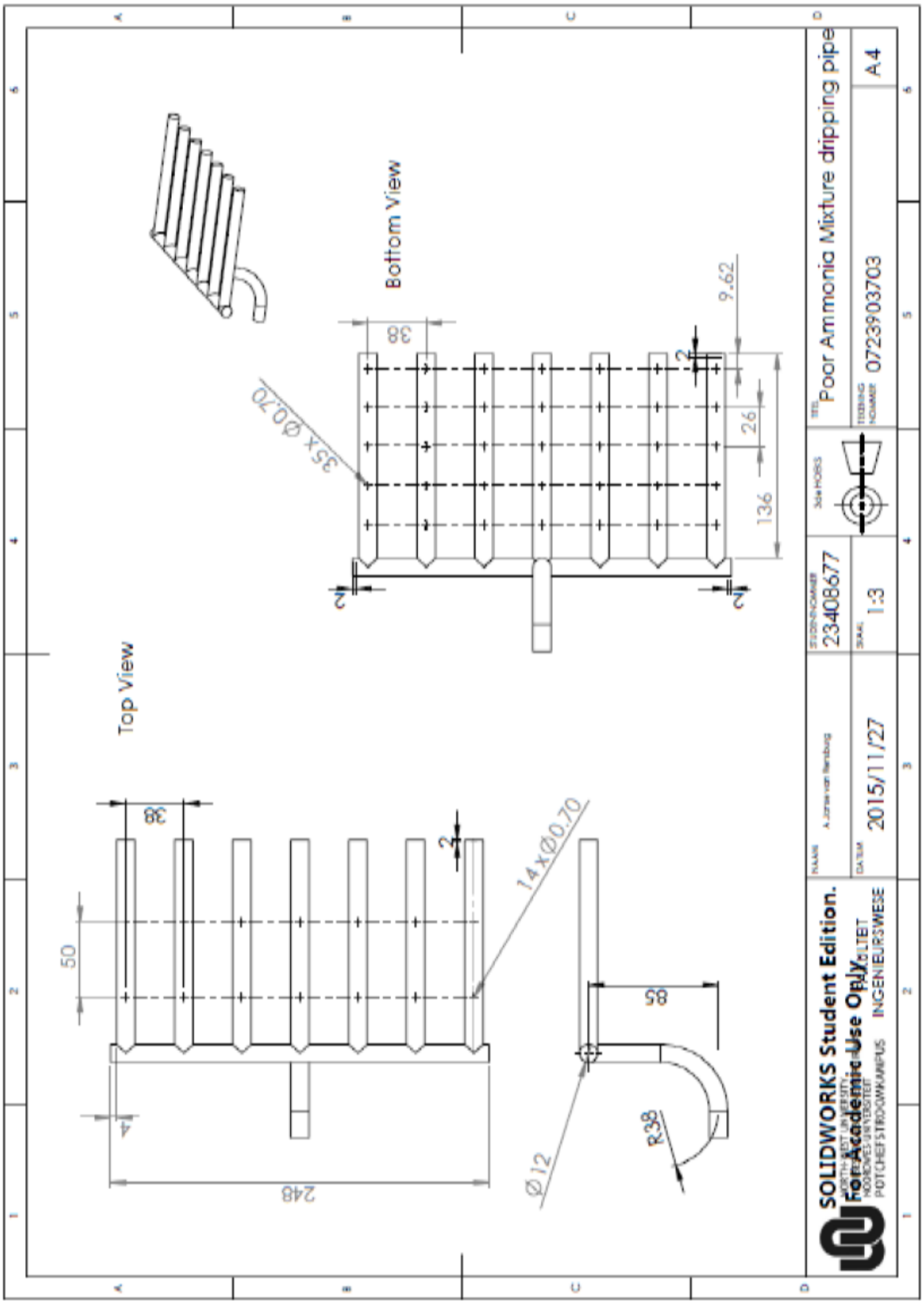
Bottom View
Top View
35x Ø0.70
14xØ0.70
38
9.62
26
136
50
248
85
R38
Ø12
Poor Ammonia Mixture dripping pipe
A4
0723903703
23408677
1:3
2015/11/27
SOLIDWORKS Student Edition.
For Academic Use Only.

APPENDIX ON CD

The following Appendices are found on the accompanying CD (available on request to the author), as it was impractical to add the contents thereof to this document:

- **APPENDIX C – VERIFICATION: EES AND EXCEL PROGRAMS**
- **APPENDIX D – DROPLET EXPERIMENTS: EXCEL SHEETS**
- **APPENDIX E – ALL EES-PROGRAMS**
- **APPENDIX F – SOLUBILITY CHARTS IN EXCEL**